IMPACTS OF ENDOPLASMIC RETICULUM STRESS ON CALRETICULIN SECRETION AND INNATE IMMUNITY

by

Larry Robert Peters

A dissertation submitted in partial fulfillment
of the requirements for the degree of
Doctor of Philosophy
(Immunology)
in The University of Michigan
2011

Doctoral Committee:

Professor Malini Raghavan, Chair
Professor Jeffrey L. Curtis
Professor Wesley Dunnick
Professor Joel A. Swanson
Associate Professor Kathleen L. Collins

DEDICATION

To my family - I can never thank you enough for your unending love and support (I could not imagine anymore).

To all my friends and people who have touched my life, near or far, old or new, casual or close: thank you so very much for the role you played and hopefully will continue to play in shaping my life.

ACKNOWLEDGEMENTS

I would like to thank all of the Raghavan lab members, past & present for their help and companionship through this challenging and rewarding period of my life. Specifically I want to thank the following people. First, my mentor Malini Raghavan, who has a relentless focus and dedication to her work, that is certainly one of the greatest I have seen. The level at which she applies all aspects of herself to every detail of her work is amazing. Furthermore, it is inspiring to see her hard work result in her continued success and career development in such an intensely competitive career. She also applied this incredible work ethic to helping me succeed in graduate school at every step of the way: publishing, presenting, staying focused on work, surveying the literature, designing experiments. For that I owe her great thanks. I also appreciate her continued efforts to make the lab a more enjoyable place to work and promote a sense of community among the members of the lab. Second, my close friend and fellow graduate student, Natasha DelCid. Thank you Natasha for stimulating discussions about our research, our field of study and our lives as a whole, throughout our careers and especially during this last year. Some of these conversations were very helpful as I sorted out my thoughts and ideas that are expressed in this dissertation. I also have to thank her for being one of my closest friends during this once in a lifetime experience. Thanks to Monem for his quiet kindness, gentle and easy-going nature. Monem is the only lab member that worked in the lab during my entire tenure here and we have shared a lot. Looking back at the past 5 years in the lab, I think I can count the number of times I heard him complain on one hand. This ability to not let the hard times in life get him down is a great trait. Sanjeeva Wijeyesakere for many helpful discussions on the dissertation/defense preparation process, computer-related issues, and most importantly, structural biology of calreticulin and ER biochemistry. I would like to give a huge thanks to Elise Jeffery for more reasons than I can list right now. Relevant to this dissertation, she often drug treated cells for me early in the morning. She also did some of the work shown in this dissertation (as

indicated & cited). Elise is one of the kindest people I know, and I was so lucky to work with her for 2 years. Ramesh was only in the lab very briefly, but I would also like to extend a big thanks to him for his incredibly kind and considerate attitude. He made the lab a warmer, friendlier place while he was here. Past and present members I would like to also mention in no particular order: Ericca, Chris, Rachel, Renata, Vil, Nasir.

I owe a huge thanks to my thesis committee for many helpful suggestions, and being so accommodating! Specifically, Jeff, Joanne Sonstein and the whole Curtis lab were very helpful in the work involving phagocytosis and some flow cytometry work. We collaborated for many experiments aimed at optimizing various assays for measuring phagocytosis of cells and exploring the potential role of MHC-I as a don't eat-me signal, but these preliminary experiments suggested it was not involved. They really made me feel at home when I was in the lab, and the time I spent there was a real pleasure. Big thanks to the Swanson lab for help with many things, and particularly the work related to phagocytosis. They were very helpful in designing experiments measuring the phagocytosis of protein-coated beads. Sam at the CLCI taught me a lot about microscopy that was used for the bead experiments and other microscopy-based phagocytosis experiments. As mentioned in the text, I collaborated on experiments examining effects of chronic ER stress on plasma cells with the Dunnick lab. They were very helpful and a pleasure to work with. As very friendly neighbors, they were always willing to lend a helping hand, use of equipment or a reagent. I also received some help from the members of the Collins lab at various times, and they were always kind and informative as well. I got the best (and most detailed) protocol for freezing and thawing cell lines from a member of the Collins lab (Chris Carter), early in my graduate career. Some of his suggestions helped me periodically throughout my graduate work while working with more sensitive cell lines.

I am so fortunate to have so many wonderful people in my life. I must extend a huge thanks to all of my friends and family. Most of you are wonderful, and are very kind to me. I cannot thank you enough for that. Many of my life experiences are fantastic, albeit in different ways, and you are part of that (Ditto for family).

Table of Contents

LIST OF FIGURES

ABSTRACT

The innate immune system must differentiate homeostatic cell stress and death from that associated with danger and infection. Failure to do so can lead to inflammatory disorders and autoimmunity on one hand, or cancer and infection on the other. Various endogenous host factors are proposed to tolerize or activate the immune system in response to cell stress/death. Antigen presenting cells (APCs), in particular dendritic cells (DC), are critical in the induction and direction of the immune response, including responses to cell stress/death. Many endogenous molecules influence APC activation in a paracrine manner following exposure to stressed/dying cells. Conversely, stress within an APC can modulate how it directs an immune response. This thesis focuses on (1) characterizing a novel pathway of increased cell-surface expression of calreticulin that occurs concomitantly with secretion of several other endogenous proteins previously defined as immunomodulatory; (2) using this pathway to examine the abilities of ER chaperones to influence innate immune responses in the context of ER stress, with a specific focus on calreticulin; (3) measuring the ability of cell-surface calreticulin to promote phagocytic uptake of ER stressed cells by DC; (4) comparing cytokine production by DCs experiencing two different forms of ER stress.

Much recent attention has been focused on the ability of cell-surface calreticulin to induce anti-tumor immune responses to dying tumor cells. We characterize a novel stimulus, thapsigargin, and the related pathway for the induction of high levels of cell-

surface calreticulin. Thapsigargin depletes ER calcium, inducing ER stress and a general handicap in ER retention mechanisms. Thapsigargin-treated cells secrete several ER chaperones previously characterized as immunomodulatory. We show that extracellular calreticulin does not modulate the ability of DCs to secrete inflammatory cytokines under sterile conditions or in the presence of an innate immune stimulus such as LPS. On the other hand, DC phagocytosed ER-stressed target cells significantly more than untreated control targets. Furthermore, the presence of cell-surface calreticulin on target cells correlated with their enhanced phagocytic uptake. Together these findings demonstrate that calcium depletion in the ER interferes with retention mechanisms of ER-resident proteins and impacts phagocytic uptake of cells in a calreticulin-dependent manner.

CHAPTER ONE
Introduction

Endoplasmic Reticulum (ER): calcium homeostasis, protein folding chaperones, and protein retention

The ER is the birthplace of virtually all secreted, transmembrane and some organelle-targeted proteins, and an important coordination center for many cell-signaling pathways (reviewed in (Braakman and Bulleid, 2010; Gorlach et al., 2006)). Most secretory proteins are co-translationally transported into the ER. Normally, the ER aids its large volume of diverse protein clientele in folding, by actively providing an appropriate folding environment. This environment includes a host of folding chaperones, oxidative conditions to allow disulfide bond formation, and sufficient concentration of calcium and ATP to promote secretory protein folding (Braakman and Bulleid, 2010; Gaut and Hendershot, 1993). The ER achieves a homeostatic luminal calcium concentration thousands of times greater than that found in the cytosol in large part using two main features. First, active cytosol to ER calcium transport is driven by transmembrane Ca^{2+} pumps that are members of the Sarco(Endo)plasmic Reticulum Ca^{2+} ATPases (SERCAs). Second, the ER membrane is largely impermeable to most molecules and tightly controls transport of other molecules (Braakman and Bulleid, 2010; Burdakov et al., 2005). The relatively high calcium concentration facilitates protein folding, and provides a sub-cellular Ca^{2+} gradient that is important in cell signaling (Gorlach et al., 2006). Consequently, the ER must also be able to vary its calcium concentration widely. The ER and the mitochondria are the two principal calcium-buffering organelles. Many ER resident proteins function in storing Ca^{2+} via calcium binding, adding another level of control to the regulation of cellular [Ca^{2+}] (Gorlach et al., 2006). ER-resident proteins that participate in calcium storage include gp96 (grp94 or

endoplasmin), protein disulfide isomerase (PDI), calreticulin (CRT), and immunoglobulin-heavy-chain-binding protein (BiP/GRP78). CRT is one of the most important intra-lumenal calcium regulators. gp96, PDI, CRT and BiP are highly expressed in the ER and contain multiple Ca^{2+} binding sites, thereby providing a large capacity of calcium storage (Braakman and Bulleid, 2010; Burdakov et al., 2005; Gorlach et al., 2006).

Interestingly, gp96, PDI, CRT and BiP are also ER folding factors, aiding newly synthesized ER proteins in proper folding. Calcium is required for proper protein folding for several reasons. First, calcium ions play a structural role in some proteins (e.g. some extracellular matrix proteins (Handford, 2000)) that traffic via the secretory pathway (Braakman and Bulleid, 2010)). Secondly, calcium binding by ER folding factors affects their structure in a concentration-dependent manner. Consequently, the functions of ER folding factors are affected by fluctuations in $[Ca^{2+}]$ (Michalak et al., 2002; Rizvi et al., 2004). By altering ER folding factor function, variations in $[Ca^{2+}]$ affect the folding of many client proteins (Gorlach et al., 2006; Michalak et al., 2002). Like most ER folding factors, BiP, PDI, gp96 and CRT, are also molecular chaperones. Molecular chaperones can directly bind to unfolded regions of protein clients preventing them from co-aggregating with other unfolded proteins. This binding alone can aid folding of nascent proteins. Some folding factors, such as ERp57 and PDI are oxidoreductases that catalyze proper disulfide bond formation in protein substrates to aid in their folding (Braakman and Bulleid, 2010).

In many cases, chaperones act co-operatively to locate, engage and fold nascent proteins. The calnexin (CNX)/CRT cycle is an example of chaperone co-operation to ensure quality control for all asparagine (*N*)-linked glycoproteins. CNX is a transmembrane molecular chaperone that is similar to CRT. Newly synthesized *N*-linked glycoproteins initially have a specific oligosaccharide structure that is added to *N*-linked glycosylation sites during or shortly following their translocation into the ER. This oligosaccharide has three terminal glucose residues, and is the universal starting carbohydrate moiety on all *N*-linked glycoproteins. The carbohydrate is also the signal that will be modified to indicate the protein folding status as proper folding progresses. Two terminal glucose residues are sequentially removed by glucosidases I & II.

CNX/CRT both specifically recognize and bind to glycan-processed monoglucosylated proteins. When clients are released from the complex with CNX/CRT, glucosidase II cleaves the terminal glucose. A glycoprotein without a terminal glucose residue is allowed to proceed through the secretory pathway. On the other hand, if the released client is not fully folded, it is recognized by a protein folding sensor, UDP-glucose glycoprotein glucosyl-transferase (UGGT) and a monoglucosylated glycan is regenerated. This modification allows CRT or CNX to bind the client and inhibit its secretion. Failure to fold after prolonged retention within the CNX/CRT cycle results in the protein being targeted for ER-associated degradation (ERAD) (reviewed in (Michalak et al., 2009)). Another layer of cooperation results in the recruitment of the thiol-oxidoreductase ERp57 to incompletely folded proteins by the specific interaction of ERp57 with CRT and CNX. By binding CRT/CNX, ERp57 is able to isomerize incorrect disulfide bonds of CNX/CRT-associated glycoproteins (reviewed in (Braakman and Bulleid, 2010)).

The collective actions of the ER folding factors execute quality control for all protein clients in the ER. This function is an important post-translational checkpoint that prevents expression of mutant gene products that could be harmful to the organism (Ellgaard et al., 1999). This is accomplished mainly by retention of incompletely folded proteins and degradation of terminally mis-folded proteins. Molecular chaperones selectively recognize and bind incompletely folded clients not only to aid in their folding, but also to ensure their retention in the ER (Braakman and Bulleid, 2010). Terminally mis-folded proteins are targeted for degradation through ERAD (reviewed in (Hebert et al., 2010)). Aggregation can also prevent ER exit of misfolded proteins. When the ER succeeds in properly folding protein clients, they escape recognition by chaperones and are actively transported to the *cis*-Golgi and subsequently continue to mature throughout the secretory pathway, often culminating in secretion or expression on the cell-surface (reviewed in (Braakman and Bulleid, 2010)).

The selective retention of fully folded ER-resident proteins and associated unfolded protein clients contrasts with the active export of fully folded client proteins. This presents a sorting problem for the ER. Many questions about how the ER overcomes this problem remain unanswered, but several mechanisms to retain ER-resident proteins

are understood in significant detail (reviewed in (Pfeffer, 2007; Sato and Nakano, 2007)). One mechanism involves the recognition and active sorting of folded protein cargo into specific transport vesicles that are coated with dedicated coat protein complexes (COP). COPII coated vesicles form at ER exit sites (ERES) and transport ER secretory cargo to the *cis* Golgi (reviewed in (Braakman and Bulleid, 2010; Sato and Nakano, 2007)). Generally, this type of sorting is dependent on signals found in the amino acid (aa) sequence of the proteins destined for export from the ER, and/or post-translational modifications of these proteins (Dancourt and Barlowe, 2010; Sato and Nakano, 2007). Some signals involved for targeting transmembrane proteins are characterized, and are located in the cytoplasmic domain of transmembrane protein clients (Sato and Nakano, 2007). In order for these same signals to concentrate soluble proteins into the ERES and COPII vesicles, the soluble proteins must bind to specific transmembrane ER cargo receptors (Dancourt and Barlowe, 2010; Sato and Nakano, 2007). In this case, additional signals in the soluble proteins and/or post-translational modifications must direct the soluble cargo to specific cargo receptors (Dancourt and Barlowe, 2010). A variety of ER cargo receptors have been identified. Current research suggests that different cargo receptors transport different soluble cargo. In some cases, the signals directing a cargo molecule to its appropriate cargo receptor are known. Characterized cargo recognition signals include general features of cargo proteins such as various oligosaccheride moieties, amino acid motifs and secondary structures (Dancourt and Barlowe, 2010). Known cargo:receptor binding is regulated by pH, receptor oligomerization, and/or calcium concentration (reviewed in (Dancourt and Barlowe, 2010)). Given the multi-layered control in concentrating secretory proteins at ERES, residence in the ER may be the default scenario for proteins entering the ER, folding properly, yet lacking an export signal. However, a percentage of a given protein not targeted for concentration at ERES does slowly escape from the ER (Braakman and Bulleid, 2010; Pfeffer, 2007). This rate of export is referred to as ‘bulk flow.’ It is believed that bulk flow contributes to the intended secretion of some protein cargo (Dancourt and Barlowe, 2010), but is suggested to be relatively inefficient (Sato and Nakano, 2007).

The cell uses a second mechanism to properly localize ER-resident proteins escaping due to bulk flow: retrieving escaped proteins from the Golgi (the downstream

organelle in the secretory pathway). ER-resident proteins have a consensus KDEL motif, recognized by a KDEL receptor residing primarily in the Golgi. The KDEL receptor binds proteins harboring a version of the KDEL sequence in a manner influenced by pH, and retrieves such proteins back to the ER through retrograde transport (reviewed in (Pfeffer, 2007)). Working together, these two described mechanisms generally maintain ER 'residence' of chaperones and co-chaperones (Pfeffer, 2007). There may be other unidentified and under studied mechanisms for ER retention (Pfeffer, 2007; Sonnichsen et al., 1994). One interesting hypothesis proposed over 20 years ago is that the high concentration of calcium in the ER allows numerous calcium-binding ER resident proteins to form a calcium-dependent matrix that holds the contents of the ER in place (Sambrook, 1990). This hypothesis may be relevant to findings described in chapter 2.

Failed retention of ER chaperones

In most cases, describing a protein as 'ER resident' refers to the majority of that protein. A minority of a given ER chaperone is often discovered outside the ER upon examination by sensitive methods. Papers published over the last 20 years from a variety of research groups characterize physiological and pathophysiological situations wherein 'ER-resident' chaperones are found in non-ER locations. An increasing number of functions have been attributed to ER chaperones in the extracellular space, but in many cases, functions are not yet fully described. Similarly, the mechanism of ER escape is not fully defined. This brief discussion will focus on chaperones that escape ER retention via the secretory pathway.

ER chaperones escape ER retention for a variety of reasons. ER chaperones escape has been characterized during particular developmental stages of a cell, and in specialized secretory cell types. In immature thymocytes, many, but not all newly synthesized ER proteins, including BiP, CRT, CNX & gp96, escape ER retention (Wiest et al., 1997). These chaperones were all found on the surface of immature but not mature thymocytes. Other examples include the release of ER chaperones in specialized, highly secretory cell types, like thyrocytes (Mezghrani et al., 2000) and pancreatic acinar cells (Bruneau et al., 2000). Thyrocytes and pancreatic acinar cells are responsible for secreting high levels of thyroglobulin and digestive enzymes, respectively. In both of

these cases, ER chaperones such as BiP, gp96 and PDI are reported to escape while bound to the primary secretory cargo, and associate with incompletely folded cargo molecules (Bruneau et al., 2000; Mezghrani et al., 2000). PDI has been reported to be a plasma membrane component of B lymphocytes with over representation in B cell chronic lymphocytic leukemia (Kroning et al., 1994; Tager et al., 1997). In another case, the chaperone CRT escapes in a different specialized cell type, cytotoxic T-cells. Cytotoxic T-cells kill target cells by release of cytotoxic granules following specific stimulation. In activated cytotoxic T-cells, CRT was exocytosed from intracellular granules along with perforins and granzyemes following immune recognition of target cells (Dupuis et al., 1993; Sipione et al., 2005).

Extracellular presence of ER chaperones is relatively uncommon. Related to this, some studies report humoral immune responses to ER chaperones in some disease states. For example, in a 2001 study by Blaβ et al., sera from rheumatoid arthritis (RA) patients was reported to more frequently (252/400) contain anti-BiP auto-antibodies in comparison with sera from patients with other rheumatic diseases (14/200) or healthy controls (1/150) (Blass et al., 2001). Furthermore, in sera from lupus patients, 13/34 samples had anti-CRT auto-antibodies, whereas no anti-CRT antibodies were detected in healthy control serum (Eggleton et al., 2000). Both necrotic and shrunken apoptotic cells (Franz et al., 2007) can non-specifically release ER proteins (i.e. release ER proteins in a way that is not specific to a particular ER protein or subset of ER proteins. Instead this refers to a general release of the contents of the ER or the cell). It is possible in these disease states, BiP & CRT are released at higher levels than in healthy individuals due to tissue damage resulting from cell death in diseased individuals. It is also possible that autoimmune responses are developed against the ER chaperones when present in the extracellular space. The question remains whether these anti-chaperone autoimmune responses are indicative of a role for chaperones in disease pathogenesis, or whether observed responses against them were merely a consequence of a higher propensity for autoimmune responses in a diseased individual. The potential contribution of extracellular chaperones to autoimmunity will be discussed in chapter 4.

As expected, genetic (Elrod-Erickson and Kaiser, 1996) or pharmacological (Di Jeso et al., 2005) interference with ER quality control is another way to disrupt retention

of proteins that are normally retained in the ER. As discussed in this section, highly secretory cells sometimes release ER chaperones. A demanding secretory load can challenge the ER quality control mechanisms described earlier. However, even in physiological situations of high secretory load, only a relatively small fraction of the total pool of a given ER chaperone is found to escape ER retention. We will now consider how cells manage an increased secretory load in an attempt to meet the increased demands of their quality control pathways.

ER response to stress (UPR)

One third of all open reading frames in the human genome are predicted to encode proteins destined for the ER. It is a challenge for the ER to accomplish its protein folding functions (Braakman and Bulleid, 2010). Furthermore, various physiological and pathophysiological changes can compound the challenge by either increasing the demand for secreted products (*e.g.*, cellular differentiation, or virus infection) or by interfering with protein folding (*e.g.*, ER calcium depletion, oxidative damage, energy depletion) (Malhotra and Kaufman, 2007). The quantity of protein clients requiring folding assistance sometimes overwhelms the folding capacity of the ER at any given time, leading to an accumulation of misfolded/unfolded proteins and ER stress. Eukaryotic cells are equipped with a specific response pathway to recognize an accumulation of unfolded proteins and attempt to restore ER homeostasis (reviewed in (Schroder and Kaufman, 2005; Todd et al., 2008)). This pathway is called the unfolded protein response (UPR).

The mammalian UPR has 3 axes mediated by 3 separate, ER-localized transmembrane proteins: activating transcription factor 6 (ATF6), inositol-requiring transmembrane kinase/endonuclease1 (IRE1) and pancreatic ER kinase (PERK) (Todd et al., 2008). Under resting conditions, these proteins are bound by the multi-functional, ER-resident molecular chaperone, BiP, maintaining them in an inactive state. When unfolded proteins accumulate in the ER, BiP is recruited to aid their folding and to prevent protein aggregation, allowing the proximal signaling molecules (ATF6, IRE1, and PERK) the potential to become activated. Activated IRE1 activates the transcription

factor X-box binding protein 1 (XBP-1) by splicing its mRNA, leading to production of the active form of the protein: XBP-1s. Activated ATF6 is cleaved, freeing the fragment ATF6f that is a transcription factor. Activated PERK inactivates (through phosphorylation) the eukaryotic translation-initiation factor (EIF2α) and induces expression of the transcription factor ATF4. These transcription factors orchestrate the UPR (Todd et al., 2008).

The UPR uses several strategies to deal with an excess of misfolded proteins. The three described UPR-activated transcription factors induce expression of three different sets of UPR target genes: ER-stress response elements (ERSEs) by ATF6f, and two different sets of UPR elements (UPREs) activated by XBP1s and ATF4 (Todd et al., 2008). ATF6f and XBP1s increase expression of molecular chaperones that assist in protein folding, and of machinery and raw materials (i.e., lipids) necessary for increasing the quantity of ER in the cell (Todd et al., 2008). ATF6f also induces expression of genes responsible for ERAD, thereby reducing the quantity of unfolded proteins in the ER. PERK-mediated phosphorylation of EIF2α, complements the induction of ERAD by blocking translation of most cellular mRNAs. The *ATF4* mRNA bypasses this translational block by having upstream open reading frames (uORFs) that recruit phosphorylated EIF2α (Todd et al., 2008). In addition to using uORFs, mRNAs encoding proteins important for the stress response, including many molecular chaperones, avoid translational block through various mechanisms (reviewed in (Yamasaki and Anderson, 2008)). As suggested, there is a great deal of interplay, and some redundancy among the signaling networks employed by the three axes of the UPR (reviewed in (Todd et al., 2008)).

Because many forms of cell stress also lead to the accumulation of unfolded proteins, there is also a great degree of interplay and redundancy in the cellular response to a diverse array of insults. For example, hypoxia (Blais et al., 2004; Koumenis et al., 2002), oxidative stress, and glucose starvation all typically induce protein misfolding, and are shown to induce some or all of the UPR signaling pathways described above (Malhotra and Kaufman, 2007). Furthermore, in addition to unfolded proteins, different types of cell stress can lead to elevated levels of reactive oxygen species (ROS) and depleted levels of ER calcium (Gorlach et al., 2006; Malhotra and Kaufman, 2007).

Reciprocally, ROS can induce ER calcium depletion (Gorlach et al., 2006) and ER calcium depletion can induce ROS (Hsieh et al., 2007). But ROS, misfolded proteins, and ER calcium depletion have unique features as well that are likely dependent on the kinetics with which each stimulus induces various responses. If severe enough, each of these stimuli can result in cell death (Gorlach et al., 2006). It should be emphasized, however, that even in the absence of cell stress, calcium levels flux naturally within the ER to maintain cellular calcium homeostasis and transducing intracellular signals (Gorlach et al., 2006).

ER stress, inflammation and autoimmunity

Due to the stressful nature of inflammatory conditions, it is logical that there would be connections between inflammation and the cell stress response. In fact, the ER stress response is connected to inflammation in a diverse range of diseases: atherosclerosis, inflammatory bowel disease, diabetes, obesity and inflammatory neurodegenerative disorders (reviewed in (Hummasti and Hotamisligil, 2010; Yoshida, 2007)). There are several proposed mechanisms that link ER stress and these inflammatory conditions. Diseases, and/or associated mouse models, including idiopathic inflammatory myopathies, ankylosing spondylitis, inflammatory colitis, and experimental autoimmune encephalomyelitis implicate an insufficient UPR in several different ways as a cause or contributor to disease development (Todd et al., 2008). Another mechanism is proposed for autoimmune diseases like lupus (Eggleton et al., 2000) and rheumatoid arthritis (Blass et al., 2001; Corrigall et al., 2001), where extracellular UPR chaperones are suggested to be autoantigens and/or adjuvants promoting the autoimmune response.

Related to connections between the UPR and inflammatory conditions, recent work revealed that UPR signaling pathways not only exhibit cross talk between themselves, but also with innate immune signaling pathways responsible for detecting infectious agents (Martinon et al., 2010; Smith et al., 2008; Zhang et al., 2006). Zhang et al. identified a liver-specific transcription factor, CREBH, which is activated by ER stress, and is responsible for expression of acute phase response genes (Zhang et al., 2006). Acute phase response genes are upregulated in the liver during infection and in the

systemic inflammatory element of innate immunity (Yoo and Desiderio, 2003). Zhang et al. established a novel, mechanistic link between ER stress and innate immunity occurring in the liver by showing that CREBH and ATF6 form heterodimers and synergistically enhance their target genes required for the acute phase response and UPR, respectively (Zhang et al., 2006). They also showed UPR activation in hepatocytes following addition of lipopolysaccharide (LPS, an activator of the pathogen recognition receptor toll-like receptor (TLR)-4) or upon addition of pro-inflammatory cytokines IL-6 and IL-1β.

Subsequent research extended the connections between ER stress and the innate immune response identified in the liver, to antigen presenting cells (APC) (Martinon et al., 2010; Smith et al., 2008). APC are found throughout the body and are responsible for initiating and directing the immune response. Smith et al. showed that macrophages subject to two different types of pharmacologically-induced ER stress responded to the pathogen associated molecular patterns (PAMPs), LPS and poly(I:C) (TLR-3 ligand), with enhanced production of the pro-inflammatory cytokine, interferon-β (IFN-β) (Smith et al., 2008). Furthermore, they showed that the synergy between TLR stimulation and ER stress induced by ER calcium depletion (induced by thapsigargin) was independent of PERK expression but dependent on XBP-1. Finally, macrophages from transgenic rats expressing the human MHC-I allotype (HLA-B27), which is prone to misfolding, also produced significantly (~4 fold) more IFN-β than control cells in response to LPS (Smith et al., 2008). These examples demonstrate connections between ER stress and the innate immune response.

Martinon et al. identified new connections between ER stress and innate immunity, in addition to extending the findings described above (Martinon et al., 2010). They showed that XBP-1 was activated following ligation of TLRs 2, 4 and 5 (but not 3, 7, 8 and 9). Unexpectedly however, TLR-2 and TLR-4 ligation actively dampened other signals associated with UPR activation. For example, TLR-4 activation did not activate the other two arms of the UPR, ATF-6 and PERK. Therefore, PRR ligation activated one arm of the ER stress response pathway, but did not induce an ER stress response.

Martinon et al. also examined the relationship between XBP-1 activation in response to PRR ligation and inflammatory cytokine production. Consistent with the

previously defined role for XBP-1 to synergistically enhance IFN-β production (Smith et al., 2008), XBP-1 expression was required for wild-type levels of pro-inflammatory cytokine production. Finally, the relevance of XBP-1 to infection was confirmed by showing that cytokine production and the innate immune response to the intracellular bacteria, *F. tularensis*, was impaired in XBP-1$^{-/-}$ macrophages and mice respectively (Martinon et al., 2010). The precise mechanism used by XBP-1 to synergize with innate immune responses is still unknown (Martinon et al., 2010). In conclusion, there is an important synergy between ER stress within an antigen presenting cell (APC) and the innate immune response directed by that APC. In this thesis (chapter 3), I address the related question of how APCs respond to cell stress in a tissue-derived cell that it encounters.

The immune response to stressed, dying and dead cells

Unlike professional APCs, other cell types are incapable of orchestrating immune responses, such as initiating or preventing an adaptive immune response to specific peptides and proteins (Savina and Amigorena, 2007). Therefore, it is necessary for APCs (particularly dendritic cells (DCs)) to sense infection or danger in surrounding cells or tissues and deliver information about potential danger (or lack thereof) to the other components of the immune system (Schenten and Medzhitov, 2011). APCs translate danger/infection into an immune response using both innate and adaptive immunity (Savina and Amigorena, 2007). APCs also promote tolerance of the adaptive immune response to peptides/proteins not associated with danger/infection (Morel and Turner, 2011). Consequently, in addition to cell stress influencing an APC's function directly as discussed in the previous section, cell stress could also alter the immune response by influencing APCs in a paracrine manner. This paracrine influence could occur at the level of the innate, the adaptive, or both arms of the immune response.

Innate immune activation to danger/infection involves the recognition of a limited number of fixed molecular patterns found in self-molecules associated with tissue damage (or 'danger' DAMPs) (Zitvogel et al., 2010) or foreign molecules from pathogens (PAMPs) (Schenten and Medzhitov, 2011) by pattern recognition receptors

(PRRs). Activation of PRRs results in the production of pro-inflammatory signals, such as cytokines and chemokines that activate surrounding cells and recruit other leukocytes. These innate signals instruct any ensuing adaptive immune response (Schenten and Medzhitov, 2011). To briefly summarize, the induction of an adaptive immune response requires an APC to first be activated by a danger/infection signal (Gallucci et al., 1999; Schenten and Medzhitov, 2011)). Immature APCs constantly survey their surrounding tissue by phagocytosing material that is targeted for uptake (opsonized), such as apoptotic cells or bacteria (Savina and Amigorena, 2007). APCs in peripheral tissues regularly migrate to draining lymph nodes to present processed peptides bound to MHC-I and II molecules to CD8+ and CD4+ T-cells, respectively (Savina and Amigorena, 2007). Some APC subsets reside in lymph nodes and are responsible for capturing and/or presenting soluble and cell-associated antigens that drain to the lymph node or which are carried to the lymph node by other types of APC (Allenspach et al., 2008; Asano et al., 2011; Lee et al., 2009). The source for APC-presented peptides are from those proteins expressed within the APC or cells/proteins phagocytosed by the APC. If the APC was exposed to any maturation stimuli (pro-inflammatory cytokines, PAMPs, or other 'danger' signals) it matures, and undergoes phenotypic changes. These phenotypic changes include up-regulation of T-cell co-stimulatory molecules on the cell surface, and expression of surface proteins which direct the APC into lymph nodes (Savina and Amigorena, 2007). Naïve T-cells specific for peptide:MHC complexes (usually foreign peptides) presented by mature APCs expressing co-stimulatory molecules will be primed (Blander, 2008). The primed, activated T-cells will carry out the adaptive immune response, including activation of antigen specific B-cells.

If an APC in the lymph node was not first exposed to maturation stimuli it will not express the co-stimulatory molecules required to activate naïve T-cells. T-cells specific to the peptide:MHC complexes (usually self peptides) presented in the absence of co-stimulation will become anergic or undergo apoptosis (clonal deletion) (Morel and Turner, 2011). Alternatively, in the presence of specific inhibitory signals (e.g., TGF-β and IL-10), a DC presenting self-peptides may induce T-cells to become regulatory cells. Regulatory cells actively suppress immune responses to their cognate peptide:MHC complexes. Induction of both T-regulatory cells and T-cell anergy are important

mechanisms in promoting peripheral tolerance to self-antigens (Morel and Turner, 2011). Central tolerance is the deletion of most developing self-reactive thymocytes prior to leaving the thymus (Kyewski and Klein, 2006). Together, peripheral and central tolerance work in tandem in an attempt to avoid autoimmunity (Kyewski and Klein, 2006; Morel and Turner, 2011).

Several questions arise relating to abilities of stressed cells to modulate an immune response through interactions with APCs. These include (i) what types of stressed cells (i.e., what types of stress) exhibit paracrine immune modulation (ii) what signals exchanged between the stressed cell and APC are relevant (iii) are the stressed cells immunosuppressive or pro-inflammatory and how does the type of stress influence the response and (iv) can stressed cells modulate the innate and/or adaptive immune response?

Cell death is the outcome of unresolved cell stress. Therefore, characterizing the signals released from cells dying as a result of different stresses is important in understanding the immune response to stresses. In fact, current research shows the type of cell stress that eventually leads to cell death alters a dying cell's immunological properties in the context of anti-tumor immunity (Zitvogel et al., 2010). Additionally, it is not always easy or experimentally possible to arrest cells at a particular stage as they travel along the continuum from viability, to stress and finally death. Consequently there is a great degree of overlap in understanding immunomodulation by stressed cells and dying cells.

Modulation of the innate immune response by dying cells

For many years, there were primarily two types of cell death recognized and studied: necrosis and apoptosis. Cells dying by apoptosis are characterized morphologically by chromatin condensation, blebbing of the cell membrane, cell shrinkage, and maintenance of organelle and plasma membrane integrity (Cohen et al., 1992; Kerr et al., 1972). Unlike apoptosis, cells dying by necrosis swell, and lose structural integrity of outer membranes and organelle resulting of the leakage of intracellular molecules (Kung et al., 2011). The immunological consequences of the signals released from or exposed by these two types of dead and dying cells are

classically thought to be quite distinct. Apoptotic and necrotic cells are generally considered to be immunosuppressive and highly inflammatory, respectively (Gallucci et al., 1999; Rock and Kono, 2008).

However, like necrotic cells, apoptotic cells eventually lose membrane integrity and are thought to non-specifically release intracellular contents. These 'late' apoptotic cells are often referred to as secondary necrotic cells. Observations (some occurring over 30 years ago) associating delayed clearance of apoptotic cells with lupus (autoimmune disease) patients also suggested similarities between late apoptotic and necrotic cells (reviewed in (Schulze et al., 2008)). Consequently, these observations led to the widespread adoption of a 'clearance deficiency' (Schulze et al., 2008) as a major factor driving the development of autoimmune diseases. Deficiency in the clearance of apoptotic cells is proposed to promote auto-immunity primarily through three mechanisms. First, interaction of apoptotic cells with phagocytes is dominantly immunosuppressive, which aids in prevention of autoimmune responses. Second, late apoptotic cells and their released intracellular contents are proposed to be pro-inflammatory. Third, increased exposure of intracellular contents, allows more opportunities for the intracellular contents to be presented inappropriately as antigens in a stimulatory context (Elliott and Ravichandran, 2010).

However, the putative immunogenic nature of late apoptotic cells and their released contents is contradicted by some observations. For example, in some *in vitro* studies, apoptotic cells did not become inflammatory or remained dominantly immunosuppressive after progressing to late apoptosis (Patel et al., 2006; Ren et al., 2001). Furthermore, some knockout mouse models have defective apoptotic cell clearance yet show no signs of inflammation or auto-immunity (Devitt et al., 2004; Stuart et al., 2005). However, these are less common than mouse models that have both signs of apoptotic cell clearance deficiency and autoimmunity (reviewed in (Elliott and Ravichandran, 2010)). More recent studies suggest that tissue-specific variations exist in the receptors used for clearing apoptotic cells (Rodriguez-Manzanet et al., 2010) and the type of immune response to apoptotic cell-associated antigens (i.e., immunogenic vs. tolerogenic) (Asano et al., 2011). This may explain some of the inconsistencies in studies of the immunogenicity of late apoptotic cells. Altogether, these studies suggest that

context is an important factor when considering the immune response to dying cells (reviewed in (Elliott and Ravichandran, 2010)).

Many studies also demonstrate that the cell stress/death stimulus leading to cell death is a critical factor determining the strength of an anti-tumor immune response to dying tumor cells (reviewed in (Zitvogel et al., 2010)). Results from these studies do not conform with the classical immunomodulatory designations of apoptotic and necrotic cells being immunosuppressive and inflammatory, respectively (Zitvogel et al., 2010). Several molecules are suggested to be determinants of the immunogenicity of cell death. These include: phosphatidylserine (PS), HMGB1, CRT, ATP/UTP, dsRNA, monosodium urate, and IL-1α, (reviewed in (Zitvogel et al., 2010)). Some of these molecules are believed to directly modulate the innate immune response: HMGB1, dsRNA, monosodium urate, and IL-1α. The three latter molecules are pro-inflammatory (reviewed in (Zitvogel et al., 2010)), whereas HMGB1 is anti-inflammatory in its oxidized state and pro-inflammatory in its reduced state (Kazama et al., 2008). Some of the dying cell signals aid location and direct or aid uptake of dying cells. Molecules or changes in the cell surface that enhance uptake of (opsonize) dying cells, cell debris or changes in how the APC perceives dying cells (benign or dangerous) could influence the adaptive immune response in multiple ways. These include a quantitative effect on antigen levels in APC or on antigen processing and presentation by APC. While extracellular CRT is suggested to be an important mediator of immunogenic cell death, relevant molecular mechanisms are not understood. Understanding the innate impacts of extracellular CRT is a major focus of this thesis.

Modulation of the adaptive immune response by dying cells - clearance of dying cells resulting in delivery of cell-associated antigens to APCs for presentation to T-cells

The most intimate interaction between an APC and a surrounding cell (or any two cells) is when one cell 'eats' the neighboring cell either through phagocytic uptake or macropinocytosis. This is a common occurrence *in vivo* due to the high levels of cell turnover in humans, and is designed to occur rapidly, allowing efficient clearance of dead cells (Elliott and Ravichandran, 2010). Rapid uptake of dead cells allows the body to

promptly re-use and recycle the valuable components found in each corpse. As discussed previously, prompt removal of apoptotic cells prevents release of their intracellular components that may have pathological consequences (Krysko and Vandenabeele, 2008; Zitvogel et al., 2010). Phagocytosis is also a critical way for foreign antigens, tumor antigens and self-proteins to be delivered to APCs. APCs can then process and present cell-derived antigens to T-cells to initiate, prevent or potentiate an adaptive immune response. Dead cells are considered to be the only physiological 'target' cells for uptake by APC. However, some recent *in vitro* analyses suggest that drug-treated, cancer cells can be eaten by APCs well before they show signs of cell death (Obeid et al., 2007b). Furthermore, in some experimental and clinical settings, manipulation of certain receptor:ligand interactions between a phagocyte and target cell can induce uptake of live cells (Chao et al., 2010; Gardai et al., 2005).

Two models exist describing the mechanism by which innate immune cells take up dead/dying cells. In one model, uptake of apoptotic cells occurs via macropinocytosis (Hoffmann et al., 2001). In another model, the mechanism of uptake depends on the type of cell death experienced by the target cell (Krysko et al., 2006). In contrast with the first model, these authors suggest that apoptotic cells are 'eaten' using a zipper-like phagocytosis resulting in tight, exclusive phagosomes. In contrast, necrotic cells are taken up by macropinocytosis, resulting in spacious macropinosomes that include other soluble material from the extracellular space (Krysko et al., 2006). Despite these suggested differences in the mechanism of uptake, some of the molecular signals responsible for inducing recognition and ingestion of various types of dying cells seem to be universal (Krysko and Vandenabeele, 2008). The most universal molecular 'eat-me' signal is the exposure of PS on the outer leaflet of the plasma membrane of dying cells. PS is retained on the inner leaflet of the plasma membrane of viable cells and dead cells expose PS on the outer layer of the plasma membrane, where it is recognized by a variety of receptors and adaptor molecules (reviewed in (Krysko and Vandenabeele, 2008; Ravichandran, 2010; Zitvogel et al., 2010)). In many experimental systems, PS is the dominant eat me signal, and may be sufficient to drive uptake of an apoptotic cell (Ravichandran, 2010).

In addition to 'eat-me' signals like PS, there is great deal of communication between the phagocytic prey and the phagocyte (Krysko and Vandenabeele, 2008;

Zitvogel et al., 2010). Currently, more is understood about the interactions between apoptotic cells (AC) and surrounding cells than necrotic cells (Krysko and Vandenabeele, 2008), so this discussion will focus on AC:phagocyte interactions. In order to ensure prompt removal, AC release 'find-me' signals that attract professional phagocytes through chemotaxis (which can also be APC) (reviewed in (Munoz et al., 2010)). Find-me signals include nucleic acids such as ATP & UTP, cleavage products of tyrosyl tRNA synthetase, lysophosphatidylcholine, fractalkine (CXC_3CL1) and others (Munoz et al., 2010) (Fig. 1.1). Some of the find-me signals are more limited in their tissue expression patterns, like fractalkine and others are universal (ATP/UTP) (Munoz et al., 2010). One of the better characterized 'find-me' signal receptors includes purinergic receptors ($P2Y_2$ and $P2RX_7$) (Zitvogel et al., 2010).

Upon finding a dying cell, a phagocyte will engage eat-me signals displayed on the surface of an apoptotic cell with specific receptors. It is interesting that many different modes of recognition exist for PS (Fig. 1.1) (Ravichandran, 2010). Some soluble molecules are soluble bridging molecules that link PS to other receptors on phagocytes, including: milk fat globule protein E8 (MFG-E8), growth arrest-specific gene 6 (Gas-6), and protein S (Fig. 1.1). Phagocyte receptors that signal through these PS-dependent apoptotic cell opsonins include $\alpha_5\beta_3$ integrin (vitronectin receptor) and the Tyro 3, Axl, and Mer family members (TAM family) that bind to MFG-E8 and gas-6, respectively (Krysko and Vandenabeele, 2008; Ravichandran, 2010; Zitvogel et al., 2010). Some receptors can bind directly to PS, such as the TIM family of receptors (such as TIM4 (Rodriguez-Manzanet et al., 2010)) and CD14 (Devitt et al., 2004) (Fig. 1.1).

The relative roles of the different mechanisms of PS recognition and how they interact are not entirely elucidated. In some cases, different receptors play only a part in a situation where different receptors cooperate to accomplish uptake of a dead cell. For example, CD14 (LRP) is suggested to 'tether' dying cells to phagocytes by PS binding, but not induce uptake (Devitt et al., 2004). In other cases, different receptors are used in tissue-specific PS-mediated dead cell clearance (Ravichandran, 2010). Consequently, some phagocytes may use different PS receptors to achieve slightly different functional outcomes. Therefore, it is interesting to consider the relative functional outcomes of ligation of these various receptors, how they interact to recognize what may be a limited

number of ligands on a target cell, and how eat-me signals from PS may be integrated with those from other eat-me signals (Ravichandran, 2010).

The second most notable eat-me signal after PS, is the ER chaperone calreticulin (Krysko et al., 2006; Zitvogel et al., 2010). CRT's role as an eat-me signal on the surface of an apoptotic cell (Gardai et al., 2005) is a new discovery relative to the eat me signal PS (Fadok et al., 1992). The increased expression and redistribution of CRT on the surface of pre-apoptotic (prior to PS exposure) and apoptotic (PS positive cells with intact plasma membranes) cells is reported to be limited to certain cell death stimuli, unlike PS exposure (Zitvogel et al., 2010). Phagocytes are suggested to recognize CRT via CD91/LDL-related protein (LRP)/α2-macroglobulin receptor (Gardai et al., 2005). Unlike PS, CRT is expressed on the surface of some viable cells (Chao et al., 2010; Gardai et al., 2005; Kuraishi et al., 2007; Park et al., 2008). Consequently, viable cells express complementary 'don't-eat-me' signals to prevent CRT-mediated uptake (Zitvogel et al., 2010). Examples include CD47 (Gardai et al., 2005) and plasminogen activator inhibitor-1, PAI-1 (on neutrophils) (Park et al., 2008). Interestingly, blocking CD47 is sufficient to drive cell-surface CRT-dependent phagocytic uptake of viable cells by macrophages (Chao et al., 2010; Gardai et al., 2005; Park et al., 2008). Furthermore, macrophage-mediated uptake of apoptotic cells expressing high levels of both cell surface CRT and PS requires CRT:LRP mediated signals in the phagocyte (Gardai et al., 2005; Park et al., 2008). These findings suggest that CRT is necessary and sufficient to drive phagocytic uptake by macrophages (Gardai et al., 2005; Park et al., 2008). CRTs function as an eat-me signal on pre-apoptotic cells was demonstrated using BMDC as phagocytes (Obeid, 2008; Obeid et al., 2007b). In a pre-apoptotic context, PS is not exposed on the PM. Therefore, the relative importance of CRT and PS-mediated uptake of apoptotic cells by BMDC is not yet known and is investigated in chapter 3.

Other eat-me signals could include changes in the glycocalix (cell-surface glycoproteins) on shrunken apoptotic cells, and the presence of chaperones such as HSP 70, HSP90 and gp96. ER chaperones are proposed to bind to a variety of receptors on phagocytes. Similarly, apoptotic changes in the glycocalix (Franz et al., 2007) are suggested to recruit a variety of binding proteins that promote uptake of dead cells (reviewed in (Zitvogel et al., 2010)). Unlike the relatively early exposure of CRT that is

seen on dying cells, changes in the glycocalix may appear later in the apoptotic time-line. Immature glycoproteins containing ER carbohydrate moieties may be exposed as a result of general donation of the ER membrane to the plasma membrane during apoptotic blebbing (Franz et al., 2007; Zitvogel et al., 2010).

In conclusion, various 'eat-me' signals, 'don't eat-me' signals, opsonins, associated receptors, and many different phagocytes (diversified, for example, by several different sub-sets of macrophages & DCs) function to ensure prompt removal of apoptotic cells *in vivo*. Furthermore, signals that accompany the phagocytic event play an important role in delivering cell-associated and particulate antigens to APCs for presentation to T-lymphocytes. The possibility that various permutations of signals & phagocytes combine to alter the way potential antigens are perceived, processed and presented is an important area of future research. It will likely further our understanding to the adaptive immune response.

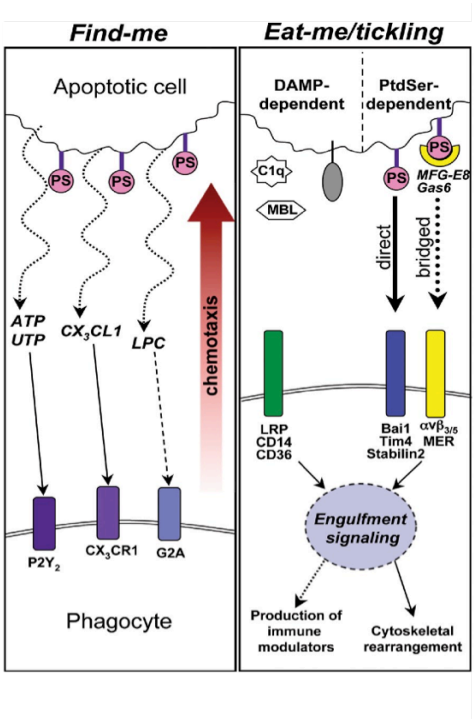

Figure 1.1 – Find-me and eat-me signals released by apoptotic cells and their receptor-mediated detection by phagocytes.
Find-me signals released from apoptotic cells create a chemotactic gradient detected by professional phagocytes. Find-me signals that are described include nucleotides ATP/UTP, fractaline (CX_3CL1) and lysophosphatidylcholine (LPC), which bind purinergic receptors ($P2Y_2$), fractaline receptor (CX_3CR1), and G-protein coupled receptor G2A (G2A), respectively. Eat-me signals are divided into phosphatidyl-serine (PtdSer)-dependent and DAMP (Danger-associated molecular patterns)-dependent mechanisms of uptake. Opsonins such as C1q, surfectant proteins A and D (SP-A and SP-D) (not shown) and mannose binding lectin (MBL) bind to immature glycoproteins (Schulze et al., 2008; Zitvogel et al., 2010) exposed on the cell surface following cell shrinkage as a result of ER membrane donation to the plasma membrane (Franz et al., 2007). Because the immature glycoproteins are endogenous molecular patterns recognized by innate immune complement proteins, they are classified as DAMPs. LRP(CD91) and the scavenger receptors CD14 and CD36 are receptors used by phagocytes to recognize various apoptotic cell opsonins (Devitt et al., 2004; Zitvogel et al., 2010). Here the three separate phagocyte receptors, LRP, CD14 & CD36 are represented by one symbol. PtdSer-dependent mechanisms of uptake include those mediated by bridging molecules like MFG-E8 or Gas6 and dedicated receptors such as αvβ5 integrin and MER (TAM-family receptors, Mer, Axl, Tyro3) and those mediated by direct receptor binding of PS (Bai1, Tim4 or stabilin2) (Elliott and Ravichandran, 2010). Figure shown here is edited from:

Elliott, M. R. and K. S. Ravichandran (2010). "Clearance of apoptotic cells: implications in health and disease." J Cell Biol 189(7): 1059-1070.

The immune response to stressed, dying and dead cells – signals with multiple effects on the immune response and future directions

Interestingly, several of the molecules that control the location and uptake of dying cells are also shown to modulate the innate immune response (Munoz et al., 2010; Zitvogel et al., 2010). For example, ATP/UTP is pro-inflammatory and, as mentioned, PS is anti-inflammatory (reviewed in (Zitvogel et al., 2010)). Other examples include the ability of lysophosphatidylcholine (LPC) to enhance phagocytic uptake after being bound by IgM molecules, and modulate the innate immune response in addition to serving as a find-me signal (Munoz et al., 2010). Other molecules associated with cell stress and death are reported to influence the innate immune response, although their effects and modes of action are not entirely clear or in some cases are quite controversial. Most notable in this later category is the heat-shock protein (HSP) including CRT and other HSPs, which are a major focus of this thesis (reviewed in (Henderson et al., 2010; Tsan and Gao, 2009)).

Immunomodulation by heat shock proteins

There is an extensive and controversial history describing the ability of HSPs to modulate the immune response. The most essential physiological role of HSPs is to serve as molecular chaperones in various intracellular locations. They are so named because they are upregulated during conditions of stress (e.g., heat shock) to help the cell cope with the stress (Feder and Hofmann, 1999). Several observations led to the attractive hypothesis that outside the cell, many HSPs are immunological 'swiss army knives (Schild and Rammensee, 2000),' including their: intracellular importance during various conditions of cell stress; ability to promiscuously bind a wide variety of proteins and peptides and induce adaptive immune responses specific to their associated proteins and peptides; and apparent stimulation of the innate immune system (Srivastava, 2002).

Much of the debate regarding their various roles in modulating immune responses stems from some of the early work (and still some current publications), in which recombinant HSPs expressed in, and purified from bacteria were shown to be inflammatory and enhance immune responses to associated or co-administered antigens. In these types of experiments it is very difficult to rule out the contribution of

contaminating bacterial molecules (Henderson et al., 2010; Tsan and Gao, 2009). The innate immune system has evolved an extensive list of receptors PRRs that recognize PAMPs, and induce inflammatory responses that initiate and/or direct the immune response (Schenten and Medzhitov, 2011). Many of these receptors and signaling pathways seem to also respond to specific endogenous 'danger-associated molecular patters' (DAMPs, also known as alarmins). These pathogen recognition pathways (described earlier) are well studied and indisputable relative to HSP's ability to stimulate innate immunity. Consequently, HSP signaling through PRRs provides an attractive mechanism to explain their putative pro-inflammatory effects. To further complicate this issue, some groups more recently report that HSPs mediate immunosuppression by signaling through some of the PRRs ((Zanin-Zhorov et al., 2006) and reviewed in (Henderson et al., 2010)). The fact that PAMPs are not classically associated with immunosuppression, is used as circumstantial evidence to support the view that some reports of immunomodulation by HSPs is independent of contaminating PAMPs (Henderson et al., 2010).

It was not initially known that several of the HSPs bind tightly to PAMPs and greatly enhance the immunogenicity of the respective PAMPs (Tsan and Gao, 2009). Following recognition of the abilities of HSPs to bind PAMPs, it became recognized that, bacterially-derived HSP preparations not only had to be free of contaminating soluble PAMPs, but also of HSP-bound PAMPs in order for proposed immunostimulatory activities to be credible. A recent review proposed that, and summarized why, HSP-bound PAMPs explain most, if not all, of the innate immune effects attributed to HSPs (reviewed in (Tsan and Gao, 2009)). On the other hand, the possibility that some HSPs modulate the innate immune response continues to be supported by current literature (Henderson et al., 2010; Murshid et al., 2008; Panayi and Corrigall, 2006; Tamura et al., 2011; Zitvogel et al., 2010).

Some HSPs do have a much less disputed role in manipulating the adaptive immune response by enhancing the cross priming of associated proteins and/or peptides (reviewed in (Murshid et al., 2008; Tsan and Gao, 2009)). CD8+ T-cell priming is the activation of a naïve CD8+ T-cell specific to a peptide-MHC-I complex presented by an activated professional APC. Cross priming is the presentation of peptides resulting from

break down of exogenously-derived proteins not expressed by the APC to allow for subsequent APC-mediated T-cell activation. This is highly relevant in the anti-tumor and anti-viral immune response (reviewed in (Raghavan et al., 2008)). Srivastava et al. showed that vaccination of mice with tumor-derived gp96 protected mice from subsequent challenge of the same tumor line but not other tumor lines (Srivastava et al., 1986). They later showed that vaccination with other tumor-derived HSPs, including CRT, displayed the same anti-tumor protection (reviewed in (Srivastava, 2002)).

Using a technology platform based on these observations and subsequent work, Srivastava co-founded a biotechnology company, Agenus (formerly Antigenics) (http://www.agenusbio.com/). The legitimacy of an HSP, namely gp96, to induce adaptive immune responses to associated antigens is evidenced by successfully clinical trials piloted by Agenus (http://www.agenusbio.com/prophage/past-trials.html); most notably, a recent, successful, phase III clinical trial using gp96-complexed tumor peptides to treat advance melanoma (Testori et al., 2008). This is the focus of Agenus' current work. However, some recent work suggests that this ability of gp96 to dramatically enhance cross-priming of T-cells to associated antigens does not occur in the context of viral infections (Lev et al., 2009). Furthermore, the ability of gp96 to stimulate innate immune responses was questioned as early as 2003 (Reed et al., 2003). As this 2003 study showed, the ability of gp96 to stimulate ROS and NFκB signaling was dependent on contamination with bacterial LPS. However, other responses appeared to be LPS-independent, consequently, Reed et al. concluded that gp96 (and CRT) were able to activate APCs (Reed et al., 2003). Additionally, genetically-induced cell-surface expression of gp96 was shown to be immunostimulatory in a transgenic mouse context (Liu et al., 2003). Thus, Agenus still includes "HSPs release from dying cells send a "danger signal" to the immune system leading to generation of immune responses" as an explanation of their technology platform (http://www.agenusbio.com/about/platforms.html). Furthermore, their website references recent work supporting the idea that gp96 can serve to stimulate innate immune responses (Oizumi et al., 2007). Further work is needed to establish in what contexts and using which mechanisms gp96 is able to initiate an innate immune response.

Similar conflict exists in defining the immunomodulatory properties of the HSP BiP. A body of work generated in the UK over the last decade shows that BiP can be immunosuppressive, and protects patients against rheumatoid arthritis (RA) (reviewed in (Henderson and Pockley, 2010; Panayi and Corrigall, 2006)). Despite the fact that much of this work was done using recombinant BiP expressed in bacteria (Corrigall et al., 2004; Corrigall et al., 2001), this work has culminated in ongoing clinical trials evaluating BiP as a treatment for RA (Henderson and Pockley, 2010; Panayi and Corrigall, 2008). In contrast with the work describing BiP as an immunsuppressive molecule, a very recent paper suggests that BiP derived from tumor cells engineered to secrete BiP by deletion of its KDEL sequence is able to cross-prime anti-tumor immune responses (Tamura et al., 2011). Although the ability of this secreted BiP to stimulate the innate immune response was not directly tested, innate stimulation by BiP was a suggested mechanism for enhanced cross-priming of CD8 T-cell responses against tumor-associated antigens (Tamura et al., 2011).

Like BiP, HSP-60 is also reported to be both inflammatory and immunosuppressive (reviewed in (Henderson et al., 2010)), although in this case, strong evidence suggests that PAMP contamination explains the former observation (Gao and Tsan, 2003). Unlike BiP, a receptor through which HSP-60 exerts its immunosuppressive effects was identified: TLR-2 (Zanin-Zhorov et al., 2006). Because the HSP-60 used in this study was recombinant protein, purified from *E. coli*, it is interesting to speculate that a bacterial PAMP signaling through TLR-2 is responsible for the reported immunosuppressive effects. This would be unexpected, as PAMPs are extensively characterized as pro-inflammatory signals. However, precedence does exist for the ability of PAMPs to suppress rather than stimulate the innate immune response (Frleta et al., 2009; Ginzkey et al., 2010). Clearly, more work is needed to understand the modulation of the innate immune response by BiP and how it may vary in different biological contexts.

CRT is the final HSP to be discussed in depth, and is a central focus of my dissertation. Like gp96, Srivastava's group also described an ability of soluble, tumor-derived CRT to induce anti-tumor immune responses to associated tumor peptides in 1999 (Basu and Srivastava, 1999). However, unlike BiP and gp96, many other

extracellular functions are attributed to CRT, both immunological and non-immunological (Gold et al., 2010). Regarding extracellular CRT's ability to influence immune responses, much work starting in 2007 shows that upregulation of CRT on the surface of dying tumor cells stimulates protective anti-tumor immune responses (Obeid et al., 2007b). Kroemer and colleagues previously showed that anthracyclin-killed tumor cells stimulated *in vitro* maturation of splenic DCs and the induction of adaptive immune responses (Casares et al., 2005). These findings suggested that part of the immunogenic apoptosis induced by anthracyclin treatment involved both innate and adaptive immune activation. However, subsequent work demonstrated that soluble CRT/peptide complexes did not stimulate innate or adaptive immune responses to associated peptides (Bak et al., 2008). This leaves open the possibility that cell-surface CRT is inflammatory, unlike soluble CRT. In fact, cell-surface CRT is currently described as a 'pro-inflammatory' signal by prominent experts in the field, despite no published work to directly test this possibility (Zitvogel et al., 2010). Furthermore, Petrovski et al showed that PS-independent uptake of autophagic cells by macrophages induced pro-inflammatory cytokine production (Petrovski et al., 2007a; Petrovski et al., 2007b). They suggested that cell-surface calreticulin may be the signal responsible for the PS-independent uptake and the pro-inflammatory cytokine production, but these hypotheses have yet to be tested (Petrovski et al., 2007a; Petrovski et al., 2007b). Currently, the relative contributions of an innate immune response (possibly stimulated by cell-surface CRT) vs. the delivery of cell-associated antigen (by enhancing uptake of apoptotic cells) in cell-surface CRT-dependent anti-tumor immunity have not been characterized, studies that are undertaken in my thesis.

Calreticulin, a traveling multi-functional protein

CRT is a soluble protein found predominantly found in the ER. In the ER, CRT serves as a chaperone for all *N*-linked glycoproteins. CRT binds proteins mainly through recognition of mono-glucosylated glycans (Hebert and Molinari, 2007). CRT can also bind and prevent aggregation of non-glycosylated protein clients *in vitro* (Hebert and Molinari, 2007; Jeffery et al., 2011; Rizvi et al., 2004; Saito et al., 1999). The functional contribution of the polypeptide based chaperone activity of CRT to protein folding *in*

vivo is debated and still unclear. This uncertainty is in part due to the inability to pinpoint a polypeptide-binding site on CRT (Jeffery et al., 2011).

CRT comprises 3 domains: a globular N-domain, an extended arm-like P-domain, and an acidic C-terminal tail ('C-domain') (Michalak et al., 2009) (Fig. 1.2). The globular domain contains the lectin binding site, the proposed polypeptide binding site (Leach et al., 2002), and a single high-affinity Ca^{2+} binding site (Kozlov et al., 2010). The C-domain has a low affinity, high capacity Ca^{2+} binding site that is reported to bind over 50% of the calcium found in the ER (Michalak et al., 2009). The P-domain is proline rich and suggested to have some structural flexibility (Michalak et al., 2009). CRT uses the tip of the P-domain to bind its partner co-chaperone, ERp57 (Michalak et al., 2009). Specifically, CRT requires amino acid W244 of the P-domain to bind ERp57 (Del Cid et al., 2010; Frickel et al., 2002). As previously mentioned, CRT and ERp57 co-operate in properly folding client glycoproteins in the ER (Frickel et al., 2002).

Figure 1.2 – Calreticulin's molecular structure
Generated in MacPyMOL

CRT is also one of a select group of five ER chaperones or specific assembly factors that are responsible for the proper folding and peptide loading of MHC-I molecules. A complex formed by these proteins is designated the 'peptide-loading complex' (PLC). MHC-I molecules are expressed by all nucleated cells and are required for CD8 T-cell immune responses against intracellular pathogens and tumor cells (Raghavan et al., 2008). CRT is bound to ERp57 both inside and outside the PLC.

In addition to its roles in the ER, CRT is found in several other sub-cellular locations: the cytosol, *cis*-golgi and plasma membrane (Gold et al., 2010). In resting cells, a portion of CRT is retrotranslocated into the cytosol in an atypical manner that avoids proteasomal degradation (Afshar et al., 2005; Carpio et al., 2010). Here it is suggested to aid in cell adhesion (Afshar et al., 2005) and gene transcription (reviewed in (Michalak et al., 2009)). Additionally, during conditions of cell stress such as cell calcium depletion, cytoplasmic arginylated-CRT associates with stress granules (Carpio et al., 2010). The specific function of CRT in the stress granules is not known. Like other ER-localized proteins, a portion of CRT escapes ER retention, and is mostly retrieved by the KDEL receptor in the Golgi. Recently, Howe et al showed that the CRT that is recycled from the

Golgi back to the ER is responsible for retrieving sub-optimally loaded MHC-I molecules (Howe et al., 2009). In doing so, CRT molecules recycling in the early secretory pathway promote optimal loading on MHC-I (Howe et al., 2009). Unlike these later two examples of CRT functions in specific locations outside the ER, many functions are reported for extra-cellular CRT, including roles in cellular adhesion, cell migration, anoikis, phagocytosis, inflammation, cell signaling, and enhancing wound healing and anti-tumor immune responses (Gold et al., 2010).

Of central interest to my thesis are the proposed abilities of cell-surface CRT to enhance phagocytosis (Gardai et al., 2005), induce inflammation and promote anti-tumor immune responses (Cheng et al., 2005; Obeid et al., 2007b). In 2005, Kroemer and colleagues first published the finding that anthracyclin-induced tumor cell apoptosis drove protective, anti-tumor immune responses in mice (Casares et al., 2005). Anthracyclins are a class of chemotherapeutics. This finding was surprising because apoptotic cells were previously known to be strongly immunosuppressive in many other contexts examined. In 2007, Kroemer and colleagues showed that anthracyclins also induced the highest levels of cell-surface calreticulin among a panel of 14 different cytotoxic drugs (some of which were chemotherapeutics) (Obeid et al., 2007b). Furthermore, anthracyclin-induced immunogenicity of cell death required cell-surface calreticulin. Kroemer et al. showed that cell surface calreticulin was strongly upregulated within a few hours of drug treatment, long before PS exposure. For this and other reasons, anthracyclin-induced upregulation of cell-surface CRT was suggested to be a pre-apoptotic event (Obeid et al., 2007b). Subcutaneous immunization with the CRT-high pre-apoptotic cells provided mice with almost complete protection from subsequent tumor challenge, and protection was dependent on cell-surface CRT. Furthermore, the immunization with surface CRT-high cells primed IFN-γ producing cells in the draining lymph node in a surface CRT dependent manner (Obeid et al., 2007b). This experiment suggested a direct involvement of CRT in generating the adaptive anti-tumor immune response. However, many related questions about CRT-dependent stimulation of the adaptive immune response remain unanswered, including: whether extracellular CRT drives an advantageous (in the context of anti-tumor immunity) innate immune response

and whether a CRT advantage resulting from tumor cell phagocytosis can translate into increased priming of T-cell responses against tumor cell antigens.

Overall summary

To begin to address the questions outlined above, we tested different conditions for extracellular CRT exposure in chapter 2, including cell treatments with an anthracyclin, UV irradiation and different types of ER stress. We showed that THP-induced, ER calcium depletion handicaps ER retention, resulting in the release of several proteins normally retained within the ER. Most notably, ER calcium depletion induced strong cell-surface calreticulin. THP induced cell-surface CRT to an extent greater than that induced by anthracyclins. This finding allowed us to identify mechanisms of cell-surface CRT exposure in THP-treated cells in chapter 2. Additionally, in chapter 3, we characterized functional impacts of stress-induced cell-surface CRT upon the innate immune response focusing on cytokine production and target cell phagocytosis by DC. In chapter 4, we summarize the findings of chapters 2 and 3 and discuss the implications of this work in understanding the effects of cell stress on ER protein retention, antigen delivery and innate immunity.

CHAPTER TWO

Specific forms of endoplasmic reticulum stress break ER retention and strongly increase cell-surface calreticulin

SUMMARY

A number of immunological functions are ascribed to cell-surface expressed forms of the endoplasmic reticulum (ER) chaperone CRT, including abilities to induce inflammation and adaptive anti-tumor immune responses. Here we examined the impact of several different ER stress inducing stimuli on cell-surface CRT induction. We show that cell-surface expression of CRT and secretion of CRT, BiP, gp96 and PDI are induced by THP treatment, which depletes ER calcium, but not by tunicamycin (TUN) treatment, which inhibits protein glycosylation. We define the mechanism of THP-induced, CRT surface expression, and show that it is distinct from the two previously described mechanisms of cell-surface CRT expression. Binding sites relevant to the polypeptide-specific chaperone activity of CRT are important for the retention of CRT on the cell surface. We also show cell-surface expression of CRT on apoptotic but not viable plasma cells, a cell type under constitutive ER stress resulting from high secretory load. Other apoptotic cells examined, including splenocytes and thymocytes, do not show elevated levels of surface CRT as assessed by flow cytometry. Together, our data show that increased cell surface CRT expression by a magnitude measurable by flow cytometry is linked to certain type of drug-induced and physiological forms of ER stress. Sections of this chapter were published in:

Peters, L.R., and Raghavan, M. (2011). Endoplasmic reticulum calcium depletion impacts chaperone secretion, innate immunity, and phagocytic uptake of cells. J Immunol *187*, 919-931.

and

Jeffery, E., L. R. Peters, and M. Raghavan. 2011. The polypeptide binding conformation of CRT facilitates its cell-surface expression under conditions of endoplasmic reticulum stress. *J Biol Chem* 286:2402-2415.

INTRODUCTION

The endoplasmic reticulum (ER) is an important site of protein folding, calcium storage, and intracellular signaling (Gorlach et al., 2006). A number of ER chaperones are important in carrying out these functions. CRT is a chaperone that maintains quality control of glycoprotein folding by binding mono-glucosylated proteins in the ER. CRT also contributes to calcium storage in the ER (reviewed in (Michalak et al., 2009)). Several recent studies showed that the cell-surface expression of CRT was induced in different cell types by different treatments, and that the increased amount and/or the re-distribution of CRT on the cell surface has important functions in the immune response (reviewed in (Gold et al., 2010; Green et al., 2009)). In 2005, Gardai et al. first characterized that CRT was upregulated and re-distributed on the surface of UV-treated, apoptotic cells. Cell surface CRT was necessary for phagocytic uptake of apoptotic cells. Although the mechanism for CRT upregulation and re-distribution was not defined in the study, the authors did show that CRT and PS co-localized in distinct clusters on the apoptotic cell surface (Gardai et al., 2005).

In the following years two different models were published explaining the increased surface expression of CRT in dying cells. The most recent model, involves the subset of CRT molecules demonstrated to reside in the cytosol (arriving via non-degrading retrotranslocation from the ER), in resting viable cells (Afshar et al., 2005; Carpio et al., 2010). In 2010, Tarr et al. proposed that the cytosolic portion of cellular CRT associates with PS on the inner leaflet of the plasma membrane in a manner that is enhanced by calcium (Tarr et al., 2010). Furthermore, Tarr et al. suggested that following the exposure of PS on the outer leaflet during apoptosis or pharmacological intervention, PS-bound CRT becomes exposed. This study did not directly address the contribution of a loss in membrane integrity due to secondary necrosis or oxidative damage to the cell surface expression of CRT (Tarr et al., 2010).

The other proposed model is described in many papers from the laboratory of Dr. Guido Kroemer. Their studies characterized chemotherapeutic drugs and relevant pathways that lead to increased cell-surface CRT expression. They showed increased co-dependent surface expression of CRT/ERp57 complexes in pre-apoptotic cells at relatively short time points following exposure to UV light, gamma-irradiation, anthracyclin chemotherapeutics (*e.g.*, mitoxantrone (MTX)), and platinum-based chemotherapeutics (*e.g.*, oxaliplatin) (Obeid, 2008; Obeid et al., 2007a; Obeid et al., 2007b; Panaretakis et al., 2008a; Panaretakis et al., 2009; Tufi et al., 2008). In addition, activation of pancreatic ER kinase (PERK), which initiates one of three branches of the unfolded protein response, induction of reactive oxygen species, pre-apoptotic cleavage of caspase 8, activation of pro-apoptotic molecules, BAX and BAK (Panaretakis et al., 2009), and ER calcium efflux (Panaretakis et al., 2009; Tufi et al., 2008) are required. Notably, BAX and BAK lead to ER calcium efflux and alterations in mitochondrial membrane permeability (Scorrano et al., 2003).

A number of other studies also suggest links between ER calcium depletion and detection of ER-resident proteins, including CRT, in the extracellular space. Treatment of NIH3T3 cells with the calcium ionophore A23167, which depletes intracellular calcium stores (Drummond et al., 1987), resulted in secretion of gp96, an ER-resident chaperone, and reduced intracellular levels of CRT (referred to in the paper as CRP55) (Booth and Koch, 1989). Furthermore, treatment of NIH3T3 cells with the sarco-endoplasmic reticulum Ca^{2+}-ATPase (SERCA) inhibitor THP (Thastrup et al., 1990) resulted in a decrease in CRT ER staining intensity and an increase in the co-localization of CRT with wheat germ agglutinin in a non-ER cellular compartment suggested to be the Golgi (Booth and Koch, 1989). Finally, two other groups showed that ER calcium depletion by THP results in secretion and surface expression of BiP (Delpino and Castelli, 2002; Zhang et al., 2010).

THP is a commonly used drug to induce the UPR pathway, and as noted above, THP induces calcium depletion (Thastrup et al., 1990). Another drug that is commonly used to induce the UPR pathway is TUN, which inhibits protein glycosylation thereby causing protein misfolding in the ER (Rutkowski and Kaufman, 2004). Both TUN and THP induce all three axes of the UPR including PERK activation, which is required for

pre-apoptotic, anthracyclin-induced surface CRT:ERp57 complex expression (Li et al., 2000; Martinon et al., 2010; Martins et al., 2011).

In the present studies, we compare the impacts of these two ER stress-inducing drugs as well as the chemotherapeutic MTX, on cell-surface expression of CRT in different cell types. We show that cell-surface expression of CRT, and secretion of other ER proteins including CRT, is specific to the ER calcium depletion-induced form of ER stress. Cell-surface expression of CRT in THP treated cells involves a failure in effective ER retention mechanisms for a number of ER-resident proteins. Furthermore, amino acid residues that contribute to the polypeptide-specific chaperone activity of CRT also influence its surface expression in THP-treated cells (Jeffery et al., 2011). This mode of CRT release from the ER is distinct from that described for anthracyclin-induced surface CRT expression, where co-translocation with ERp57 is suggested and other ER proteins are not secreted (Obeid, 2008; Panaretakis et al., 2008a).

Finally, splenocyte differentiation into plasma cells is used as a physiological model of constitutive ER stress based on previous findings that the UPR-induced transcription factor XBP-1 is required for plasma cell differentiation (Iwakoshi et al., 2003). Indeed B-cell to plasma cell differentiation is characterized by expression of the expansion of the ER (Kirk et al., 2010). We report that surface CRT is not found on viable plasma cells during the days following initiation of differentiation. However, in contrast with other apoptotic cells examined, apoptotic plasma cells showed elevated levels of surface CRT. Together, our data show that increases in cell surface CRT expression that are measurable by flow cytometry are a feature of some but not all apoptotic cells and are consistent with a model in which both ER chaperone upregulation and reduction in ER calcium levels are required to liberate resident chaperones from ER retention.

METHODS

Drugs and antibodies

TUN and MTX were purchased from Calbiochem or Sigma, and used at 10 μg/ml or 1 μM, respectively unless indicated otherwise. THP was purchased from both Sigma and Alexis Biochemicals (now Enzo Life Sciences) and used at 5 μM, unless indicated otherwise. MTX, THP and TUN were all dissolved in DMSO and stored in single use aliquots at -20^{o} C at stock concentrations of 1 mM, 5 mM and 10 mg/ml, respectively. Frozen aliquots and freshly dissolved drugs did not show differences in measured activities. Chicken-anti-CRT or rabbit-anti-CRT were purchased from Affinity Bioreagents, now part of Thermo Scientific (PA1-902A), and Abcam (ab2907), respectively and used for flow cytometry at a concentration of 2.5 μg/ml and a dilution of 1:200, respectively. Annexin-V (AnnV)-FITC was purchased from Biovision and BD biosciences. 7AAD was purchased from Sigma. Mouse-anti-H2b (Y3) (1:100) and mouse-anti-H2d (34-1-2S) (1:100) were used to detect MHC-I in flow cytometry, and rabbit anti-K^{b} antiserum EX8 (P8) (1:6000) was used in MHC-I immunoblots (kindly provided by Dr. Jonathan Yewdell). Streptavidin-APC (BD biosciences, 554067) was used at a 1:100 dilution. All other fluorescent secondary antibodies were purchased from Jackson Immunoresearch. For immunoblots, goat-anti-CRT (Santa Cruz, sc-7431) was used at a dilution of 1:2500, and secondary antibodies conjugated to horseradish peroxidase were purchased from Jackson Immunoresearch and used at a dilution of 1:30,000. Mouse-anti-BIP (BD biosciences, 610978) and rabbit-anti-CRT (Abcam, ab2907) were used in immunoprecipitations at a concentration of 1:1000 or 1:1666 respectively. Rabbit-anti-PDI (1:2500, Santa Cruz, sc-20132), mouse-anti-BIP (BD biosciences, 610978), rabbit-anti-HMGB1 (Abcam, ab18256) and rabbit-anti-GP96 (1:1000, Cell Signaling Technologies, 2104S) were used in immunoblots.

Cell culture

All cell lines, and primary thymocytes and splenocytes were maintained in RPMI 1640 media (Gibco) supplemented with 100 μg/ml streptomycin, 100 U/ml of penicillin (some media additionally contained 0.25 μg/ml of the anti-mycotic amphotericin B) and 10%

FBS (v/v) (Invitrogen). One exception was that during experiments in which immunoblotting analyses of ER proteins in the supernatants or conditioned media of drug-treated cells were undertaken, the samples were generated in 1% serum instead of 10% serum to minimize background bands from serum proteins. CRT deficient ($CRT^{-/-}$ K42) and WT (K41) mouse embryonic fibroblasts (MEFs) were a kind gift from Dr. Marek Michalak. The CT26 mouse colon cancer cell line was purchased from American Tissue Culture Collection. CRT deficient MEFs expressing wild type or mutant CRT or an expression vector with no inserted gene were generated as described (Del Cid et al., 2010; Jeffery et al., 2011). Human multiple myeloma lines NCI H929 (H929) and RPMI8226 were the kind gift of Dr. Malathi Kandarpa and Andrzej Jakubowiak. Murine thymi from C57BL/6 or BALB/c mice were homogenized with a syringe plunger and cell strainer. Murine spleens were prepared as the thymi, with an additional 2-minute treatment with red cell lysis buffer and subsequent wash before being plated. All cells were maintained at 37^{o} C and 5% CO_2.

For the generation of plasma cells, splenocytes (1.5E6 cells/ml) were cultured for the indicated times in RPMI 1640 supplemented with 10% FBS, penicillin, streptomycin, glutamine, 20 μM 2-ME, 35 ng/ml recombinant murine IL-4, at a 1:10 ratio of CD40L-expressing Sf21 insect cells to splenocytes.

Flow cytometry

For CRT, MHC-I, and ERp57 surface analysis by flow cytometry, cell lines were detached with PBS + 8 mM EDTA, washed in PBS and resuspended in PBS containing 2% FBS (flow cytometry buffer). 1.5-2x10^5 cells were stained in 70 μl flow cytometry buffer containing the respective antibody. For CRT + block stains, the same dilution of chicken anti-CRT was pre-incubated for 15-30 minutes at room temperature with a saturating concentration of peptide (KEQFLDGDAWTNRWVESKHK) corresponding to the sequence in CRT that the antibody was generated against and affinity purified with. Cells were washed two times with flow cytometry buffer, resuspended in 70 μl buffer containing donkey anti-chicken conjugated to PE (1:250) for CRT stains, goat-anti-rabbit-FITC (1:125) for ERp57 stains, or goat-anti-mouse-phycoerythrin (1:250) for MHC-I stains and incubated for 30-60 minutes rocking at 4^{o} C. Cells were then washed

two times. Finally, cells were resuspended in a 1x dilution of AnnV-FITC and 7AAD in AnnV binding buffer (10 mM HEPES (pH 7.4), 140 mM NaCl, and 2.5 mM $CaCl_2$), and

Plasma cells were harvested at the indicated times. Samples were stained with AnnV-FITC and 7AAD as described to monitor progression through apoptosis. Parallel samples were stained with anti-CRT and 7AAD as described, except flow cytometry buffer was made with 2% rabbit serum instead of FBS, in addition to CD138-biotin, followed by streptavidin-APC.

In all cases, data for each sample was collected on a FACSCanto flow cytometer (BD). Analysis was performed using Flowjo 8.8.6 (Treestar Inc.).

Immunoprecipitations

The day before drug treatment, 1-2x10^6 cells were seeded in a 10 cm dish and allowed to grow overnight. The next day, the media was removed and cells were treated with different drugs for 5 hours as described above. Supernatants from each treatment were centrifuged to remove cell debris, transferred to fresh tubes, and incubated overnight with indicated antibodies at 4˚C, with gentle agitation. The following day, samples were centrifuged to remove precipitated proteins, transferred to new tubes and incubated for at least 5 hours with Protein G beads (GE Healthcare). The beads were washed three times with 1 ml of 1% NP-40 in PBS and then boiled in the presence of SDS and DTT. The samples were analyzed by SDS-PAGE and immunoblotting with indicated antibodies. In parallel, cells from each plate were harvested and lysed in triton X-100 lysis buffer (10 mM Na_2HPO_4, 10 mM Tris, 130 mM NaCl, 1% Triton X-100, complete EDTA-free protease inhibitors, pH 7.5) on ice for at least 1 hour, followed by a 30-minute centrifugation at 4^o C to remove cell debris. Protein concentrations of cleared lysates were determined with Pierce bicinchoninic acid (BCA) assay and these lysates were included in the immunoblotting analysis of the immunoprecipitated proteins.

RESULTS

Differential impacts of ER-stress inducing drugs on cell-surface CRT and MHC-I

THP inhibits sarco-endoplasmic reticulum Ca^{2+}-ATPase pumps and causes a reduction in levels of ER calcium (Thastrup et al., 1990). We recently showed that THP treatment of MEFs for short times (5-6 hours) induces cell-surface expression of CRT (Jeffery et al., 2011), as previously shown in neuroblastoma cells (Tufi et al., 2008), and additionally that THP treatment of the MEFs also induced CRT secretion (Jeffery et al., 2011). In the present studies, we asked whether treatment of cells with another drug commonly used to induce ER stress, TUN, would also result in cell-surface and secreted CRT. Additionally, the effect of treating cells with the anthracyclin chemotherapeutic mitoxantrone (MTX) was also tested, as previous studies have suggested that MTX is a strong inducer of cell-surface CRT in pre-apoptotic and apoptotic cells (Obeid et al., 2007b; Panaretakis et al., 2008a; Panaretakis et al., 2009).

We first examined cells subject to short drug exposures, which left the large majority of cells intact. To distinguish the apoptotic population that had exposed PS on the outer leaflet of the plasma membrane (Fadok et al., 1992), annexin-V (AnnV) was used. Furthermore, 7-Aminoactinomycin D (7AAD) was used, which is impermeable to live and early apoptotic cells, but stains late-apoptotic/secondary necrotic cells that have lost membrane integrity. The analyses were initially conducted with fibroblasts derived from wild-type (WT MEFs) or CRT deficient mouse embryos ($CRT^{-/-}$ MEFs) to control for the specificity of antibody binding. Untreated cells, or cells exposed to TUN, THP or MTX for 5-7 hours were triple stained with AnnV-FITC, chicken-anti-CRT followed by anti-chicken-PE, and 7AAD, and analyzed by flow cytometry. As previously shown (Jeffery et al., 2011), in the AnnV(-), 7AAD(-) gate (which comprised 80-90% of cells in all treatment groups (**Fig. 2.1A**)), THP treatment induced a significant enhancement in surface CRT relative to untreated cells (**Fig. 2.1B)**. THP-induced increase in CRT surface staining of treated cells relative to untreated cells was observed in WT MEFs but not in CRT deficient MEFs, demonstrating specific staining for CRT (**Fig. 2.1B**). The THP-

induced increase in CRT stain was also inhibited by pre-treatment of the anti-CRT antibody with the CRT-derived, peptide epitope (peptide block) that had been used as an immunogen for generating the anti-CRT antibody (anti-CRT+block), demonstrating that the staining was specific to the F_{ab} region of the antibody. Consistent with a previously published study by Obeid et al. (Obeid et al., 2007b), TUN did not induce surface CRT expression in viable cells. In contrast with the same study, however, we saw little pre-apoptotic induction of surface CRT in response to short MTX treatments relative to the CRT up-regulation induced by short THP treatments of cells (**Fig. 2.1B**).

Figure 2.1 A specific form of ER stress induces cell-surface CRT.
Cell death profiles (A and C) and surface CRT expression profiles (B and D) of different treatment conditions were analyzed by flow cytometry. WT or CRT deficient ($CRT^{-/-}$) MEFs were incubated in 5 μM THP (THP), 1 μM MTX (MTX), 10 μg/ml TUN (TUN), or media alone (UNT) for 5-7 hours (A-B) or 17 hours (C-D). Cells were then stained with anti-CRT (anti-CRT), anti-CRT pre-incubated with the CRT-derived peptide used as the immunogen and used to affinity purify the antibody (anti-CRT+block), or secondary antibody alone (control). All cells were also stained with AnnV and 7AAD and analyzed by flow cytometry. The median fluorescence values of anti-CRT staining of treated cells were measured for the AnnV(-)7AAD(-) (B and D as indicated) or the AnnV(+)7AAD(-) populations (D as indicated) and plotted as a ratio relative to the median fluorescence of AnnV(-)7AAD(-), untreated cells stained under the same condition (B and D). In B, inset shows representative histogram overlays of untreated (UNT, (fill)) or THP-treated (THP (dashed)) CT26 cells stained with anti-CRT antibody. THP-treated cells were stained in the presence (block (line)) or absence (THP (dashed)) of the peptide block. (A and C) Percentage of cells in the AnnV(-)/7AAD(-) (viable/pre-apoptotic), AnnV(+)/7AAD(-) (early apoptotic) and AnnV(+)/7AAD(+) (late apoptotic/secondary necrotic) populations are shown. Graphs show averages of 5-10 (A), 5-7 (B), 3-5 (C), or 2-3 (D) experiments. The p-values from two-tailed, paired t-tests are indicated.

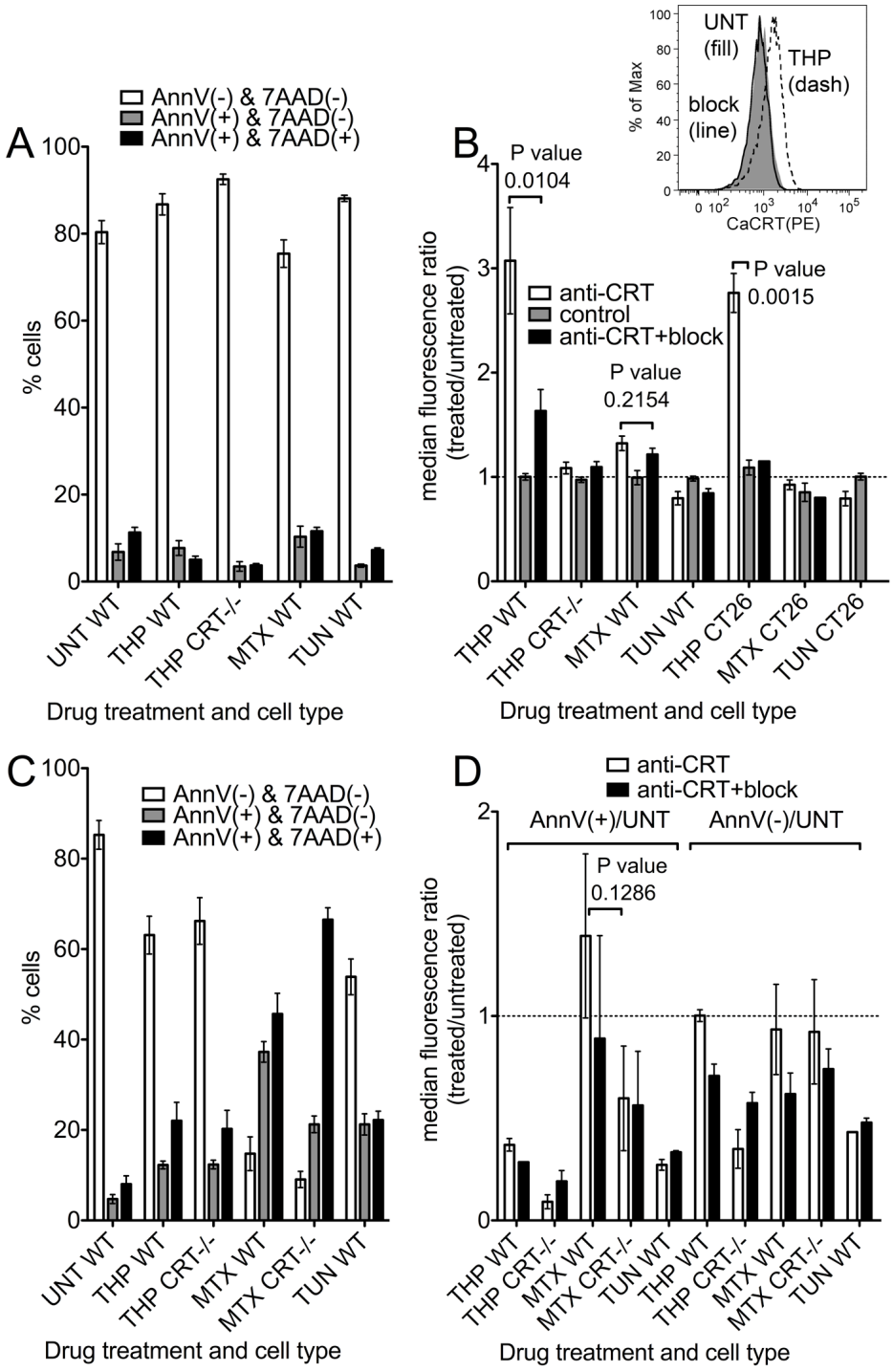

Because of the contrast of our data with the findings presented by Obeid et al. (Obeid et al., 2007b), we measured changes in surface CRT levels in the CT26 mouse colon cancer cell line used in that study. The strong induction of cell-surface CRT seen in

THP-treated WT MEFs was also seen in CT26 cells. In contrast, MTX-treatment did not expose surface CRT in CT26 cells, similar to the results obtained with WT MEFs (**Fig. 2.1B**). It is possible that expression of cell-surface CRT in MTX–treated cells occurs with different kinetics than those in THP-treated cells, or in cells that are at a different stage of cell death. To examine impacts of longer time-points of each drug treatment upon surface CRT induction, we next examined cells treated with each drug for 17 hours, which induced approximately 2-5 times more apoptotic cells (**Fig. 2.1C**). This allowed us to compare surface CRT levels on AnnV+ apoptotic cells and AnnV(-) pre-apoptotic cells to those on viable, AnnV(-), untreated cells (**Fig. 2.1D**). None of the long drug treatments induced a significant increase in CRT staining in apoptotic or pre-apoptotic MEFs although the MTX-treated, apoptotic cells had a trend suggesting a slight up-regulation of surface CRT relative to viable, untreated cells (**Fig. 2.1D**).

The interpretation of some of the data presented in Figure 2.1D may be complicated by the fact that apoptotic cells are smaller than viable cells (**Fig. 2.2A**). To further examine this point, we compared the level of surface CRT staining in the presence or absence of the anti-CRT peptide block within a given viable or apoptotic cell population (**Fig. 2.2B-C**). Figures 2.2B-C include some of the same data shown in Figure 2.1B and D, but analyzed differently as described. We also sought to further characterize the ability of the drug treatments to induce cell-surface CRT expression in other cell types. Therefore, we analyzed experiments performed with additional cell types using the anti-CRT/anti-CRT+block ratio (**Fig. 2.2B-C & 2.3**). These analysis showed similar trends of induction in AnnV(-) cells as measured in Figure 2.1B. Interestingly, MTX-treated AnnV(-) cells had slightly higher levels of CRT than untreated AnnV(-) WT MEFs. This difference was statistically significant, and specific to the WT MEFs (**Fig. 2.2B**). These data analyses also confirmed that apoptotic cells resulting from long THP treatments do not have elevated levels of cell surface CRT, suggesting that the association of CRT with the cell surface is transient or unstable (**Fig. 2.2C**).

Figure 2.2 Impacts of cell size, cell type and drug treatment on surface CRT expression and detection.
(A) Representative forward scatter (FSC-A) and side-scatter (SSC-A) density plot of MTX-treated apoptotic WT MEFs showing the gating of larger, higher forward scatter cells and smaller, lower forward scatter cells which are AnnV low (larger cells represented by the grey filled peak) and high (smaller cells represented by the black line), respectively, in the adjacent AnnV histogram overlay. (B-C) Graphs show cell surface CRT expression of indicated cell types subjected to the indicated treatments for short (B) or long (C) time points unless described otherwise. Levels of cell surface CRT are represented here by the median fluorescence of the anti-CRT stain relative to that of the anti-CRT+block stain. WT MEF, CRT-/- MEF and CT26 bars show data from Figure 2.1 (with the exception of CT26 long time point/AnnV+ data not shown in Figure 2.1D which is shown here) re-analyzed in this graph as the CRT/CRT+block ratio for a given cell population. Drug treatment times for the data not shown in Figure 2.1 were (B and C) THP (H929 & RPMI8226), 4.5 or 6 hrs and (C) TUN (CT26) 17 hrs, THP (CT26) 17 or 21 hrs, MTX (CT26) 14-21 hrs, MTX (Splenocytes and thymocytes), 7-15 hrs. The average cell death profiles (AnnV&7AAD double negative/AnnV single positive) and n values for cell types not described in Figure 2.1 were: (B and C) H929 (n=2) UNT-82/3.6, THP-56/25; RPMI8226 (n=2) UNT-63/4.3, THP-51/10; (B) splenocytes UNT-58/16.5 (n=5); thymocytes UNT-72/17.9 (n=11) (C) CT26, UNT 94/0.5 (n=4), TUN 93/0.3 (n=1), MTX 68/2.9 (n=3), THP 76/4.3 (n=2); Splenocytes MTX-14.4/17.8 (n=4); thymocytes MTX-7.3/62 (n=7). Unless indicated otherwise, long drug treatments analyzed the combination of non-adherent and adherent cells and short drug treatments analyzed adherent cells only. RPMI8226 & H929 are naturally non-adherent cells. (C) In one experiment, only adherent CT26 cells were analyzed following a 14-hour MTX treatment. The p-values from two-tailed, paired t-tests are indicated.

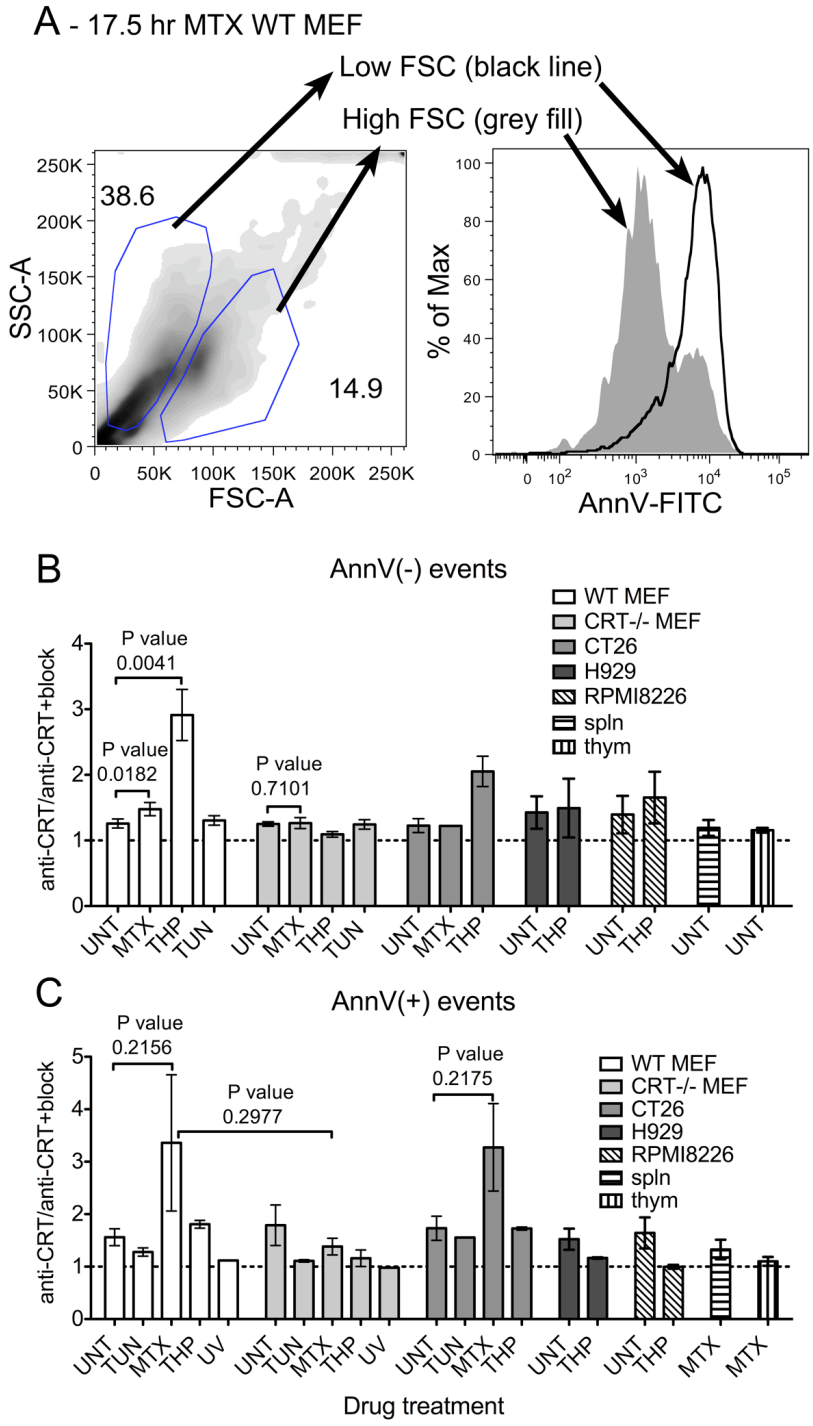
A - 17.5 hr MTX WT MEF
Low FSC (black line)
High FSC (grey fill)
38.6
14.9
SSC-A
FSC-A
% of Max
AnnV-FITC
B
AnnV(-) events
WT MEF
CRT-/- MEF
CT26
H929
RPMI8226
spln
thym
P value 0.0041
P value 0.0182
P value 0.7101
anti-CRT/anti-CRT+block
UNT
MTX
THP
TUN
C
AnnV(+) events
P value 0.2156
P value 0.2977
P value 0.2175
UV
Drug treatment

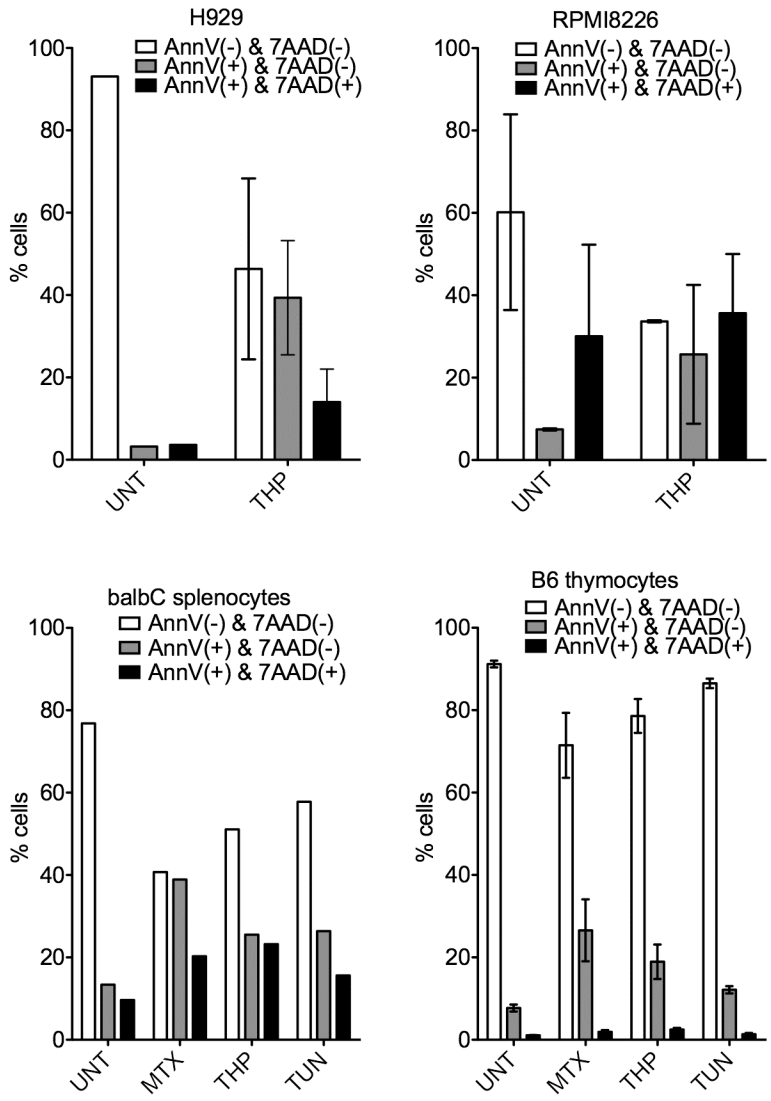

Figure 2.3 Cytotoxicity of MTX, TUN & THP on various additional cell types.
The indicated cell lines were treated and stained as in Figure 2.1 and 2.2 with data from slightly altered time points averaged together in the graphs. Times of drug treatments for separate experiments include: C57BL/6J (B6) thymocytes 2.3, 5.3 or 6.3 hrs (n=3, average shown), and BALB/cJ (balbC) spleens 5.75 hrs (n=1), multiple myelomas RPMI8226 4.5 or 6 hrs (n=2) and H929 4.5 or 8.5 hrs (n=1).

Consistent with the data analyses from Figure 2.1D, the analyses of Figure 2.2C suggest that apoptotic cells resulting from longer MTX treatments have elevated levels of CRT, although the differences did not achieve statistical significance. Overall, it appears that MTX-induced surface CRT is lower in AnnV(-) cells at early time points relative to

that induced by THP, and quite variable in AnnV(+) cells at later time points. Additionally, whereas THP-induced CRT surface expression was observable in WT MEFs and CT26 cells following short time points of drug treatment, similar treatments of other cell types including primary murine splenocytes, thymocytes, and other cancer cell lines did not strongly induce cell-surface CRT **(Fig. 2.2B-C**). It is possible that the cancer cell lines display cell surface CRT in the absence of drug treatments as recently suggested (Chao et al., 2010), which could account for the lower levels of THP-induced surface CRT (**Fig. 2.2B-C**). However, it should be noted that the various cell types differed in their susceptibility to each drug's cytotoxicity (**Fig. 2.3**). Further investigations will be needed to understand the cell type specific effects of THP treatments on cell-surface CRT induction.

To examine how the different drug treatments affect surface expression of other proteins, we measured surface expression of MHC class I, a protein that is constitutively expressed on the cell surface of most cell types under normal cellular conditions (**Fig. 2.4A-B**). As previously described (Jeffery et al., 2011), short THP treatments reduced cell-surface MHC class I. TUN treatment also resulted in consistent decreases in cell-surface MHC-I, whereas MTX treatment did not decrease surface MHC class I (**Fig. 2.4A-B**). TUN treatment resulted in an average decrease of 36, 48 and 39% in CRT deficient MEFs, WT MEFs (H-2K^{b}) and CT-26 cells (H-2D^{d}), respectively (**Fig. 2.4A-B**). The average decrease in MHC-I in response to THP was less: 26, 39 and 18% in CRT deficient MEFs, WT MEFs (H-2K^{b}) and CT-26 cells (H-2D^{d}), respectively (**Fig. 2.4A-B**). As noted, two different MHC-I haplotypes responded with the same trend. Consistent with the decrease on the cell surface, both TUN and THP decreased total cellular MHC-I heavy chain levels in cell lysates (note that deglycosylation by TUN induces a significant mobility shift of the MHC-I heavy chain, indicated by *d.g.) (**Fig. 2.4C**). However, in contrast with the relative effects of the two drugs on cell surface MHC-I, THP more dramatically reduced levels of total cellular MHC-I heavy chains (**Fig. 2.4C**).

Figure 2.4 TUN and THP, but not MTX, decrease surface and total expression of MHC-I.

Flow cytometric analyses of MHC class I cell-surface expression were conducted following different treatments of cells. (A) WT or CRT-/- MEFs or (B) CT26 mouse tumor cells were treated as in Fig. 2.1A-B. Cells were then stained with indicated anti-MHC-I antibodies or secondary antibody alone (control). All cells were also stained with AnnV and 7AAD and analyzed by flow cytometry. The AnnV(-)7AAD(-) populations were analyzed in all cases. Graphs show averages of 3 experiments. The p-values from two-tailed, paired t-tests are indicated. (C) Anti-MHC-I heavy chain immunoblot of lysates from cells treated as in A-B. MHC-I heavy chains (*MHC-I H.C.), d.g.=deglycosylated.

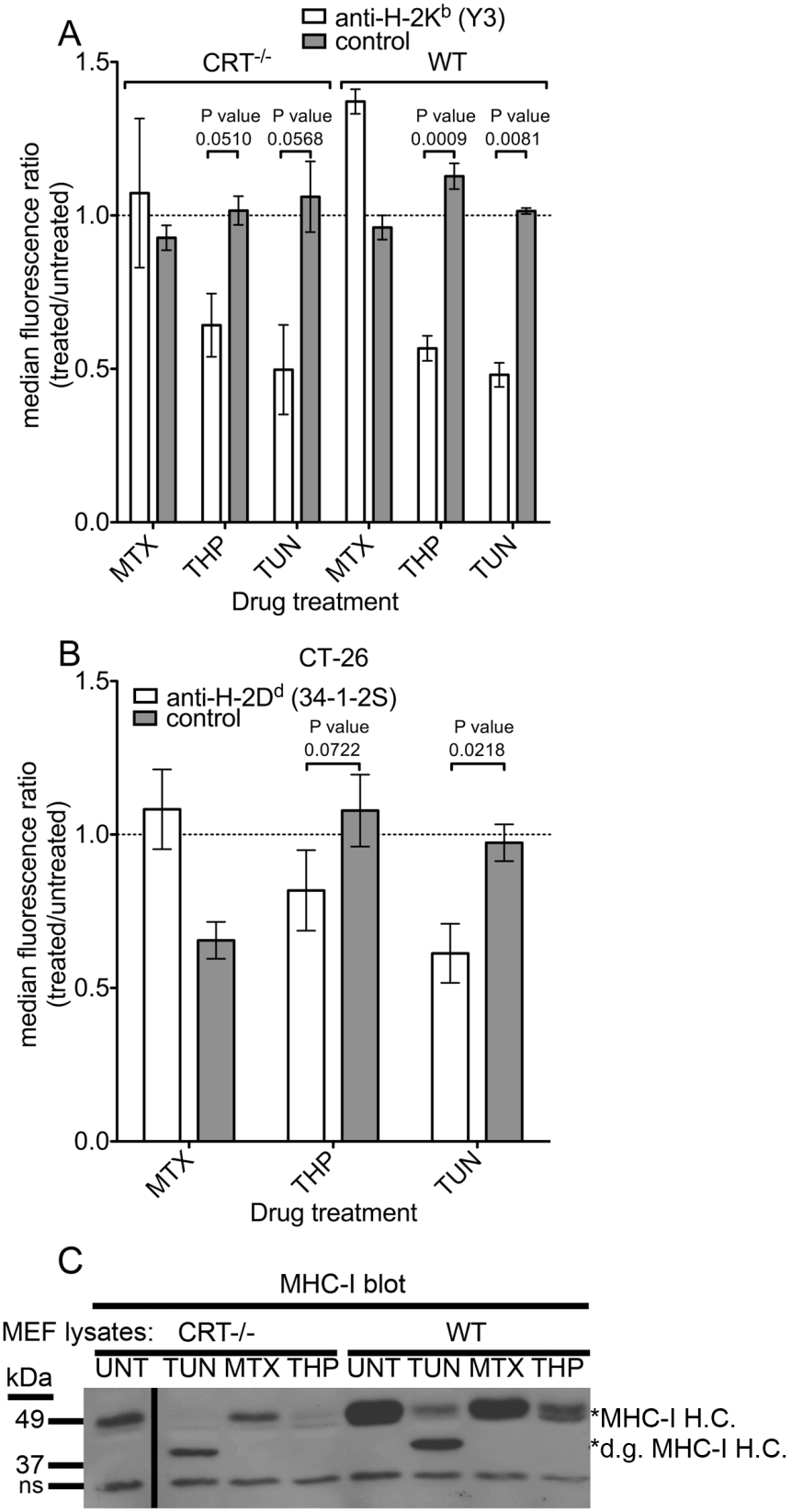
A
anti-H-2K^b (Y3)
control
CRT$^{-/-}$
WT
P value 0.0510
P value 0.0568
P value 0.0009
P value 0.0081
median fluorescence ratio (treated/untreated)
1.5
1.0
0.5
0.0
MTX
THP
TUN
MTX
THP
TUN
Drug treatment
B
CT-26
anti-H-2D^d (34-1-2S)
control
P value 0.0722
P value 0.0218
median fluorescence ratio (treated/untreated)
1.5
1.0
0.5
0.0
MTX
THP
TUN
Drug treatment
C
MHC-I blot
MEF lysates: CRT-/-
WT
UNT TUN MTX THP UNT TUN MTX THP
kDa
49
37
ns
*MHC-I H.C.
*d.g. MHC-I H.C.

Consistent with these analysis, MHC-I was recently shown to be significantly decreased on human thyrocytes following longer exposures to TUN or THP (Ulianich et al., 2011). Furthermore, MHC-I was significantly decreased on mouse cells subject to two different non-pharmacological ER stresses: exposure of cells to the saturated fatty acid palmitate, or glucose deprivation of cells (Granados et al., 2009). Thus, the ER stress inducing drugs differentially impact surface expression of cellular proteins. Both reduce surface expression of MHC class I, a constitutively secreted cell-surface protein, whereas only THP treatment induces the cell-surface expression of CRT at early time points post-treatment. Based on these results, we conclude that cell surface expression of various proteins in the secretory pathway is differentially effected by different ER stress stimuli.

Several ER resident proteins are released in THP but not TUN-treated cells

We examined secretion of ER resident proteins in response to 5-hour treatments of WT MEFs with different drugs. Supernatants from the different drug-treated cells were separated by SDS-PAGE and immunoblotting analyses were performed with antibodies directed against gp96 and PDI. In addition, as neither CRT nor BiP were detectable by direct immunoblotting analyses, proteins present in supernatants were immunoprecipitated with antibodies against CRT and BiP, followed by immunoblotting analyses to detect those proteins. THP, but not TUN or MTX induced secretion of at least four proteins that are normally retained within the ER: CRT, gp96, PDI and BiP (**Fig. 2.5A**). Although depletion of ER calcium is expected to occur almost immediately following THP treatment (Thastrup et al., 1990), THP-induced secretion of ER chaperones was not detectable at 1.25 or 2.5 hours following THP treatment (**Fig. 2.5C**). These findings suggest that ER calcium depletion alone is insufficient to induce a detectable loss of ER retention of chaperones. Previous studies with other cell types indicate that BiP (Okada et al., 2003; Winnay et al., 2010) and CRT (Llewellyn et al., 1996; Waser et al., 1997) mRNA levels are upregulated following 2-5 hours of TUN and THP treatment and that BiP protein levels are increased within 5 hours of TUN treatment (Winnay et al., 2010). Consistent with these UPR induction kinetics, an examination of

changes in BiP and CRT protein levels revealed small increases in CRT and BiP expression at 3 hours, and stronger induction 5 hours post-TUN treatment (**Fig. 2.5D**). Over the same time-frame, THP treatment decreased the levels of cellular CRT and BiP, with stronger reduction seen at 5 hours compared to 3 hours (**Fig. 2.5D**). This is consistent with the observed increases in ER chaperone secretion during this time-frame (**Fig. 2.5C**). Therefore, the increase in expression of ER chaperones in response to TUN and THP is not sufficient to induce detectable secretion of ER chaperones. Taken together, these findings suggest that both depletion of ER calcium and increases in ER chaperone expression are required for chaperones to escape ER retention in THP-treated cells.

Figure 2.5 Various ER chaperones are released from THP-treated fibroblasts
(A) Immunoblotting of cell supernatants and lysates for the presence of various ER chaperones. Supernatants (CM1) from cells treated with TUN, MTX or THP or untreated cells were harvested in parallel with the corresponding cell lysates. Direct immunoblotting analyses of each fraction were performed for PDI and gp96. For CRT and BiP, proteins in cell supernatants were first immunoprecipitated (IP) with anti-CRT or anti-BiP, prior to immunoblotting analyses. (B) Kinetics of PDI and gp96 secretion. Analyses were performed as in A, but immunoblotting analyses were undertaken at the indicated time points. (C) Kinetics and magnitude of BiP and CRT induction in response to TUN & THP. Indicated microgram amounts of total cell lysates were analyzed as in A at the indicated time-points post-drug treatments. Representative blots of 3-4 experiments are shown in A. Data are based on (B) 1 experiment and (C) 1 experiment shown, representative of 2 total experiments (A) Approximately 8500 cells per lane contributed to the CM1 used to blot for PDI and gp96. The blots of corresponding lysates show approximately 30,000 cells worth of lysate. (A-C) Vertical black lines in blots indicate places where lanes of the blot were re-arranged to match the labeling scheme used in adjacent immunoblots or to digitally remove lanes containing size standard (relevant bands from size standard are shown digitally for each blot).

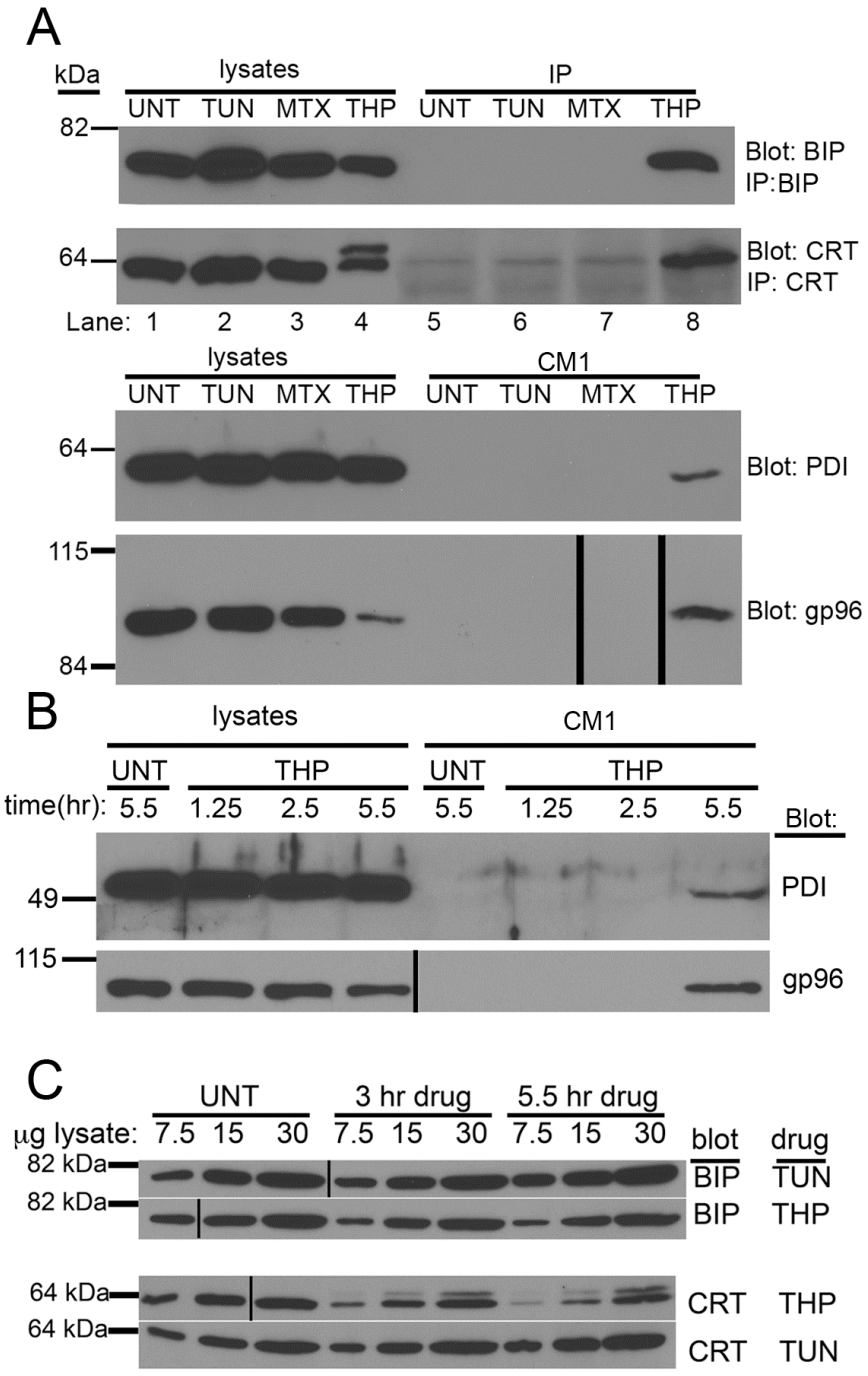
A
kDa
lysates
IP
UNT TUN MTX THP UNT TUN MTX THP
82
Blot: BIP
IP:BIP
64
Blot: CRT
IP: CRT
Lane: 1 2 3 4 5 6 7 8
lysates
CM1
UNT TUN MTX THP UNT TUN MTX THP
64
Blot: PDI
115
84
Blot: gp96
B
lysates
CM1
UNT THP UNT THP
time(hr): 5.5 1.25 2.5 5.5 5.5 1.25 2.5 5.5
Blot:
49
PDI
115
gp96
C
UNT
3 hr drug
5.5 hr drug
μg lysate: 7.5 15 30 7.5 15 30 7.5 15 30
blot
drug
82 kDa
BIP
TUN
82 kDa
BIP
THP
64 kDa
CRT
THP
64 kDa
CRT
TUN

In THP-treated cells, ER chaperones follow the secretory route to gain access to the extracellular compartment

As previously described (Rizvi et al., 2004), analysis of cell lysate-derived CRT by immunoblotting revealed that THP treatment of cells induced CRT glycosylation (**Fig. 2.5A**, CRT blot, lane 4) in a subset of CRT molecules present in the cell. The glycosylation site of CRT appears to be buried under normal conditions, but becomes partly exposed under calcium-depleting conditions (Jeffery et al., 2011). It was of note that the glycosylated CRT species was absent from cell supernatants, suggesting that the glycosylated form of CRT was either ER retained, or preferentially retained on the cell surface (**Fig. 2.5A**) (Jeffery et al., 2011).

Since CRT glycosylation is partial and induced by specific cellular conditions, we assessed the glycosylation status of gp96, a constitutively glycosylated protein, in order to further understand the cellular exit route for ER chaperones in THP-treated cells. A cytosolic route has recently been described for CRT release from apoptotic cells (Tarr et al., 2010). Since cytosolic localization of proteins induces their de-glycosylation, we assessed the glycosylation status of extracellular gp96 in order to further understand whether a secretory or cytosolic route was used in the trafficking of gp96 (and by inference, other ER proteins) to the extracellular space in THP-treated cells. Previous findings indicate that gp96 secreted in response to cellular calcium perturbation exits the cell through the secretory pathway and becomes differentially glycosylated as it travels through the Golgi (Booth and Koch, 1989). Consistent with these findings, gp96 from cell supernatants migrated more slowly than gp96 in cell lysates (**Fig. 2.6A**). When supernatants from THP-treated cells were digested with Peptide:N-Glycosidase F (PNGase F), which cleaves carbohydrate residues from glycoproteins, and analyzed by immunoblotting with an anti-gp96 antibody, a decrease in molecular weight was observed, indicating that secreted gp96 is indeed glycosylated (**Fig. 2.6B,** gp96 blot, lanes 8 and 9). Finally, the induction of cell-surface CRT in response to THP was reduced when the cells were pre-treated with brefeldin-A (BFA), which blocks ER-Golgi trafficking (**Fig. 2.6C**). Together, these findings indicate that THP treatment of cells

perturbs normal ER retention mechanisms, and that ER proteins exit the cell via a secretory route in response to THP treatment.

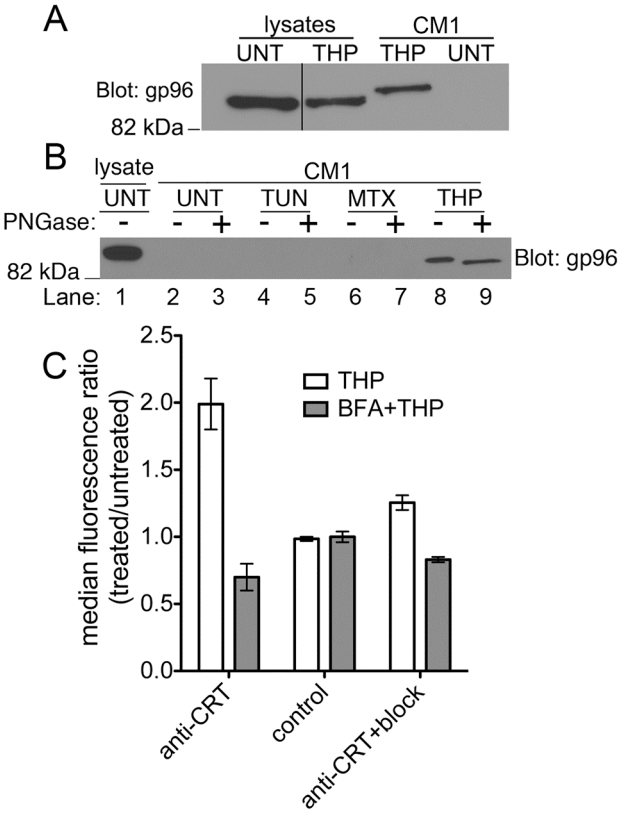

Figure 2.6 Release of ER chaperones from THP-treated cells involves the secretory pathway.

(A and B) Immunoblotting analyses with anti-gp96 of supernatants (CM1) and lysates from THP-treated or untreated cells to analyze the presence of glycosylated forms of gp96 in cell supernatants following THP treatment. (A) For this immunoblot, SDS-PAGE-based protein separation was undertaken on an 8% polyacrylamide gel, and separation optimized compared to that shown in 3A, to allow for resolution of different forms of gp96. The supernatant sample (CM1) was also run adjacent to the lysate sample to better resolve alterations in electrophoretic mobility resulting from post-translational modifications. The vertical black line in the gp96 blot denotes lanes that were cut and pasted from the same blot. B) Indicated cell supernatant samples were first digested with Peptide:N-Glycosidase F (+) or left undigested (-), prior to the immunoblotting analyses. C) BFA blockade of the secretory pathway inhibits THP-induced surface CRT expression. Cells were pre-treated with BFA for 45 minutes followed by addition of THP for 6-7 hours. Cells were harvested and surface CRT expression was measured in the AnnV(-) and 7AAD(-) population by flow cytometry as described. Graph shows ratio of surface CRT median fluorescence of BFA+THP-treated/untreated cells. The blot shown in B is representative of 3 experiments and the data in C are the average of 2 experiments.

CRT surface expression in response to THP is independent of ERp57 co-translocation

The data of Figure 2.5A indicate that THP-treatment does not result in a specific release of CRT, but rather in a generalized loss of ER retention of various ER proteins. This mechanism of CRT release from the ER is distinct from that suggested for anthracyclin-induced CRT surface expression, where the specific co-translocation of CRT-ERp57 complexes was indicated (Obeid, 2008; Panaretakis et al., 2008a). In the ER, CRT and ERp57 interact via the P-domain of CRT, and amino acid W244 within the P-domain of CRT is important for binding to ERp57 (Del Cid et al., 2010; Frickel et al., 2002; Martin et al., 2006). To test the requirement for ERp57 co-translocation for CRT surface expression, we first measured ERp57 surface expression under the conditions that we detected surface CRT. A rabbit-anti-ERp57 antibody (used in the published work characterizing anthracyclin-induced CRT:ERp57 complex surface expression (Obeid, 2008; Panaretakis et al., 2008b)) did not detect cell-surface ERp57 in THP-treated CT-26 tumor cells, or in WT or CRT deficient MEFs (**Fig. 2.7B**). To further test the requirement of the CRT:ERp57 interaction for CRT surface expression in THP-treated cells, wild-type CRT, or CRT mutants unable to bind to ERp57 (Del Cid et al., 2010) (a W244A point mutant and a delta P (ΔP) truncation mutant lacking the P-domain) were expressed in CRT deficient MEFs using retroviral infections. Both mutant CRT proteins were induced on the cell surface in response to THP treatment at levels that correlated with their total expression in the lysates (**Fig. 2.7B**), rather than with their abilities to interact with ERp57 (**Fig. 2.7C**). Thus, CRT does not require association with ERp57 to be expressed on the cell surface in response to ER calcium depletion. Whether ERp57 is present in supernatants of THP-treated cells is unclear as ERp57 was not detectable in cell supernatants by immunoblotting analyses (data not shown); however ERp57 migrates in close proximity to background bands present in the cell supernatants, and low levels of secreted ERp57 may be masked by the background signals.

Figure 2.7 THP-induced surface CRT expression is independent of CRT-ERp57 binding.

(A) Flow cytometric assessments of surface ERp57 expression. CT26 mouse colon cancer cells, WT MEFs or CRT-/- MEFs were treated with 5 μM THP for 5-7 hours, and stained with the indicated primary antibody (anti-CRT or anti-ERp57) and/or the respective secondary antibodies (control–secondary antibody alone). Anti-CRT-stained cells were additionally stained with AnnV and 7AAD and anti-ERp57 stained cells were stained with PI. Cells were analyzed by flow cytometry and the median fluorescence of treated cells relative to untreated cells is shown for the respective AnnV(-)7AAD(-), or PI (-) populations. The surface CRT data in (A) are the same as those shown in Fig. 2.1, shown again in this figure as a comparison to ERp57 surface expression (B) Immunoblotting analyses of lysates from CRT-/- MEFs infected with retroviruses encoding wild CRT (WT), a CRT construct lacking the P-domain (ΔP), a CRT point mutant that is unable to interact with ERp57 (W244A), or a virus lacking CRT (vec). (C) Flow cytometric analysis measuring cell-surface CRT before and after THP treatment of the MEFs described in B. Representative blots of 3-4 experiments are shown in B. Flow cytometric data are the averages of (A) 6-8 (MEFs) and 4 (CT26) experiments for anti-CRT stains and 2-4 experiments for anti-ERp57 stains or (C) 3-5 experiments. The p-values from two-tailed, paired t-tests are indicated.

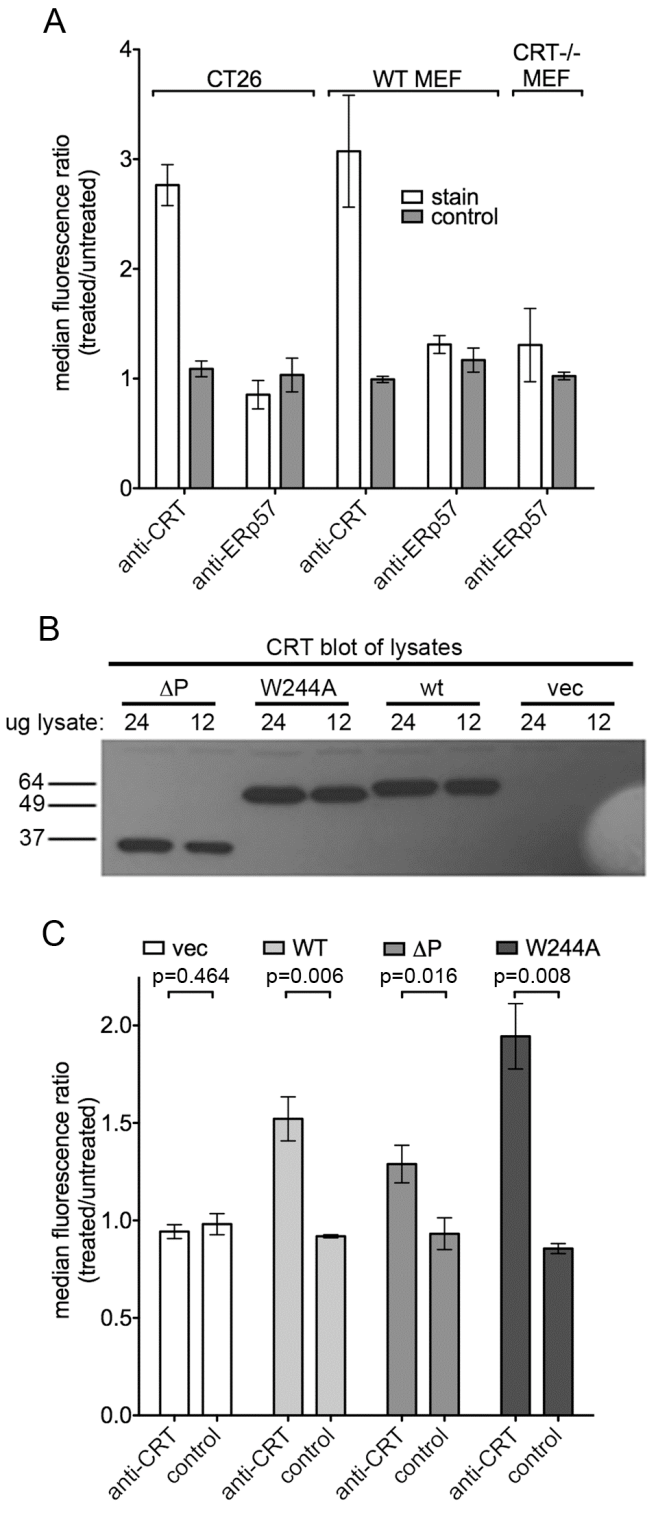
A
CT26
WT MEF
CRT-/-
MEF
median fluorescence ratio
(treated/untreated)
stain
control
anti-CRT
anti-ERp57
anti-CRT
anti-ERp57
anti-ERp57
B
CRT blot of lysates
ΔP
W244A
wt
vec
ug lysate:
24
12
64
49
37
C
vec
WT
ΔP
W244A
p=0.464
p=0.006
p=0.016
p=0.008
median fluorescence ratio
(treated/untreated)
anti-CRT
control

Polypeptide-based interactions contribute to CRT binding to the cell surface of ER calcium-depleted fibroblasts

We next asked what types of protein:protein interactions were used by CRT to bind to the cell surface. As an ER chaperone, CRT binds and promotes folding of immature glycoproteins in the ER. CRT recognizes and binds immature glycoproteins by a single, terminal glucose molecule found on the carbohydrate moiety $Glc_1Man_9GlcNAc_2$ (Glc=Glucose, Man=Mannose, GlcNAc = *N*-Acetyl Glucosamine). The terminal glucose is removed from a secretory protein following its proper folding and prior to ER exit. Glycan-mediated binding of CRT to protein clients or co-chaperones could allow for the co-trafficking of protein-CRT complexes through the secretory pathway, preventing Golgi glycosidase access to substrate glycans. Wiest et al. suggested this model for surface expression of CNX in immature thymocytes, where calnexin molecules traffic to the thymocyte surface in complex with glycosylated CD3 molecules (Wiest et al., 1997). In addition to glycan-based binding, CRT displays direct polypeptide-based binding under ER stress conditions including calcium depletion and heat shock (Rizvi et al., 2004). In response to ER stress, CRT also demonstrates an ability to bind and prevent aggregation of several non-glycosylated protein substrates *in vitro* (Mancino et al., 2002; Saito et al., 1999). Therefore, generic polypeptide binding sites of CRT could become relevant to CRT-protein interactions in ER-calcium-depleted cells.

To examine whether CRT was binding to cell-surface proteins via its glycan or generic polypeptide binding sites, we expressed CRT mutants with various defects in their protein binding abilities in $CRT^{-/-}$ MEFs. The cell-surface expression and secretion of these CRT mutants was measured in the various THP-treated, $CRT^{-/-}$ MEFs. Tested mutants included those with the lowest (mCRT(L139A)) or highest (mCRT(H153A)) polypeptide-specific chaperone activities, a glycan binding-deficient mCRT(W302A) mutant, and a mutant designated mCRT(VLI) mutant. The mCRT(VLI) triple mutant has the same L139A mutation as mCRT(L139A), but also has V138A and I140A mutations, resulting in lower conformational stability than mCRT(L139A) (Jeffery et al., 2011). Therefore, comparing mCRT(L139A) to mCRT(VLI) assessed the relative contributions of site specificity and conformational effects in the observed phenotypes. We found that,

compared with mCRT(WT), the conformationally stable mCRT(L139A) was strongly impaired in its cell-surface expression after THP treatment of cells (**Fig. 2.8, A and E**). Surface expression of the triple mutant, mCRT(VLI), was significantly enhanced relative to mCRT(L139A). These findings indicate the conformational stability of mCRT(L139A), rather than a direct involvement of leucine 139 in cell-surface protein binding, contributes to the low cell-surface expression of mCRT(L139A) in THP-treated cells (**Fig. 2.8, B and E**). Mutant mCRT(H153A) was found at higher levels on the cell surface than mCRT(WT) within individual experimental comparisons undertaken (e.g., that shown in **Fig. 2.8C**), although the difference did not achieve significance when averaged values were compiled (**Fig. 2.8E**). Furthermore, mCRT(L139A) was secreted in response to THP, generally at higher levels than other mutants that were detected on the surface. This strongly implicates CRT's polypeptide binding function in its ability to bind to the cell surface (Jeffery et al., 2011).

Proper folding and subsequent ER exit of glycoprotein clients en route to the cell surface normally results in removal of monoglucosylated carbohydrate moities, the primary protein client targeting mechanism used by CRT. However, during THP-induced ER stress and calcium depletion, it is possible that the normal glycoprotein folding checkpoints, namely UDP-glucose:glycoprotein glucosyltransferase's (UGGT) recognition of an incompletely folded substrate, fail. Additionally, co-trafficking of CRT-client complexes through the Golgi could protect monoglucosylated glycans from cleavage in the Golgi and result in cell-surface expression of glycoproteins containing monoglucosylated glycans bound by CRT. As noted above, this model was previously proposed for binding of the CRT homolog, calnexin, to the immature thymocyte cell surface (Wiest et al., 1997). It appears, however, that glycan-mediated binding is not relevant to CRT's cell surface expression after ER calcium depletion, as mCRT(W302A), which is deficient in glycan binding (Del Cid et al., 2010), displayed cell-surface expression at a level similar to that of mCRT(WT) (**Fig. 2.8, D and E**). Together, these findings indicate that the cell-surface expression of mCRT in THP-treated cells is dependent on its polypeptide-receptive conformation (**Fig. 2.8E**).

Figure 2.8 Polypeptide-based interactions contribute to CRT binding to the cell surface of ER calcium-depleted fibroblasts.
(A–D) representative histograms show THP-induced cell-surface CRT in K42 cells expressing mCRT(WT) or indicated mutants. Analyses were performed as described in Fig. 2.1. (E) Results are averaged across 2-4 independent analyses for each mutant. MFI indicates mean fluorescence intensity. NS indicates not significant. ** Indicates $p<0.01$. *** Indicates $p<0.001$. All p values were generated using a two-tailed, unpaired t test. PE=Phycoerythrin. Elise Jeffery performed these experiments. Figure taken from Jeffery, E., Peters, L.R., and Raghavan, M. (2011). The polypeptide binding conformation of calreticulin facilitates its cell-surface expression under conditions of endoplasmic reticulum stress. J Biol Chem 286, 2402-2415.

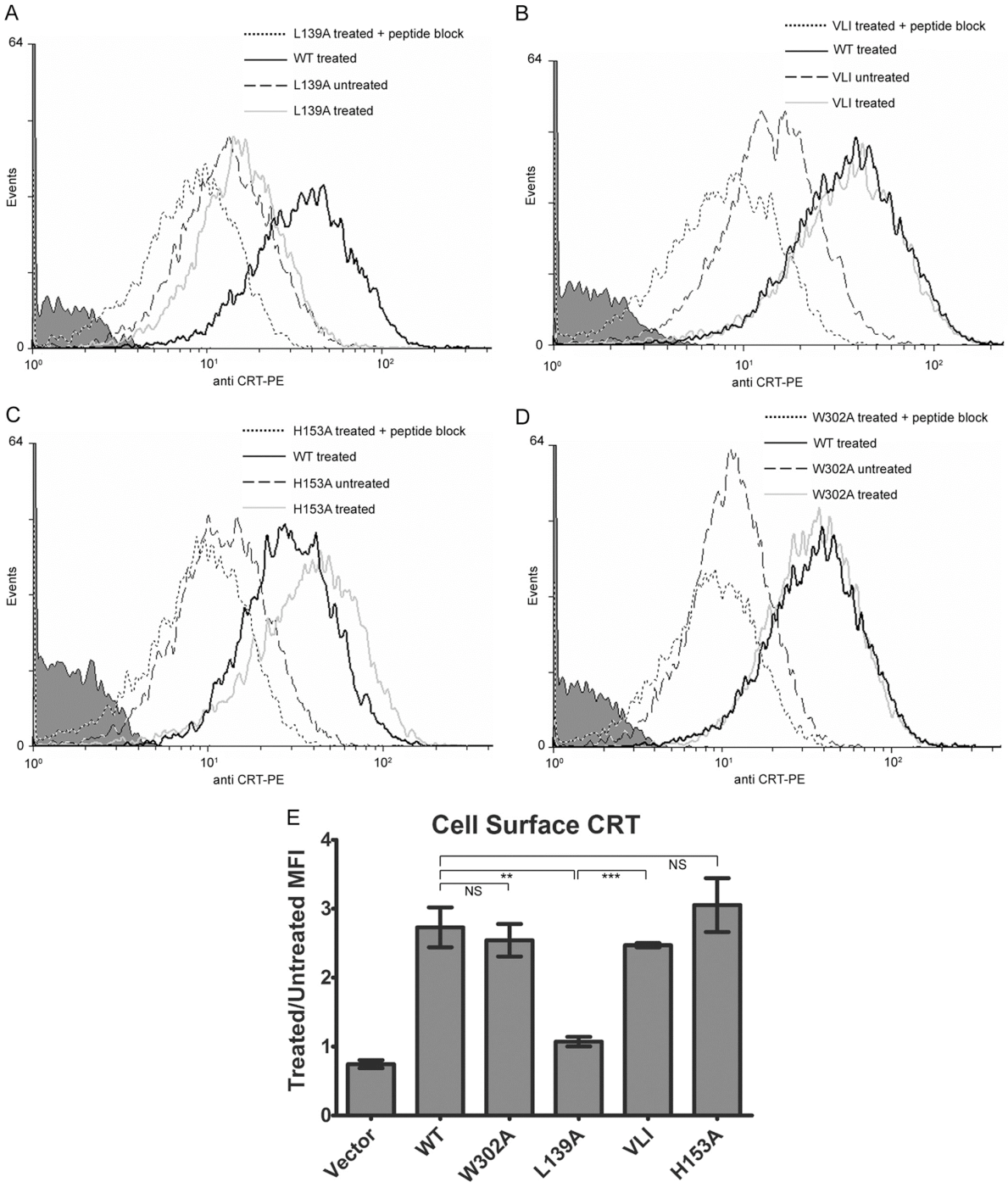
A
L139A treated + peptide block
WT treated
L139A untreated
L139A treated
Events
anti CRT-PE
B
VLI treated + peptide block
WT treated
VLI untreated
VLI treated
C
H153A treated + peptide block
WT treated
H153A untreated
H153A treated
D
W302A treated + peptide block
WT treated
W302A untreated
W302A treated
E
Cell Surface CRT
Treated/Untreated MFI
NS
**
***
Vector
WT
W302A
L139A
VLI
H153A

Surface CRT is not upregulated during plasma cell differentiation, but is elevated on apoptotic plasma cells, unlike other primary apoptotic cells

As a model of physiological ER stress, we examined levels of cell surface CRT on plasma cells. Plasma cells are highly secretory and are under constitutive ER stress (reviewed in (Todd et al., 2008)). The UPR-activated transcription factor Xbp-1 is required for plasma cell differentiation (Reimold et al., 2001). Stimuli often used *in vitro* to induce plasma cell differentiation include LPS and CD40L+IL4 treatments of splenocytes. The spliced form of *Xbp1* mRNA, which encodes the active Xbp1 protein, is detected following 48 hours of CD40L+IL4 treatment of splenocytes and is increased following 72 hours of CD40L+IL4 treatment, which correlates with maturation of plasma cells (Iwakoshi et al., 2003). Thus, we IL-4 treated splenocytes co-cultured with CD40L expressing insect cells to induce plasma cell differentiation. Plasma cells in the splenocytes culture were measured by the plasma-cell specific marker, CD138/syndecan-1 (**Fig. 2.9A**). The percentage of plasma cells in the culture was maximal following 3 and 4 days of stimulation at which point ~10-40% of the cells were non-apoptotic (**Fig. 2.9A-B**). For technical reasons, the simultaneous AnnV stains of the CRT-stained plasma cells were not performed. However, upon exposing phosphatidylserine (widely used as criteria to classify a cell as apoptotic) cells show a significant and almost discrete shift from a higher FSC, higher SSC profile (annexin-V(-) and viable) to a lower FSC, lower SSC profile (annexin-V(+) and apoptotic). Therefore, in the absence of an AnnV stain, a cell's position in a FSC/SSC plot serves as a fairly reliable indicator of whether or not a cell exposed phosphatidylserine. This is demonstrated in Figure 2.2. Therefore, FSC/SSC gating was used to infer the apoptotic status of the plasma cells in Figure 2.9. On days 3 and 4 of stimulation, apoptotic (low FSC) but not live (high FSC) plasma cells had levels of surface CRT elevated 2-4 fold indicated by the CRT/block ratio (**Fig. 2.9C**). Thus the UPR experienced by live plasma cells does not interfere with ER retention of CRT to a degree measurable by flow cytometry, in contrast with that induced by THP-treatment of live fibroblasts (**Figs. 2.1 & 2.9**).

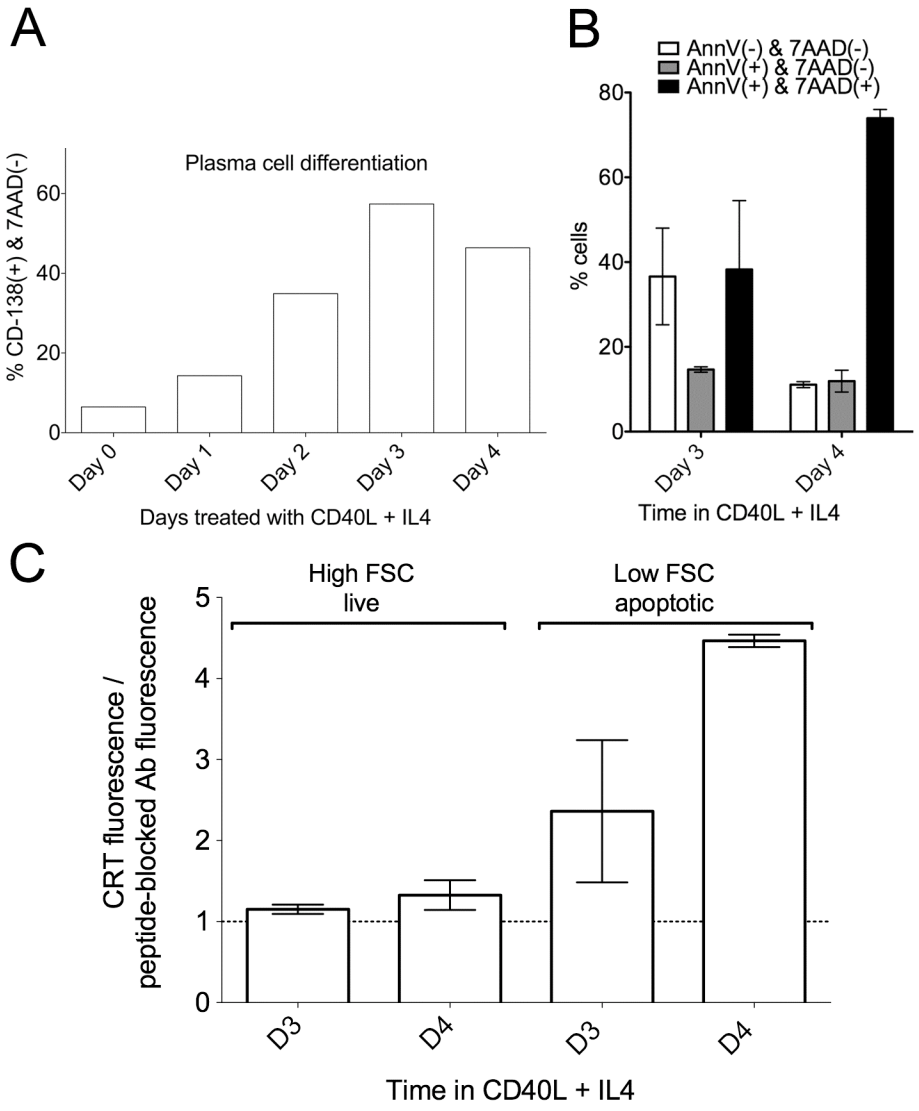

Figure 2.9 Surface CRT is upregulated on apoptotic but not live plasma cells.
(A) Kinetics of plasma cell differentiation in splenocytes treated with IL-4 and co-incubated with CD40L-expressing insect cells. As suggested, the percentage of 7AAD(-), CD138(+) cells shown includes both live and apoptotic plasma cells. (B) Cell death profiles on days 3 and 4 of treatment (C) Cell-surface CRT measured as in Fig. 2.1B on live or apoptotic 7AAD(-), CD138(+) cells. Annexin-V was not included in these stains, so cell size and granularity was used to differentiate apoptotic and viable cells (as shown in Fig. 2.4A). The data represent (A) 1 and (B-C) 2 experiments respectively. These experiments were performed in collaboration with the lab of Dr. Wesley Dunnick.

To determine if the elevated levels of cell surface CRT seen on primary, apoptotic plasma cells were also present on other primary lymphocytes we measured the CRT

median fluorescence of apoptotic or non-apoptotic lymphocytes (**Fig. 2.10A**). Untreated thymocytes and splenocytes had ~20% or 7% 'early' (AnnexinV single positive) apoptotic cells, respectively, following culture for 6-15 hours in unsupplemented media (**Fig. 2.10B**). The observed apoptosis was likely a result of lymphocytes undergoing 'death by neglect.' Further apoptosis was induced in parallel cultures treated with dexamethasone (**Fig. 2.10B**). Neither 'death by neglect' nor dexamethasone-induced apoptotic splenocytes and thymocytes had increased cell surface CRT expression (**Fig. 2.10A**). Plasma cells have increased expression of CRT and other ER chaperones relative to unstimulated splenocytes (Skalet et al., 2005), which may explain the differences in cell surface CRT levels on apoptotic plasma cells versus apoptotic splenocytes and thymocytes.

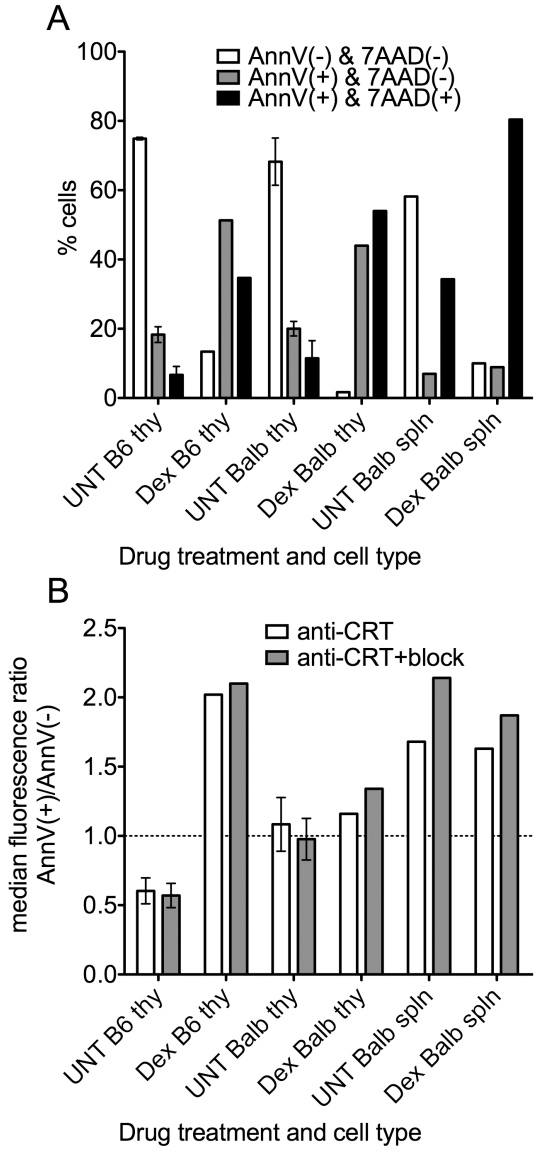

Figure 2.10 Surface CRT is not found on other live or apoptotic primary lymphocytes.

(A) Cell death profiles of freshly harvested thymocytes and splenocytes following 6-15 hours in unsupplemented media or in media containing the cytotoxic drug dexamethasone (Dex). Thymocytes die as a result of death by neglect in unsupplemented media. (B) Cell surface CRT measured in AnnV+ (apoptotic) relative to AnnV(-) (live) cells that were treated as in A. (A-B) Data on UNT thymocytes are the average of 3 experiments and data on UNT splenocytes and dex-treated splenocytes and thymocytes are based on a single experiment.

DISCUSSION

Cell-surface CRT is characterized as an important factor in inducing anti-tumor immune responses (Martins et al., 2011; Obeid et al., 2007b; Panaretakis et al., 2008a; Panaretakis et al., 2009). Anti-cancer regimens that induce an anti-tumor immune response are likely to be more effective than non-immunogenic regimens with similar cancer cell cytotoxicity (Green et al., 2009). Identifying conditions that induce cell-surface CRT, and understanding mechanisms and functional consequences of cell-surface CRT expression could help design more effective anti-tumor therapies. Our findings indicate that THP induces transient, pre-apoptotic, cell-surface CRT exposure in some cell types (**Figs. 2.1-2.4**), yet significant decreases in cell surface MHC-I expression (**Fig. 2.4**). The cell-surface CRT corresponds to a general interference with ER retention in response to THP; a mechanism with distinct features from both previously published mechanisms of increased cell-surface CRT expression on dying cells (**Figs. 2.6 & 2.7**). Furthermore, we identify a novel connection between poly-peptide-based protein binding by CRT and its cell surface expression in response to THP (**Fig. 2.9** and (Jeffery et al., 2011)). Finally, primary, apoptotic plasma cells, which are highly secretory and under constitutive ER stress, have elevated levels of apoptotic, cell-surface CRT measurable by flow cytometry, unlike other primary cell types examined (**Fig. 2.9 & 2.10**).

Our data indicate a secretory route for ER proteins (**Fig. 2.6**), as also suggested for the CRT-ERp57 co-translocation mechanism (Panaretakis et al., 2009). It is noteworthy that several of the ER resident proteins detectable in supernatants of THP-treated cells (**Fig. 2.5**) are known calcium binding proteins of the ER (Coe and Michalak, 2009). As is the case with CRT (Sonnichsen et al., 1994), ER retention of BiP, PDI and gp96 may in part involve calcium-dependent processes. However, calcium-depletion alone appears insufficient to induce secretion of the ER chaperones (**Fig. 2.5C-D**). Rather, the combined effects of KDEL receptor saturation and calcium-depletion appear to be the mechanism that drives secretion of the ER chaperones in THP-treated cells. Related to this, UPR induces expression of ER chaperones, but TUN and THP-induced UPR was shown not to induce expression of the KDEL receptor (Llewellyn et al., 1997). If KDEL receptor expression is not matched to that of the ligands it is expected to

retrieve following inappropriate ER escape, a constant occurrence even in unstressed cells (as described in chapter 1), one might expect a failure in KDEL-mediated ER retention. Similar mechanisms may be relevant to the extracellular localization of ER chaperones under physiological protein misfolding conditions, known to induce the UPR and alter ER calcium homeostasis.

It is important to consider that increases in surface CRT by a magnitude measurable by flow cytometry were, in general, difficult to detect in apoptotic cells (**Figs. 2.1-2.4**). Stronger non-specific protein binding to apoptotic cells could render a specific signal more difficult to detect by flow cytometry. Microscopic observations allow for visualization of CRT redistribution and possibly better detection of CRT upregulation on apoptotic cells as described in other studies (Gardai et al., 2005; Kuraishi et al., 2007; Park et al., 2008). Related to this, it should be noted in the case of *Drosophila melanogaster*, apoptotic cells do not upregulate cell-surface CRT (Kuraishi et al., 2007). Rather, the viable and apoptotic *Drosophila* cells examined had equal quantities of cell-surface CRT. However, on apoptotic *Drosophila* cells cell-surface CRT redistributed into distinct puncta (Kuraishi et al., 2007), as also reported in mammalian cells (Gardai et al., 2005). Importantly, CRT on the apoptotic *Drosophila* cell surface was sufficient for CRT to significantly increase phagocytic uptake despite absence of a measurable increase in the level of cell-surface CRT relative to viable cells (Kuraishi et al., 2007). It is of interest to further examine whether THP-induced cell-surface CRT expression is present in patches similar to that observed on apoptotic mammalian (Gardai et al., 2005) and invertebrate cells (Kuraishi et al., 2007).

The mechanism of increased cell-surface CRT expression we describe has key differences from the other two published models. Tarr et al. proposed a model wherein CRT is co-expressed on the surface with PS, and is bound to PS (Tarr et al., 2010). In contrast, we see high levels of cell surface CRT on THP-treated PS(-) cells, and low levels, if any, on THP-treated PS(+) cells (**Fig. 2.1-2.2**). The other described mechanism for increased cell surface CRT exposure (induced by specific stimuli like anthracyclin chemotherapeutics) was initially identified and thoroughly characterized by Guido Kroemer's group (reviewed in (Martins et al., 2010)). The THP-induced pre-apoptotic increase in CRT cell-surface expression we describe here is distinct in several ways from

anthracyclin-induced pre-apoptotic cell-surface CRT (reviewed in (Martins et al., 2010)). Unlike Kroemer's published specific co-translocation of CRT:ERp57, our THP-induced surface CRT model: a) is independent of CRT-ERp57 binding, b) does not result in increases in cell-surface ERp57 expression measurable by flow cytometry (**Fig. 2.7**), and c) results in the secretion of several additional ER proteins. On the other hand, the two mechanisms have several key similarities: CRT travels through the secretory pathway and appears on the surface within hours of stimulus (**Fig. 2.5**) (Obeid et al., 2007b; Panaretakis et al., 2009); and PERK activation (Gass et al., 2008) and reactive oxygen species production (Hsieh et al., 2007) both result from THP treatment (within hours) and are required for inducing CRT:ERp57 complex surface expression (Panaretakis et al., 2009).

We show that plasma cells, a primary cell type undergoing physiological ER stress, do not have elevated levels of pre-apoptotic cell surface CRT (**Fig. 2.9**). This might be because plasma cell differentiation only activates the ATF6 and IRE1a/XBP1 axes of the UPR, and not the PERK axis (Gass et al., 2008). These observations are consistent with the idea that PERK activation (or downstream signals) may be a general requirement for cell surface CRT expression. Relevant to this, the PERK axes of the UPR is thought to be activated by toxic or pathologic stimuli resulting from chronic ER stress to subsequently prepare the cell to undergo apoptosis (reviewed in (Todd et al., 2008)). Since chronic unresolved ER stress leads to PERK activation and subsequent apoptosis, PERK activation may occur in cultured plasma cells that are continually stimulated, thereby explaining the high levels cell-surface CRT measured on apoptotic plasma cells (**Fig. 2.9**). Thus, PERK involvement in increased cell-surface CRT exposure may be part of the general mechanism for increased expression (and/or redistribution) of the known eat-me signal, CRT, on cells undergoing apoptosis. If PERK activation is involved in CRT exposure on apoptotic cells, it would couple a known apoptosis-inducing pathway with induction of a known eat-me signal. This interesting model suggests a system where the cell prepares to be 'properly buried' prior to its death.

CHAPTER THREE

Impacts of extracellular calreticulin on phagocytosis and innate immunity

SUMMARY

The cellular response to ER stress plays an important role in cell survival and is increasingly recognized as a factor that modulates the immune response. Furthermore, it is widely published that many proteins involved in the cellular response to stress, particularly heat shock proteins (HPSs), also modulate the immune response. However, immunomodulation by HSPs is highly controversial and often described using bacterially expressed or over-expressed HSPs. Here we examined the immunological consequences of secretion of several HSPs including BiP, gp96 and CRT. We used THP treatment of MEFs, which depletes ER calcium, to induce cell-surface expression of CRT, and secretion of CRT, BiP, gp96 and PDI. We show that incubation of bone marrow-derived dendritic cells (BMDC) with THP-treated MEFs enhances sterile IL-6 production, and LPS-induced generation of IL-1β, IL-12, IL-23 and TNF-α. However, extracellular CRT is not required for enhanced pro-inflammatory responses and the presence of the other secreted ER chaperones does not induce sterile production of IL-1β, IL-12, IL-23 and TNF-α, or diminish the BMDC response to LPS. Importantly, the pattern of pro-inflammatory cytokine induction by THP-treated cells and cell supernatants resembles that induced by THP itself, and indicates that other ER chaperones present in supernatants of THP-treated cells also do not contribute to inducing the innate immune response. On the other hand, we show that ER stress significantly enhances phagocytic uptake of THP-treated target cells by BMDC. Surface expression of CRT in viable, THP-treated fibroblasts correlates with their enhanced phagocytic uptake by BMDC. These studies show that while cell surface CRT is able to promote phagocytic uptake of calcium-depleted cells, it is unable to modulate the innate immune response. Additionally, there is a strong synergy between calcium-depletion in the ER and sterile IL-6 as well as LPS-dependent IL-1β, IL-12, and IL-23 innate responses, findings that

have implications for understanding inflammatory diseases that originate in the ER. This chapter is published in part by:

Peters, L.R., and Raghavan, M. (2011). Endoplasmic reticulum calcium depletion impacts chaperone secretion, innate immunity, and phagocytic uptake of cells. J Immunol *187*, 919-931.

INTRODUCTION

Among the functions attributed to cell-surface CRT (reviewed in (Gold et al., 2010; Green et al., 2009)), several have important immunological implications. For example, cell-surface CRT on dead and dying tumor cells stimulates therapeutic and protective anti-tumor immune responses in mice (Obeid et al., 2007a; Obeid et al., 2007b; Panaretakis et al., 2009). CRT on the surface of apoptotic and dying tumor cells also functions as an eat-me signal in the phagocytosis of these cells (Gardai et al., 2005; Kuraishi et al., 2007; Obeid et al., 2007b); by this mechanism, CRT could promote the presentation of antigens derived from dying cells to T cells to induce anti-tumor immunity. However, other mechanisms could also account for, or contribute to, the immunostimulatory effects of cell-surface CRT. Purified ER chaperones such as heat shock protein 90 (HSP90), CRT (Hong et al., 2010) and gp96 (HSPC4) are implicated in the induction of co-stimulatory molecule expression and cytokine production by dendritic cells (reviewed in ((Henderson et al., 2010)). While it has been suggested that TLR ligand contamination could account for the reported immunogenicity of these and other soluble HSP's, studies demonstrating immunogenicity of cell-associated HSPs, including HSP90 and gp96, suggest that HSPs can be immunomodulatory independently of microbial contaminants (Liu et al., 2003; Spisek et al., 2007; Tsan and Gao, 2009).

ER calcium depletion, which causes ER stress, is reported to induce secretion or cell surface expression of some endogenously expressed HSPs (Booth and Koch, 1989). Additionally, we identified ER calcium depletion as a strong inducer of pre-apoptotic cell-surface CRT expression (Jeffery et al., 2011; Peters and Raghavan, 2011a). Recently, several papers identified interesting connections between ER stress (including ER calcium depletion-induced ER stress) and innate immunity (Goodall et al., 2010;

Martinon et al., 2010; Smith et al., 2008; Zhang et al., 2006). In particular, ER stress induction in macrophages caused them to produce higher levels of pro-inflammatory cytokines in response to several innate stimuli (Smith et al., 2008). It is possible that cell-surface CRT expression and/or HSP-secretion in response to ER stress were involved in the enhanced these inflammatory responses.

Martinon et al., subsequently showed that the transcription factor XBP-1, which is important in orchestrating the ER stress response, was activated by Toll-Like Receptor (TLR) ligation (Martinon et al., 2010). Yet, the two other arms of the UPR were absent or suppressed. XBP-1 was required for wild-type levels of pro-inflammatory cytokines in response to TLR ligation or infection (Martinon et al., 2010). Together, these results suggest that XBP-1 plays alternative roles in promoting innate immune responses and UPR. Other studies have linked inflammation with UPR induction or ER calcium depletion. For example, atherosclerosis (Li et al., 2004; Li et al., 2005) and familial dementia (Davies et al., 2009) have been associated different forms of ER stress. A specific inherited mutant of the protein neuroserpin that is associated with familial dementia, was recently shown to induce ER calcium depletion in the absence of a traditional UPR. Inflammation is important in the pathogensis of atherosclerosis (Li et al., 2005) and speculated to be involved in the development of dementia (Leonard, 2007). Consequently it is of interest to characterize inflammatory responses to different forms of ER stress and the role of extracellular chaperones.

In the present chapter, we examined the innate immunological consequences of cell-surface CRT using THP-treated wild-type and $CRT^{-/-}$ MEFs, which have impaired ER retention (**Fig. 2.5**) and increased cell-surface CRT expression (**Fig. 2.1** (Jeffery et al., 2011)). THP-induced secretion of various extracellular chaperones, including CRT, BiP, gp96 and PDI (**Fig. 2.5**), also allowed us to examine abilities of the soluble, extracellular forms of these ER chaperones to modulate the innate immune response. We found that incubation of BMDC with THP-treated fibroblasts or conditioned media from the treated cells enhances production of IL-6 under sterile conditions, but not IL-1β, IL-12 or TNF-α, cytokines previously shown to be induced by macrophages following exposure to extracellular gp96 (Liu et al., 2003) or a CRT fragment (Hong et al., 2010). We also found that ER stress induced phagocytic uptake of cells by BMDC. Furthermore,

phagocytosis of THP-treated cells by BMDC was significantly enhanced in a CRT-dependent manner. Finally, direct THP treatment of BMDCs enhanced IL-6 production under sterile conditions as previously shown in macrophages (Bost and Mason, 1995), and enhanced various pro-inflammatory responses to LPS more significantly than did BMDC treatment with TUN. Together the findings point to strong synergies between ER calcium depletion and innate immune responses and suggest that the combined presence of several ER chaperones in the extracellular environment *per se* is not strongly pro-inflammatory.

MATERIALS AND METHODS

Generation of BMDC

C57BL6 femurs & tibias were flushed with media and cultured in 24 well plates (roughly 2*24 well plates per mouse). Bone marrow cells were cultured for 5-7 days in BMDC media: RPMI 1640 supplemented with 100 mg/ml streptomycin, 100 U/ml of penicillin, 10% FBS (v/v), 1 mM HEPES, 1 mM sodium pyruvate, 0.1 mM MEM Non-Essential Amino Acids (Life Technologies), GMCSF (conditioned media diluted 1:5000) and 50 mM 2-ME. BMDC media were changed every other day, and non-adherent and loosely adherent cells were harvested by pipetting. Phenotype of generated cells was examined by measuring upregulation of CD80/86 and MHC-II on the surface of CD11c+ cells from LPS-treated cultures of bone marrow derived cultures. These analyses confirmed that the generation protocol stimulated the differentiation of the bone marrow cells into DC (data not shown).

Cytokine profiling of BMDC and generation of MEF CM

For data in Figure 3.1, MEFs were drug-treated as indicated for 5-6 hours (**Fig. 3.1**) or 20.5 hours (**Fig. 3.2)**. Next, cells were harvested, washed 2-3 times (first in 25 ml media, then either twice in 10 ml or once in 25-40 ml media) and incubated alone or with BMDC as described below. For data shown in Figure 3.3, MEFs were treated with indicated drugs for 5-6 hours, supernatants collected (CM1), cells washed 3 times in 7 ml of PBS, following which 4 ml of BMDC media were added to the cells. After a 5-6 hour collection period, conditioned media, called conditioned media 2 (CM2), were harvested. CM1 and CM2 were centrifuged to clear any floating cells or cellular debris. For Figure

3.3, a portion of CM2 was added to BMDC (MEF CM2+DC) and another portion directly tested for the presence of specific cytokines (MEF CM2). For Figure 3.6, CM1 or CM2 were added directly to BMDC as in Figure 3.3.

For Figure 3.7 CM1 and CM2 were first dialyzed using 3 kDa or 10 kDa centricon filters as indicated (using at least 3 successive concentrations and dilutions), before adding retentate or flow-through to BMDC. Separate wells of dendritic cells were directly treated with the indicated concentrations of the described drugs (Direct treatment), or left untreated. In parallel analyses, a second set of MEF plates were treated as described above for generation of the CM2. MEFs were then harvested and stained with AnnV and 7AAD (to measure cell viability at the end of the MEF CM2 collection).

Protocols for BMDC incubations with treated cells, CM or drug were adapted from Torchinsky et al. 2009 (Torchinsky et al., 2009). Day 5 or 6 BMDCs ($5x10^5$) were mixed with $1x10^6$ washed target cells, co-sedimented and incubated for 19-23.5 hours (**Fig. 3.1**), 18.5 hours (**Fig. 3.2**) or treated separately with drugs for 21-23 hours (**Fig. 3.6**) or with MEF CM for 15-23 hours (**Fig. 3.3-3.6**) in 24 well plates in the presence or absence of described amounts of LPS before centrifuging the plates for 5 min at 241**g* and harvesting the resulting supernatants. Supernatants were finally submitted to the University of Michigan Cancer Center Immunology Core (UMCCIC) for cytokine measurements by ELISA. Duoset ELISA development systems were purchased from R&D systems (Minneapolis, MN).

ATP measurements

ATP was measured as directed using the ENLITEN® ATP Assay System Bioluminescence Detection kit (Promega). MEF CM1 and CM2 were prepared using opti-MEM I Reduced Serum Media (Invitrogen) as published (Selzner et al., 2004), or DC media as is used in the cytokine assays. We mixed 50 μL of CM with 50 μL of the provided recombinant luciferase in 96 well plates and used a Biotek Synergy HT plate reader to measure the luminescences of the samples. Relative luminescence units were converted to mass ATP using an ATP standard curve performed with the provided ATP standard. Controls include the respective media that was never added to cells (media), or

THP-CM2 that was pre-mixed with 10-20 U/ml of apyrase and incubated at room temperature for 20-40 minutes before measuring its ATP levels as described.

Assays measuring phagocytosis of MEFs

Target cells were labeled with CellTracker™ Green CMFDA (5-chloromethylfluorescein diacetate) (Invitrogen) in 10 cm plates that were seeded with 2-2.5x10^6 target MEFs per plate 12-20 hours before labeling. Each plate was labeled as directed with 0.1-0.35 μM CMFDA diluted in optimem serum free media for 20-40 minutes at 37^o C. Media was removed and replaced with previously described tissue culture media (RPMI with 10% serum) and incubated at 37^o C for 30-60 minutes. After this, the media was replaced with media, respective plates were then exposed to 3 minutes of UV light on a UV light box or left untreated and plates were incubated overnight in tissue culture incubator. The respective plates were then treated with 5 μM THP or 10 μg/ml TUN for 5-6 hours or left untreated. Cells were finally harvested (UV) or washed twice in 10-12 ml PBS (untreated and drug-treated), then harvested with 8 mM EDTA in PBS and diluted in RPMI for counting (a third wash) before pelleting and resuspending at the appropriate concentration. 1x10^5 Day 5 or 6 BMDC were then mixed with 4x10^5 targets in 96 well plates and the plates were then incubated at 37^o C or 4^o C for 60 minutes. Cells were then fixed for 10 minutes with formalin (fisher PROTOCOL) diluted 1:10 in flow cytometry buffer (PBS+2% FBS), washed twice, stained with anti-CD11c-APC (1:220, BD-Biosciences) for 20-40 minutes at 4^o C. Cells were washed twice and data for each sample was collected on the FACS Canto flow cytometer (BD). Analysis was performed using Flowjo 8.8.6 (Treestar Inc.). CMFDA was read on the FITC channel.

RESULTS

In a CRT-independent manner, THP-treated cells, cell supernatants and THP itself induce and enhance innate immune responses more broadly and significantly than corresponding TUN treatments

Using THP-treated WT or $CRT^{-/-}$ MEFs, we investigated whether cell surface and/or extracellular soluble CRT were linked to enhanced pro-inflammatory cytokine production. We first examined production of IL-6, a cytokine previously shown to be induced by direct treatments of murine macrophages with THP (Bost and Mason, 1995) or TUN (Martinon et al., 2010). WT or CRT deficient MEFs were treated with TUN, MTX & THP for short (5-6.5 hr) or long (20.5 hr) times as described in Chapter 2 Materials and Methods, harvested, washed extensively with PBS, co-incubated with BMDC or alone, and then the cytokines in the supernatants of these cultures were quantified by ELISA. BMDC co-incubations with MEFs treated with THP resulted in higher levels of sterile/spontaneous IL-6 compared to BMDC co-incubations with other target cells (**Fig. 3.1A**). However, these effects were independent of CRT expression, as shown by similar levels of IL-6 resulting from BMDC co-incubations with THP-treated CRT-/- or WT MEFs (**Fig. 3.1A**). THP-induced increase in IL-6 production was also seen with MEFs subjected to longer time points of drug treatments (**Fig. 3.2B),** although the levels of IL-6 measured were lower (**Fig. 3.1A** compared to **Fig. 3.2B**). These findings are consistent with higher levels of MEF apoptosis following long drug treatments (**Fig. 3.2A** compared to **Fig. 2.1A**), and the expected immunosuppressive effects of apoptotic cells (Voll et al., 1997). It is noteworthy that MTX-treated, pre-apoptotic (**Fig. 3.1**) or apoptotic (**Fig. 3.2)** cells did not induce significant pro-inflammatory cytokine production by BMDC, despite being reported to induce strong anti-tumor immune responses in mice (Obeid et al., 2007b).

Figure 3.1 Co-culture of THP-treated pre-apoptotic target cells with BMDC induces and enhances pro-inflammatory cytokine production in a CRT-independent manner.

(A-E) Cytokine production by DCs, MEFs, and DC+MEF co-cultures. WT or CRT-/- MEF target cells were treated with TUN, MTX or THP for 5.5 or 6.5 hours or left untreated. Adherent target cells were then harvested, washed and incubated in media alone (MEF alone) or co-incubated with BMDC (MEF+DC) in the absence (described as 'sterile') (A) or presence (B-E) of 0.5-2 ng/ml LPS for 18.5-23.5 hours and the concentrations of the indicated cytokine were measured in duplicate by ELISA. Wells of DC incubated in the presence (B-E) or absence (A) of LPS were included in each experiment as an additional control (DC alone). The THP(-)LPS bars indicate conditions where THP-treated WT MEF or CRT-/- MEFs were incubated with DC, but in the absence of LPS, to illustrate the LPS dependence of enhanced production of indicated cytokines. The data from co-incubations of DC and MEFs show the mean and standard error of 3 (WT) or 5 ($CRT^{-/-}$) experiments. The data from MEFs alone or DC alone show the mean and standard error of 1-3 experiments in the presence of LPS, or 2-4 experiments in the absence of LPS. The p-values from two-tailed, paired t-tests are indicated.

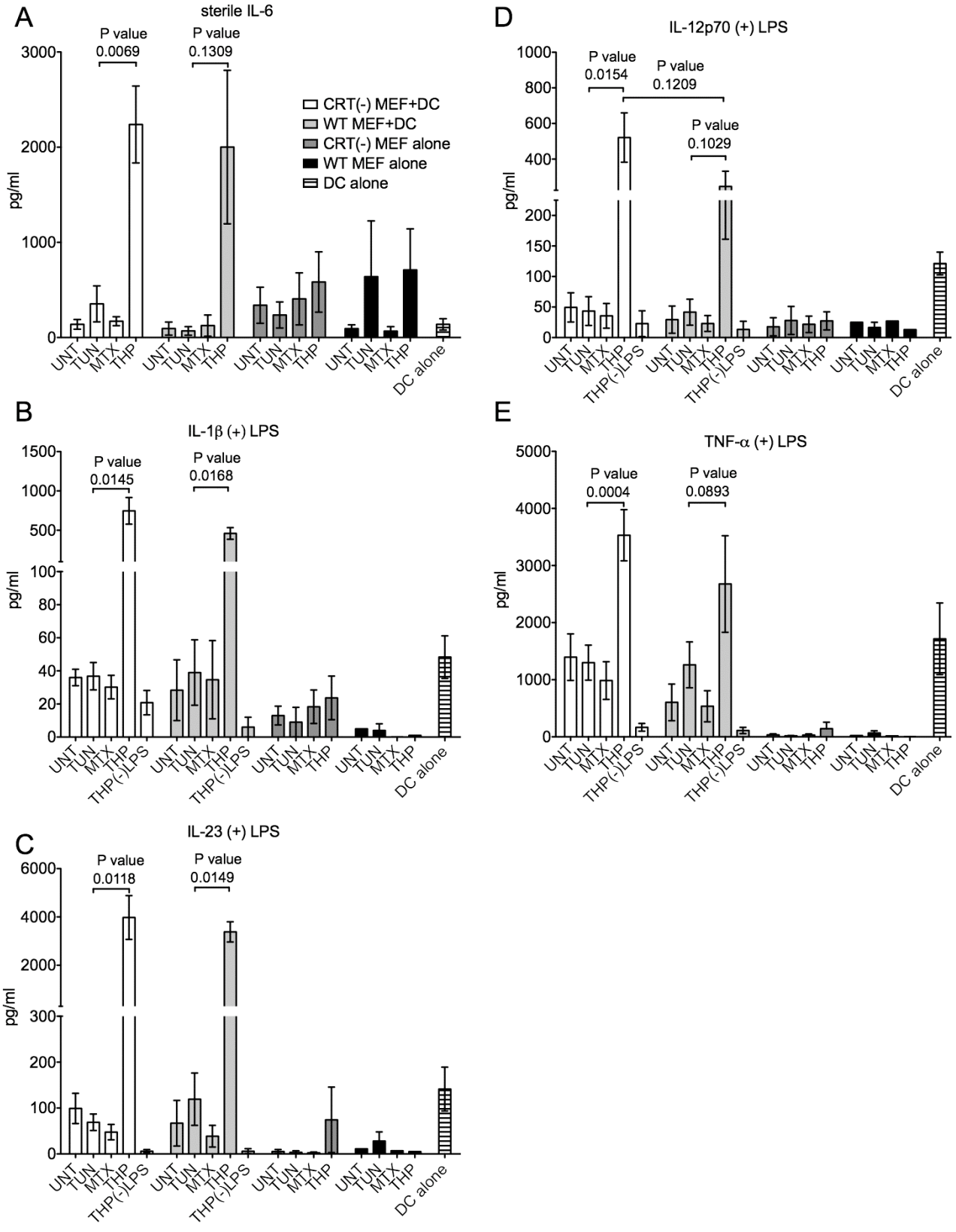
A
sterile IL-6
P value
0.0069
P value
0.1309
pg/ml
3000
2000
1000
0
CRT(-) MEF+DC
WT MEF+DC
CRT(-) MEF alone
WT MEF alone
DC alone
UNT
TUN
MTX
THP
DC alone
B
IL-1β (+) LPS
P value
0.0145
P value
0.0168
1500
1000
500
100
80
60
40
20
0
THP(-)LPS
C
IL-23 (+) LPS
P value
0.0118
P value
0.0149
6000
4000
2000
300
200
100
0
D
IL-12p70 (+) LPS
P value
0.0154
P value
0.1209
P value
0.1029
1000
800
600
400
200
150
100
50
0
E
TNF-α (+) LPS
P value
0.0004
P value
0.0893
5000
4000
3000
2000
1000
0

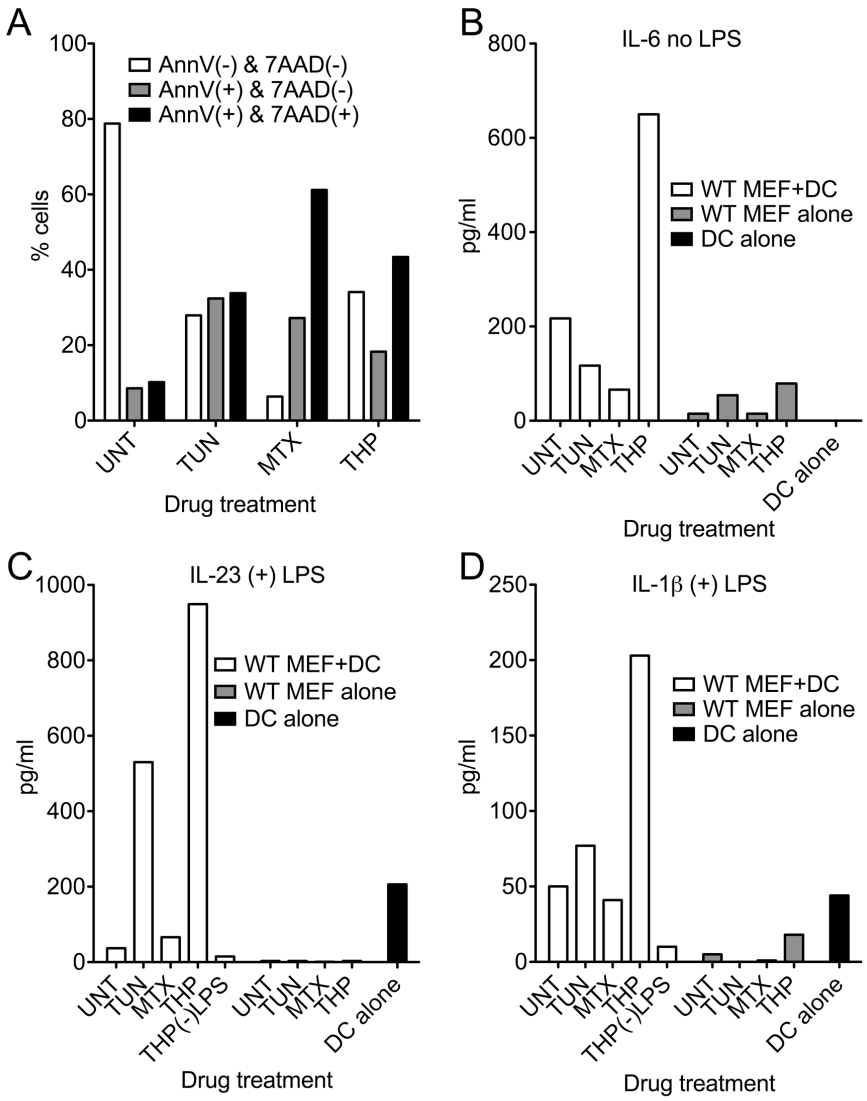

Figure 3.2 Co-culture of THP-treated, apoptotic target cells with BMDC induces and enhances pro-inflammatory cytokine production but to a lesser extent than that seen with pre-apoptotic THP-treated cells.

(A-D) WT MEFs were treated with indicated drugs for 20.5 hours, prepared and co-cultured with BMDC as described for Fig. 3.1, with or without 0.5 ng/ml LPS (as indicated) for 18.5 hours. (A) An aliquot of treated MEFs were stained with AnnV and 7AAD to measure their viability. (B-D) IL-6, IL-23 and IL-1β in the co-cultures' supernatants were measured in duplicate by ELISA. Data shown are from one experiment and are representative of 1-2 experiments for each analyte.

We also examined the effect of THP-treated MEFs on production of IL-12, IL-1β, and TNF-α, cytokines that were previously shown to be induced by a membrane-linked extracellular form of gp96 (Liu et al., 2003) or a bacterially-expressed CRT fragment (Hong et al., 2010). Additionally, we compared induction of IL-23, as both THP and TUN were recently reported to enhance expression of this cytokine in the presence of TLR agonists (Goodall et al., 2010). Co-incubating THP-treated MEFs with BMDCs strongly enhanced TLR-dependent (0.5-2 ng/ml LPS) production of IL-1β, IL-12p70 and IL-23 compared to co-incubating other drug-treated or untreated MEFs with BMDC (**Fig. 3.1B-E**). CRT was not required for enhanced cytokine production in response to THP-treated cells, and in fact, CRT-deficiency in the THP-treated MEFs appeared to correlate with higher levels of cytokine production. However, observed differences between wild type and CRT-deficient cells were not statistically significant (**Fig. 3.1B-D**). Compared to other drug treatments, THP-treated cells subjected to long (20.5 hours) drug treatments also stimulated IL-1β and IL-23 (**Fig. 3.2C-D**), although at reduced levels compared to co-incubations with MEFs subjected to short drug treatments (**Fig. 3.1**). Immunostimulatory effects of TUN-treated apoptotic cells upon IL-23 production were also measurable following longer drug treatments, but at reduced levels compared to THP-treated cells (**Fig. 3.2C**).

To better understand the molecular basis for the immunostimulatory effects of THP-treated cells (**Fig. 3.1-3.2**), we next examined the impacts of conditioned media (CM) from various drug-treated cells (**Fig. 3.3**) on induction or enhancement of pro-inflammatory cytokine production. We were particularly interested in asking whether secreted ER chaperones present in supernatants of THP-treated cells or residual THP itself might be responsible for the observed pro-inflammatory effects of THP-treated cells. For these analyses, following each drug treatment of 5-6.5 hours, media containing drugs (CM1) were removed, and cells were washed three times with at least 7 ml PBS to remove soluble drug present in the media. Following these wash steps, fresh media were collected from the washed cells over a 5-6 hour period to generate different MEF CM

(CM2). We noted that secretion of PDI and gp96 was detectable for several hours following THP removal from target cells, although at significantly reduced levels compared to those detected during drug treatment (**Fig. 3.4**, CM1 compared to CM2). Nonetheless, THP CM2 was able to induce pro-inflammatory cytokine production by BMDC with patterns resembling those induced by co-incubation of BMDC with THP-treated cells (**Fig. 3.1 and 3.3**). Only trace amounts of cytokines, if any, were directly detectable in CM2 from various drug-treated, washed MEFs (**Fig. 3.3**). BMDC mixed with THP CM2, but not BMDC co-incubated with other CM2, produced IL-6 under sterile conditions (**Fig. 3.3**). Additionally, LPS-dependent production of IL-12p70, IL-23 and IL-1β strongly synergized with stimulation by THP CM2 to yield more IL-1β, IL-12p70, and IL-23 than other BMDC treatments (**Fig. 3.3**). However, BMDC cytokine production in response to THP CM2 was clearly independent of CRT expression in MEFs (**Fig. 3.3**).

Figure 3.3 Differential induction of pro-inflammatory cytokines by conditioned media (CM) from drug-treated MEFs.
BMDC were treated with MEF CM or drugs either under sterile conditions (top panel for IL-6 measurements) or in the presence of 1 ng/ml LPS (lower panels for IL-1β, IL-23 and IL-12p70 measurements) for 21-23 hours. The concentrations of the indicated cytokines were then measured by ELISA. Concentrations of the indicated cytokines in MEF CM2+DC co-incubations, or DC alone were measured in duplicate by ELISA. The THP(-)LPS bars indicate conditions where CM2 from THP-treated WT or CRT-/- MEFs were incubated with DC. CRT-/- MEF CM2 and WT MEF CM2 bars indicate direct cytokine measurements of the indicated CM2 samples without further treatment with LPS. The results with WT MEFs show the average of three independent experiments, and the results with the CRT-/- MEFs are from a single experiment.

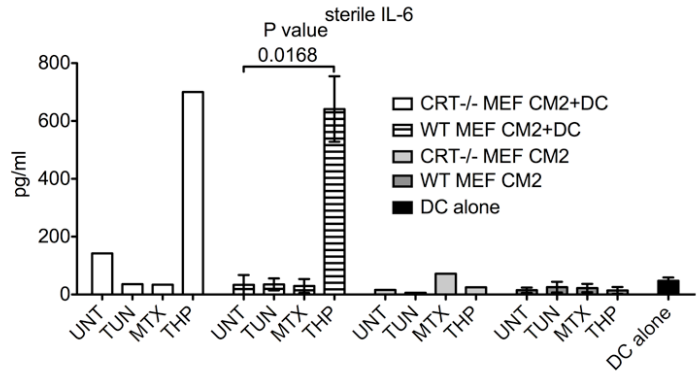
sterile IL-6
P value
0.0168
pg/ml
800
600
400
200
0
CRT-/- MEF CM2+DC
WT MEF CM2+DC
CRT-/- MEF CM2
WT MEF CM2
DC alone
UNT
TUN
MTX
THP
DC alone

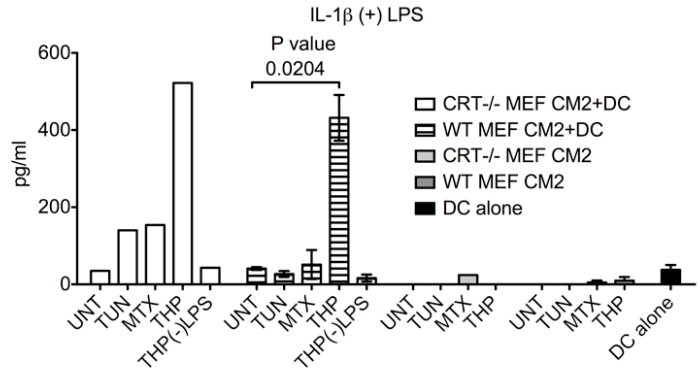
IL-1β (+) LPS
P value
0.0204
pg/ml
600
400
200
0
CRT-/- MEF CM2+DC
WT MEF CM2+DC
CRT-/- MEF CM2
WT MEF CM2
DC alone
UNT
TUN
MTX
THP
THP(-)LPS
DC alone

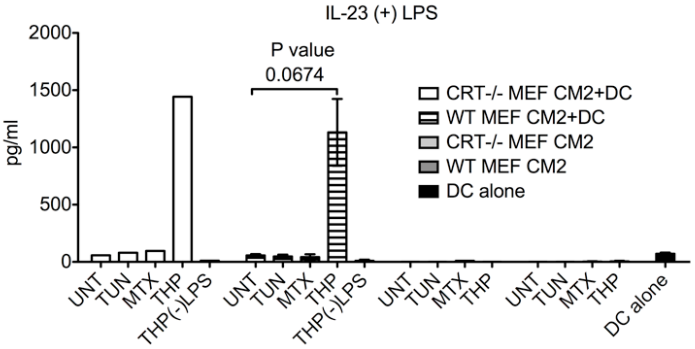
IL-23 (+) LPS
P value
0.0674
pg/ml
2000
1500
1000
500
0
CRT-/- MEF CM2+DC
WT MEF CM2+DC
CRT-/- MEF CM2
WT MEF CM2
DC alone
UNT
TUN
MTX
THP
THP(-)LPS
DC alone

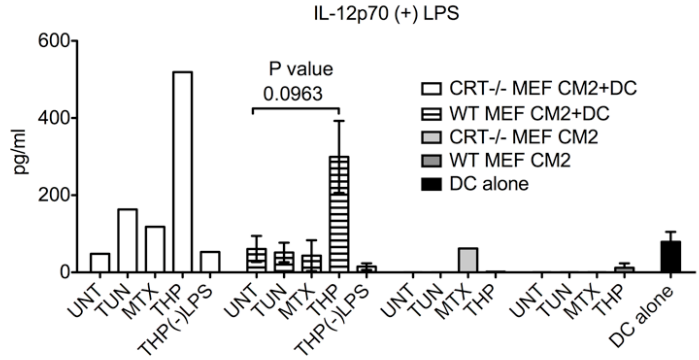
IL-12p70 (+) LPS
P value
0.0963
pg/ml
600
400
200
0
CRT-/- MEF CM2+DC
WT MEF CM2+DC
CRT-/- MEF CM2
WT MEF CM2
DC alone
UNT
TUN
MTX
THP
THP(-)LPS
DC alone

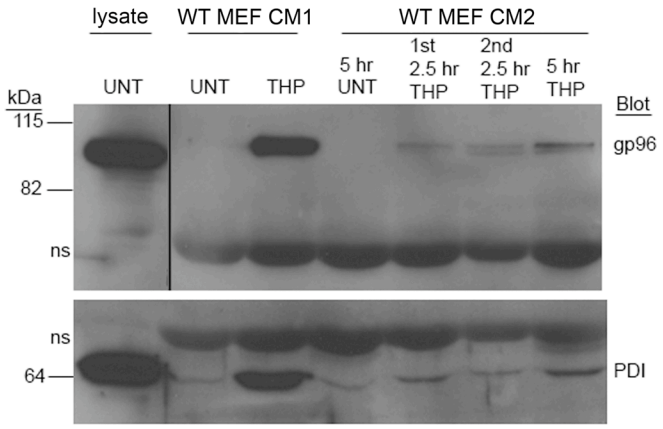

Figure 3.4 THP-induced secretion of ER chaperones continues at reduced levels for several hours following drug removal.
Gp96 and PDI secretion by untreated or THP-treated cells over the 5 hour drug treatment period (CM1) and at indicated time points following removal of drug via washing of cells (CM2). Cell lysates are shown to mark migration positions of gp96 and PDI.

The different drug-treated, washed cells used to generate CM2 were also harvested and stained with AnnV and 7AAD and analyzed by flow cytometry. These analyses indicated that, compared to other treatments, the THP CM2 generation protocol did not enhance levels of apoptotic/secondary necrotic cells (**Fig. 3.5A**). Consistent with these measurements of cell death, HMGB1 was not released from TUN or THP-treated cells used to generate CM2 (**Fig. 3.5B**). Moreover, there was no apparent correlation between the level of secondary necrotic cells in a given treatment group and its ability to stimulate the BMDC (**Fig. 3.5A and 3.3**). Therefore, necrosis-related factors were not a likely explanation for the immunostimulatory properties of THP-treated cell supernatants.

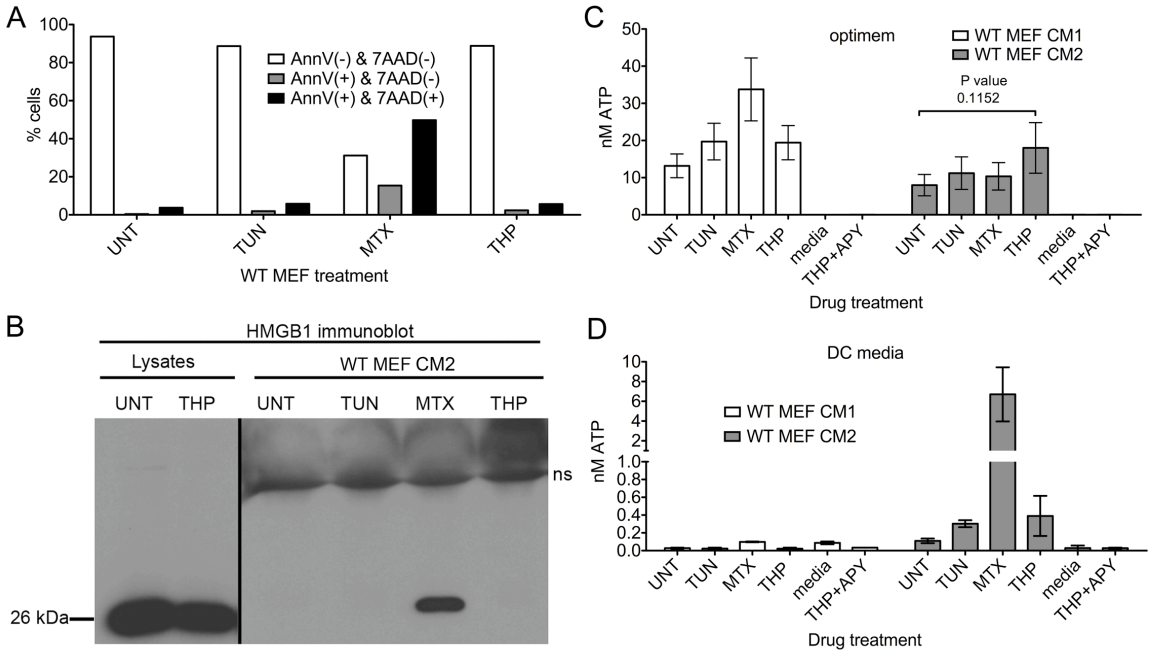

Figure 3.5 Cell viability and ATP and HMGB-1 secretion by drug-treated MEFs
(A) Cell viability: Following collection of CM2 as described in Figure 3.3, cells were harvested and stained with AnnV and 7AAD to measure cell viability. (B) WT MEF CM2 and lysates from cells subjected to the indicated treatments were immunoblotted for HMGB1. (C-D) The ATP concentrations of indicated CM from WT MEFs prepared as in (A) (or in (C) using using opti-MEM low serum media instead of DC media) were measured with the ENLITEN® ATP Assay System Bioluminescence Detection kit (Promega). The control (THP+APY) was THP WT MEF CM that was apyrase-treated prior to measuring ATP levels.

Because we detected enhanced IL-1β production in the presence of LPS and THP CM2, and ATP is implicated as an important alarmin/DAMP (Ogura et al., 2006) for activating the NALP-3 inflammasome leading to IL-1β production (Mariathasan et al., 2006), we examined the ATP concentrations in the various CM2 used to stimulate the BMDC (**Fig. 3.5 C-D**). Although ATP levels in the CM2 of THP-treated cells were not significantly enhanced relative to those in any of the other treatment groups, they were elevated above background levels in the CM2 of all treatment groups (**Fig. 3.5 C-D**). These findings suggest that extracellular ATP in the THP CM2 is not the primary stimulus responsible for enhanced IL-1β production in the presence of LPS.

It is noteworthy that IL-12p70, IL-23, IL-1β and TNF-α were not significantly induced by THP CM2 or THP-treated cells under sterile conditions (**Fig. 3.1B-D**, **Fig. 3.3**, THP(-)LPS bars). In contrast, IL-12p40 and IL-1β were both previously reported to be induced under sterile conditions by a membrane-linked form of gp96 (Liu et al., 2003). Furthermore, a recombinant, N-terminally truncated CRT fragment purified from *E. coli* induced TNF-α production by mouse peritoneal macrophages and human PBMC in the absence of a TLR agonist (Hong et al., 2010). However, TNF-α was also not induced by THP CM2 or THP-treated cells (wild type or CRT-deficient) under sterile conditions (data not shown and **Fig. 3.1E**). THP CM2 did moderately enhance TNF-α production mediated by LPS but it was independent of CRT expression by the target cells (data not shown). Thus, despite containing various extracellular ER chaperones, THP-treated cell supernatants and cells induced only the production of IL-6 under sterile conditions, and therefore were not as broadly immunostimulatory as predicted by the presence of extracellular gp96 or CRT (Hong et al., 2010; Liu et al., 2003).

Previous studies have shown that treatment of cells with TUN or THP stimulates activation of NF-κB in HeLa cells (Pahl and Baeuerle, 1995), production of reactive oxygen species (ROS) in MEFs (Hsieh et al., 2007), and significantly enhanced production of type I IFN, TNF-α (Smith et al., 2008), ISG15 and IL-6 (Martinon et al., 2010) by LPS-treated macrophages. Furthermore, THP and TUN were both shown to enhance IL-23 but not IL-12 production by human monocyte-derived DC in response to a mixture of LPS and a TLR-8 agonist (CL-097) (Goodall et al., 2010). We asked whether direct addition of TUN or THP to murine BMDC could stimulate production of any of the cytokines measured in Figures 3.1, and 3.3. The levels of cytokines resulting from drug treatment of BMDC and CM treatments of BMDC were compared within the same experiment (**Fig. 3.6**). THP and TUN treatment of BMDC both stimulated production of IL-6 in the absence of LPS, although THP stimulated on average ~9.8-fold more IL-6 than TUN at the drug concentrations and time points used in the analyses (**Fig. 3.6**, 9.8 fold was the average enhancement from five experiments, of which four are shown). THP and TUN treatments of BMDC stimulated production of IL-1β and IL-23 (**Fig. 3.6**) in response to 1-10 ng/ml LPS. However, under the conditions tested, THP was a stronger inducer of IL-1β. As noted previously with human monocyte-derived DC (Goodall et al.,

2010), lower concentrations of THP resulted in higher levels of IL-23 compared to higher concentrations of THP.

Figure 3.6 Differential induction of pro-inflammatory cytokines by different types of pharmacological ER stress

BMDC were treated with MEF CM or drugs either under sterile conditions (top panel for IL-6 measurements) or in the presence of 1-10 ug/ml LPS (lower panels for IL-1β, IL-23 and IL-12p70 measurements) for 15-22 hours. Indicated cytokine measurements followed CM+DC, drug+DC or DC-media (DC alone) co-incubations in the presence or absence of LPS. THP 200 nM CM represents CM prepared as other CM, but by incubating MEFs with 200 nM THP instead of 5 μM THP. Direct DC treatment represents cytokine production by BMDC that were directly treated with THP (black bars), or TUN (vertically striped bars) at their specified concentrations or left untreated (horizontally striped bars). The (-)LPS bars represent measurements from DC treated with THP CM1 or 5 μM THP as indicated, but in the absence of LPS. Data are averages of four experiments with the exception of CM1 stimulated cytokines, which was from a single experiment.

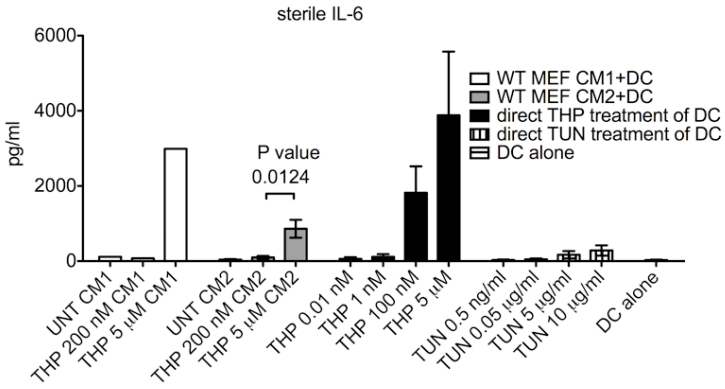
sterile IL-6
pg/ml
6000
4000
2000
0
P value
0.0124
WT MEF CM1+DC
WT MEF CM2+DC
direct THP treatment of DC
direct TUN treatment of DC
DC alone
UNT CM1
THP 200 nM CM1
THP 5 μM CM1
UNT CM2
THP 200 nM CM2
THP 5 μM CM2
THP 0.01 nM
THP 1 nM
THP 100 nM
THP 5 μM
TUN 0.5 ng/ml
TUN 0.05 μg/ml
TUN 5 μg/ml
TUN 10 μg/ml
DC alone

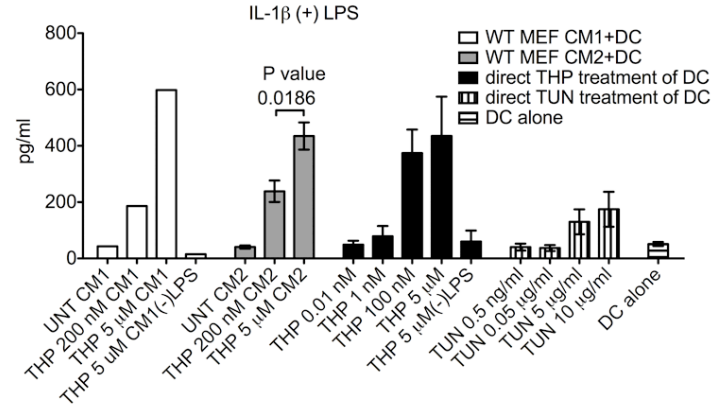
IL-1β (+) LPS
pg/ml
800
600
400
200
0
P value
0.0186
WT MEF CM1+DC
WT MEF CM2+DC
direct THP treatment of DC
direct TUN treatment of DC
DC alone
UNT CM1
THP 200 nM CM1
THP 5 μM CM1
THP 5 uM CM1(-)LPS
UNT CM2
THP 200 nM CM2
THP 5 μM CM2
THP 0.01 nM
THP 1 nM
THP 100 nM
THP 5 μM
THP 5 μM(-)LPS
TUN 0.5 ng/ml
TUN 0.05 μg/ml
TUN 5 μg/ml
TUN 10 μg/ml
DC alone

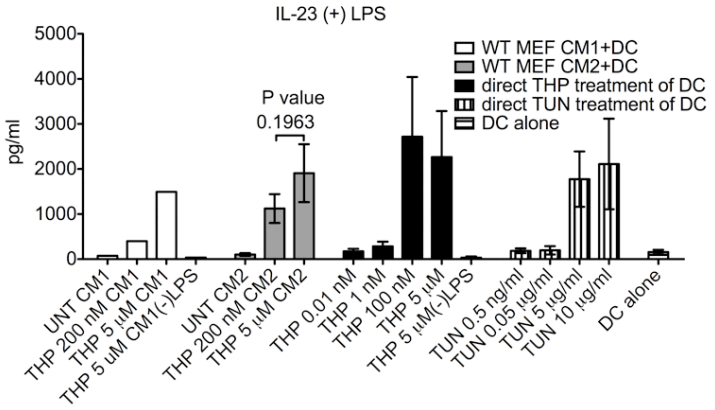
IL-23 (+) LPS
pg/ml
5000
4000
3000
2000
1000
0
P value
0.1963
WT MEF CM1+DC
WT MEF CM2+DC
direct THP treatment of DC
direct TUN treatment of DC
DC alone
UNT CM1
THP 200 nM CM1
THP 5 μM CM1
THP 5 uM CM1(-)LPS
UNT CM2
THP 200 nM CM2
THP 5 μM CM2
THP 0.01 nM
THP 1 nM
THP 100 nM
THP 5 μM
THP 5 μM(-)LPS
TUN 0.5 ng/ml
TUN 0.05 μg/ml
TUN 5 μg/ml
TUN 10 μg/ml
DC alone

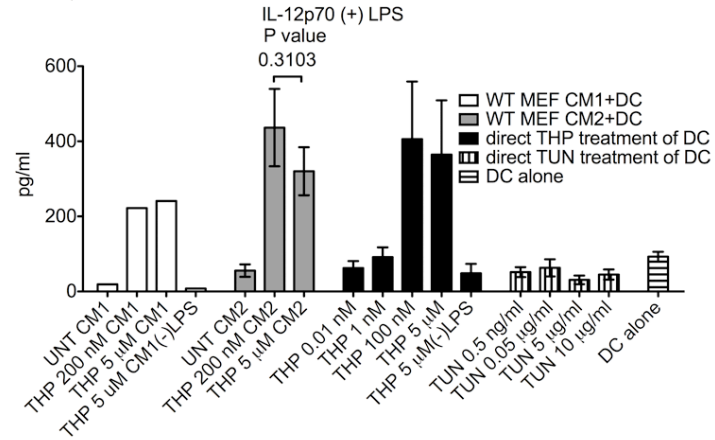
IL-12p70 (+) LPS
P value
0.3103
pg/ml
600
400
200
0
WT MEF CM1+DC
WT MEF CM2+DC
direct THP treatment of DC
direct TUN treatment of DC
DC alone
UNT CM1
THP 200 nM CM1
THP 5 μM CM1
THP 5 uM CM1(-)LPS
UNT CM2
THP 200 nM CM2
THP 5 μM CM2
THP 0.01 nM
THP 1 nM
THP 100 nM
THP 5 μM
THP 5 μM(-)LPS
TUN 0.5 ng/ml
TUN 0.05 μg/ml
TUN 5 μg/ml
TUN 10 μg/ml
DC alone

In contrast to the previous studies with human myeloid DCs, THP (but not TUN) treatment also enhanced IL-12p70 production in response to LPS (**Fig. 3.6**). However, as mentioned, a TLR-8 agonist was present in the studies with the human DCs, and the signaling cascade activated by TLR-8 may interfere with the signals leading to IL-12p70 production in the presence of LPS and THP. It has been previously described that IL-12 secretion requires *N*-linked glycosylation of the p35 subunit's signal sequence (Murphy et al., 2000). Therefore, it is possible that TUN treatment of LPS-stimulated BMDC would lead to IL-12 secretion but it is not detected because of TUN-mediated inhibition of protein glycosylation. Altogether, these results suggest that the stimulation induced by TUN and THP is qualitatively similar, although THP more strongly induces IL-6 and IL-1β (**Fig. 3.6**).

Importantly, the patterns of cytokine induction by THP-treated cell supernatants were strikingly similar to those induced by direct THP treatment of BMDC (**Fig. 3.6**). As noted above, in generating THP CM2 for Figure 3.3, THP was removed from the MEFs, and MEFs were washed sufficiently to reduce the extracellular, soluble drug concentration to < 15 pM, prior to collection of CM2. However, it is possible that THP was sequestered within cell membranes or intracellularly and subsequently partitioned into the media. In support of this possibility, we found that when CM1 (cell supernatants from drug-treated cells) and CM2 (cell supernatants from drug-treated, washed cells) were extensively dialyzed in centricons (3 KDa or 10 KDa) to remove free soluble drug that was present, the majority of cytokine-inducing activity was present in the retentates rather than in the flow through, even though THP has a molecular weight of 650 Da (**Fig. 3.7**). Based on these findings, it is likely that the activity of THP-treated cell supernatants (CM1 and CM2) (**Figs. 3.3 and 3.7**) and their resemblance to direct THP treatment of BMDC (**Fig. 3.6**) result from sequestration of THP within cell membranes or intracellularly during drug treatment of MEFs, and subsequent partitioning of active drug from MEFs into the CM within higher molecular weight membrane vesicles or protein complexes. This would allow THP to directly stimulate BMDC. THP is hydrophobic and

requires organic solvents (such as DMSO) for its solubilization, and thus its partitioning into membranes is perhaps not unexpected.

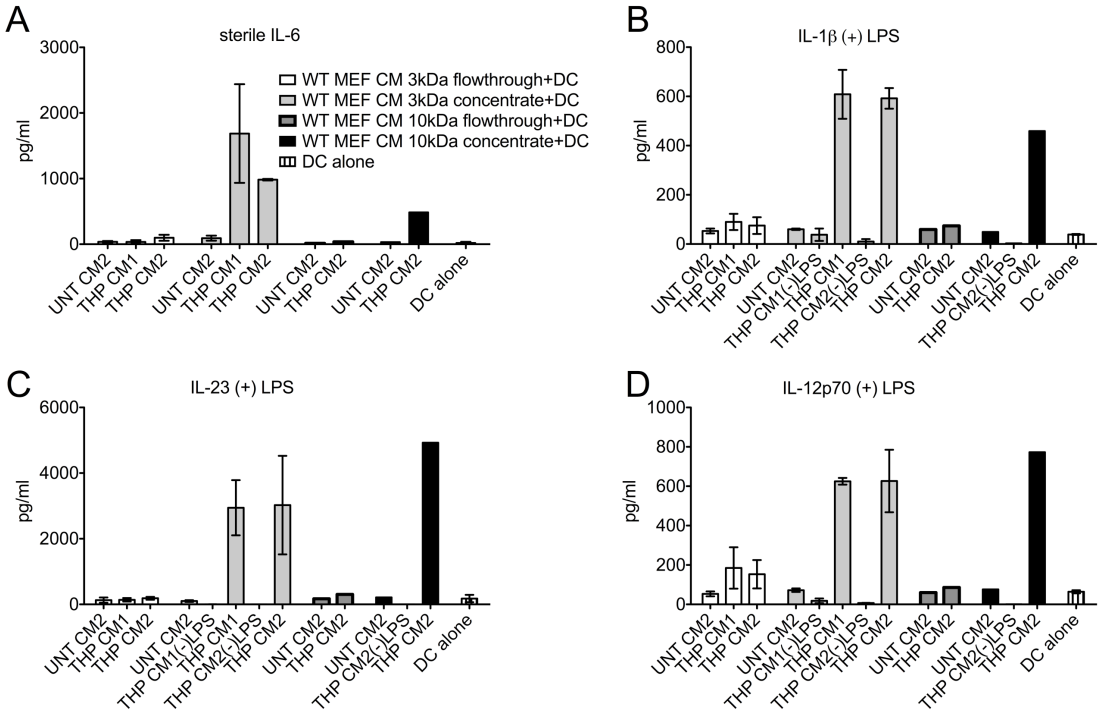

Figure 3.7 Extensive dialysis of THP CM1 and CM2 does not change inflammatory profile induced by THP CM.
These alternate conditions were performed in parallel with experiments described in Figure 3.6, except that the indicated CM were first dialyzed with either a 3 kDa or 10 kDa centricon to remove any residual drug monomers (THP has a molecular mass of 650 Da). Samples were concentrated and diluted at least 3 successive times while remaining at 4^{o}C. Cytokines induced by both the retentate and flow-through were measured as indicated.

If residual drug in THP-treated cells was responsible for the BMDC stimulating activity, we expected that reducing the concentration of THP used to treat MEFs during the CM generation would reduce the immunostimulatory capacity of THP-treated cells. Thus, we compared abilities of 5 μM or 200 nM THP CM1 and CM2 to induce production of various pro-inflammatory cytokines (**Fig. 3.6**). Cells treated with 200 nM or 5 μM THP secreted similar levels of gp96 and PDI and showed similar elevations of surface CRT expression (**Fig. 3.8**). Whereas treatments of BMDC with 5 μM THP CM1 or CM2 induced IL-6 production, treatments of BMDC with 200 nM THP CM1 or CM2

did not induce sterile IL-6 production (**Fig. 3.6**). Furthermore, reduced levels of LPS-induced IL-1β and IL-23 (**Fig. 3.6**) were observed when the 200 nM THP CM1 or CM2 were compared to the 5 μM THP CM1 or CM2. As noted, levels of chaperone secretion were very similar in 200 nM and 5 μM THP CM1 (**Fig. 3.8**).

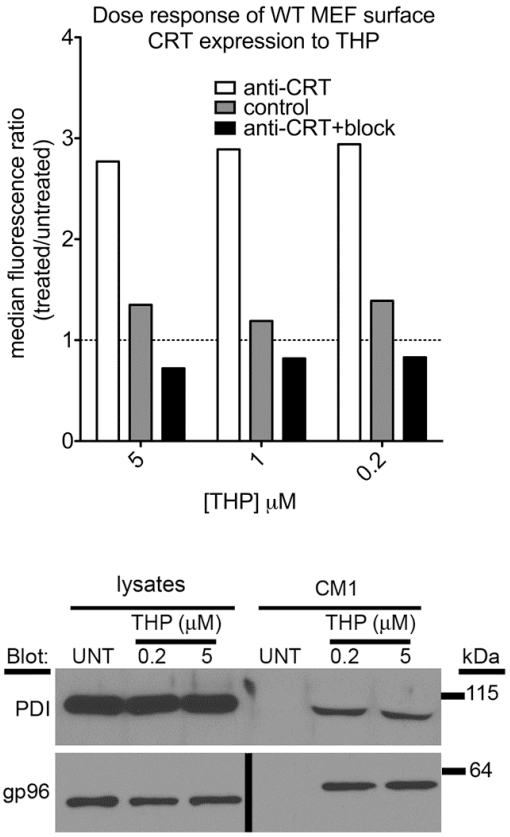

Figure 3.8 Dose response of compromised ER retention in WT MEFs exposed to THP

(A) Cell surface CRT as induced and measured in Figure 2.1B, with indicated variations in THP concentration. (B) Comparisons of PDI & gp96 release in response to low or high THP dose (200 nM or 5 μM) measured as in Figure 2.6. (A) and (B) are representative of 1 and 2 experiments respectively.

Together, these findings indicate that production of pro-inflammatory cytokines induced by THP-treated cells or CM was not enhanced by CRT expression by target cells (**Fig. 3.1 and 3.3**). Notably, the profiles of pro-inflammatory cytokine induction by THP-treated cells and dialyzed CM closely resembled those induced by THP itself, suggesting that residual THP within protein/lipid complexes was responsible for enhanced cytokine

production (**Fig. 3.3, 3.6 & 3.7**). Significantly, the effects of direct BMDC treatments with THP were qualitatively similar, but more strongly pro-inflammatory than those induced by TUN.

CRT expression enhances phagocytic clearance of THP-treated cells, but not of TUN or UV-treated cells

Because cell-surface CRT is an eat-me signal in the context of apoptotic cells (Gardai et al., 2005), pre-apoptotic tumor cells (Obeid et al., 2007b), and live tumor cells subject to CD47 blockade (Chao et al., 2010) we asked if THP-treated cells would also be phagocytosed in a CRT-dependent manner. A previously published flow-cytometry-based assay (Obeid et al., 2007b) was used to measure phagocytosis. WT or CRT deficient MEFs were labeled with a fluorophore, then drug or UV-treated, washed and incubated with BMDC. The co-cultures were then fixed and stained with an antibody specific for the DC-specific marker CD11c. The percentage of CD11c+ events that were also positive for the target-cell marker were recorded as a measure of target-cell:DC association. The ratio of DC:target cell association in co-cultures incubated at 37^{o} C relative to that of co-cultures incubated at 4^{o} C is reported as the phagocytic index (the 37 °C readings quantify adhesion and phagocytosis, whereas the 4 °C readings quantify adhesion alone). Uptake of UV-treated MEFs was significantly greater than untreated MEFs, but was independent of CRT expression by the MEFs (**Fig. 3.9A**). The latter finding was surprising in light of a previously suggested role for CRT in the phagocytic uptake of apoptotic UV-treated fibroblasts using fibroblasts, a macrophage cell line or peritoneal macrophages as the phagocytes (Gardai et al., 2005). Therefore surface CRT expression was tested in the UV-treated fibroblasts, which were triple stained for CRT as well as markers of apoptosis and plasma membrane integrity, as defined in the analyses of Figure 2.1. Our analyses indicated that CRT is not present or significantly induced on the surface of AnnV+PI- (**Fig. 3.9B**) or AnnV-PI- (data not shown) MEFs in response to UV treatment to a degree measurable by flow cytometry, consistent with the absence of significant, CRT-dependent uptake of UV-treated cells. Several differences in protocol may explain these discrepancies. These include the use of a different phagocyte (BMDC

(**Fig. 3.9**) rather than macrophages or fibroblast (Gardai et al., 2005)), a different phagocytosis assay (flow cytometry (**Fig. 3.9**) rather than microcopy (Gardai et al., 2005)), and the use of both adherent and non-adherent UV-treated target cells (**Fig. 3.9**), rather than non-adherent UV-treated target cells (Gardai et al., 2005). Additionally, expression of CD91 (the proposed CRT receptor on macrophages used for clearing apoptotic targets) on the BMDC surface may be lower than that on macrophages. Differential expression of CD91 may also explain the discrepancy between the results of Gardai et al. with macrophages as phagocytes and our results with BMDCs as phagocytes. If this were the case, THP-treated target cells would presumably have to increase CD91 expression on the BMDC to observe the CRT-dependent uptake of THP-treated cells.

Figure 3.9 CRT enhances phagocytic uptake of THP-treated target cells, but not of UV or TUN-treated target cells.
Cell Tracker Green (5-chloromethylfluorescein diacetate; CMFDA) labeling of MEFs, cell death profiles, phagocytic uptake, and surface CRT expression following different treatments. WT or CRT-/- MEFs were labeled with Cell Tracker Green, exposed to UV light for 3 minutes and then cultured for an additional 16-24 hrs, or exposed to THP or TUN for 5-6 hours, or left untreated. (A) Phagocytic uptake: Labeled and treated cells were washed 3 times, mixed with BMDC at an effector to target ratio of 1:5, and incubated for 1 hour at 37o C or 4 o C. Co-cultures were fixed, stained with anti-CD11c and analyzed by flow cytometry. For each cell type and treatment condition, the percentages of CMFDA+ events in the CD11c+ gate were measured for the 4 ^{o}C and 37 ^{o}C plates, and phagocytic index is plotted as the 37 °C/4 °C ratio of those percentages. The phagocytic index data are averages of 8 total experiments for all conditions with the exception of TUN, which shows the average of four experiments. On average 3-6% of the total added target cells were phagocytosed (B) Surface CRT expression was measured in UV-treated WT & CRT-/- MEFs as described in Fig. 2.1, and data are representative of 3 experiments. (C) Cell death profiles of target cells: CMFDA-labeled MEFs subject to indicated treatments were stained with AnnV-PE and 7AAD to quantify the percentages of MEFs in the indicated populations. Graphs show the averages of 6 experiments for all conditions except TUN treatments, which show the average of 3 experiments. AnnV/7AAD data were not collected in 2/8 experiments. (D) CMFDA fluorescences of various treated MEFs were measured on the FITC channel. Averages of 8 total experiments are shown for all conditions except TUN treatment, which shows the average of 4 experiments. The p-values from two-tailed, paired t-tests are indicated.

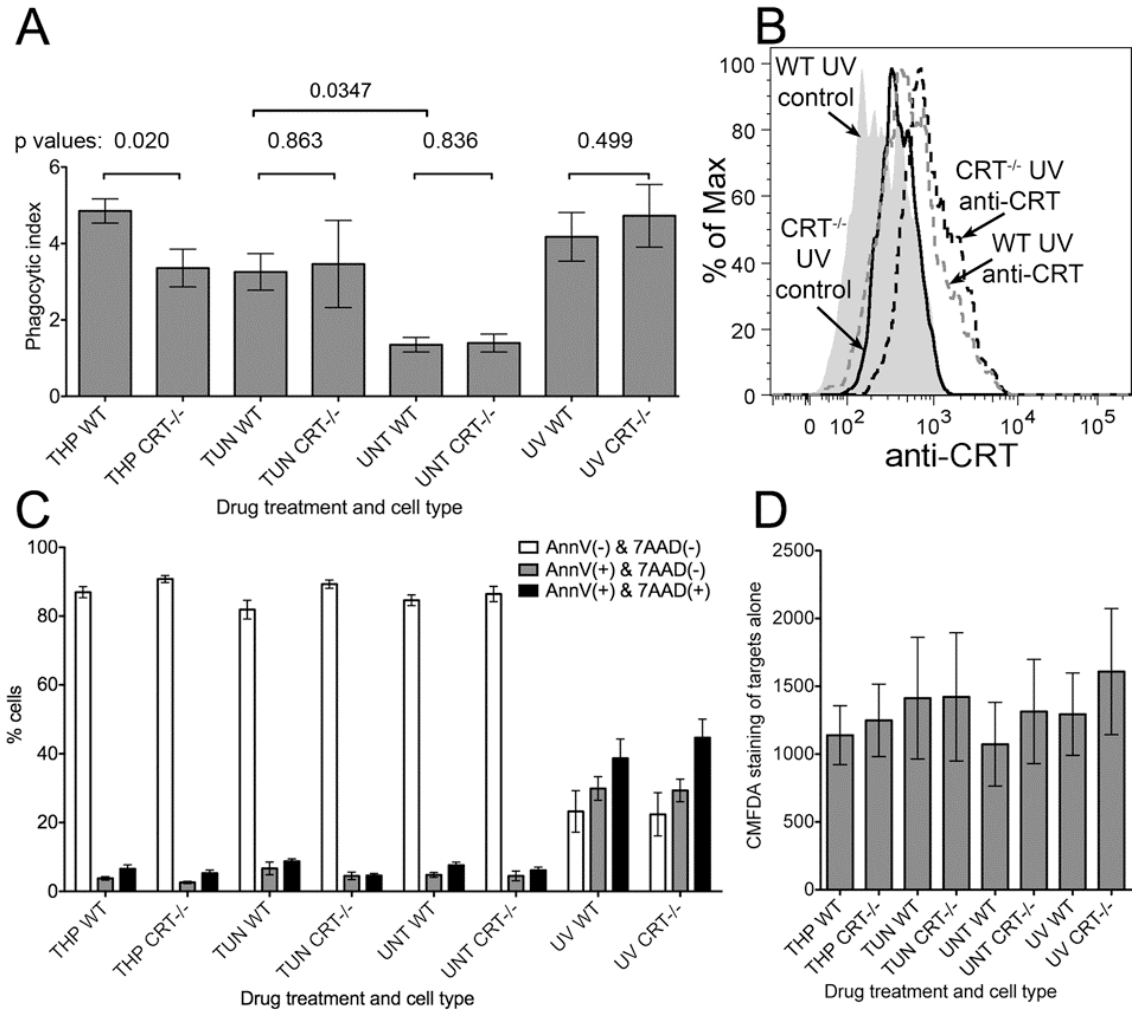

In contrast to UV-treated MEFs, THP-treated WT MEFs were phagocytosed with significantly higher efficiency than THP-treated CRT deficient MEFs and untreated MEFs (**Fig. 3.9A**). The levels of target cell death were similar between WT and CRT deficient MEF target cells within a treatment group (**Fig. 3.9C**). Additionally, the level of dead target cells in the untreated group was least as high as that in the THP-treated group (**Fig. 3.9C**), a result which indicated that cell death in the THP-group was insufficient to account for the level of phagocytic uptake observed. Finally, although TUN treatment

enhanced phagocytic uptake of target cells relative to untreated cells, there was no CRT-dependence to this effect, consistent with the inability to observe cell-surface CRT in TUN-treated cells (**Fig. 2.1B and 2B**). The fluorescence intensities of the various labeled target cells were similar, and could not explain the observed differences in the phagocytic indices (**Fig. 3.9D**). Taken together, these results suggest that THP-treated cells with measurable cell-surface CRT are phagocytosed in a manner that is partially CRT-dependent.

DISCUSSION

Our results show that THP treatment of target cells increases pro-inflammatory cytokine production by BMDC in a manner independent of target cell-derived CRT (**Fig. 3.1**), that extracellular CRT either in a cell-surface bound (**Fig. 3.1**) or soluble form (**Fig. 3.3** and data not shown) is unable to stimulate production of IL-1β, TNF-α, IL-23 or IL-12p70, and that THP treatment of cells impacts their phagocytic uptake in a CRT-dependent manner (**Fig. 3.9**).

Previous studies in HeLa cells have shown that NF-κB activation in response to agents that induce ER stress involves the release of calcium from the ER and the subsequent generation of ROS (reviewed in (Pahl and Baeuerle, 1997)). This mechanism likely accounts for sterile IL-6 production in response to direct THP treatments of BMDC (**Fig. 3.6**). THP is a stronger activator of the sterile IL-6 response than TUN (**Fig. 3.6**) likely due to a rapid effect of THP on cytosolic calcium elevation, whereas elevation of cytosolic calcium in response to TUN treatment may be more modest as well as kinetically delayed. Many recent studies have shown synergies between TLR-derived signals and transcription factors induced by the UPR, including XBP-1 and C/EBP homologous protein (CHOP). Of the cytokines measured in Figures 3.1 and 3.3, XBP-1 was previously shown to synergize with TLR signals in enhancing IL-6 production by murine macrophages (Martinon et al., 2010). In human, monocyte-derived DC, CHOP binding to the IL-23p19 promoter enhanced IL-23 production in response to TLR ligation (Goodall et al., 2010).

Similar mechanisms could account for the synergy of ER stress signals and LPS in IL-23 production by BMDC (**Fig. 3.6**). We found that THP also strongly synergizes with LPS in the generation of IL-1β and IL-12p70. Recent findings showed that high avidity ligation of ITAM-containing receptors such as DAP12 can synergize with TLR signals to activate pro-inflammatory gene expression (reviewed in (Ivashkiv, 2008; Turnbull and Colonna, 2007)). High avidity ligation of DAP12 triggers an acute, transient calcium increase (reviewed in (Ivashkiv, 2008)). Here we show that, compared to TUN, THP treatment more strongly enhances various pro-inflammatory responses to LPS (**Fig. 3.6**), consistent with similar findings from previous studies (Hsieh et al., 2007; Smith et al., 2008). These results point towards direct synergies between cytosolic calcium and TLR responses. Interestingly, it was suggested that ER calcium depletion could occur under certain conditions of ER overload and protein polymerization, even in the absence of classical UPR induction (Davies et al., 2009). Thus, findings described here may be relevant to a better understanding of inflammatory protein folding disorders that do not induce a classical UPR pathway.

A truncated, bacterially-expressed, CRT construct was shown to induce TNF-α production by murine macrophages and human PBMC (Hong et al., 2010). N-terminal truncation of CRT induces self-association likely via the exposure of hydrophobic surfaces (Del Cid et al., 2010; Hong et al., 2010), and it is possible that protein truncation induces enhanced binding to bacterial pathogen-associated molecular patterns (PAMPs). We show here that full-length extracellular CRT derived from an endogenous source does not enhance the production of various pro-inflammatory cytokines in a THP-treated BMDC context (**Figs. 3.1, 3.3** and data not shown). CRT is known to be present in the extracellular environment under a number of physiological conditions, and a number of extracellular functions are described for CRT (reviewed in Ref. (Gold et al., 2010)). Given these extracellular roles of the protein, the lack of innate immune induction by endogenously-derived, extracellular CRT is perhaps not surprising.

BMDC phagocytosed CRT-high, THP-treated, target cells more efficiently than untreated cells in a manner partly dependent on CRT expression by the target cells (**Fig. 3.9**). Experiments performed by Natasha Del Cid and myself (not shown) demonstrated that the level of target cell uptake and association (measured using co-incubations at 37

degrees) increased over time and eventually saturated. This supports the conclusion that this assay is in fact measuring phagocytic uptake. Correlating with undetectable levels of surface CRT in UV-treated cells, an effect of CRT on the phagocytosis of UV-treated cells was not observed (**Fig. 3.9**). In the UV-treated apoptotic cell context, other changes are expected that promote phagocytic uptake (reviewed in (Krysko and Vandenabeele, 2008)), including the exposure of PS, which likely explain why significant uptake was observed in the absence of any CRT expression by the target cells (**Fig. 3.9**). Correspondingly, UV-treated target cells had a higher level of total association (i.e., the combination of uptake and adherence indicated by the 37^{o} C condition) with BMDC than any other target cell group (**Fig. 3.10**). This is likely the result of molecules that are upregulated on the surface of apoptotic cells and responsible for bridging apoptotic phagocytic cargo to potential phagocytes (reviewed in (Krysko and Vandenabeele, 2008)). It is noteworthy that cell-surface CRT functions in the context of several other key eat-me and don't-eat-me signals in viable and apoptotic cells (Gardai et al., 2005; Krysko and Vandenabeele, 2008; Park et al., 2008). The data of Figure 3.9 show that TUN-treated cells displayed enhanced phagocytic uptake compared to untreated cells, although this uptake was not CRT-dependent. This observation correlates with the absence of detectable cell-surface CRT in TUN-treated cells (**Fig. 2.1B**). The same level of uptake was seen with THP-treated, CRT-deficient cells (**Fig. 3.9A**). As shown in Figure 2.4, both TUN and THP significantly reduce cell-surface MHC-I. It is possible that interference with proper protein folding resulting from these treatments also decreases surface expression of don't-eat-me signals like CD47 (Chao et al., 2010; Gardai et al., 2005) and plasminogen activator inhibitor-1 (PAI-1) (Park et al., 2008). This potential decreased surface expression of don't-eat-me signals may explain the increased level of uptake of TUN-treated and THP-treated, CRT-deficient cells by BMDC.

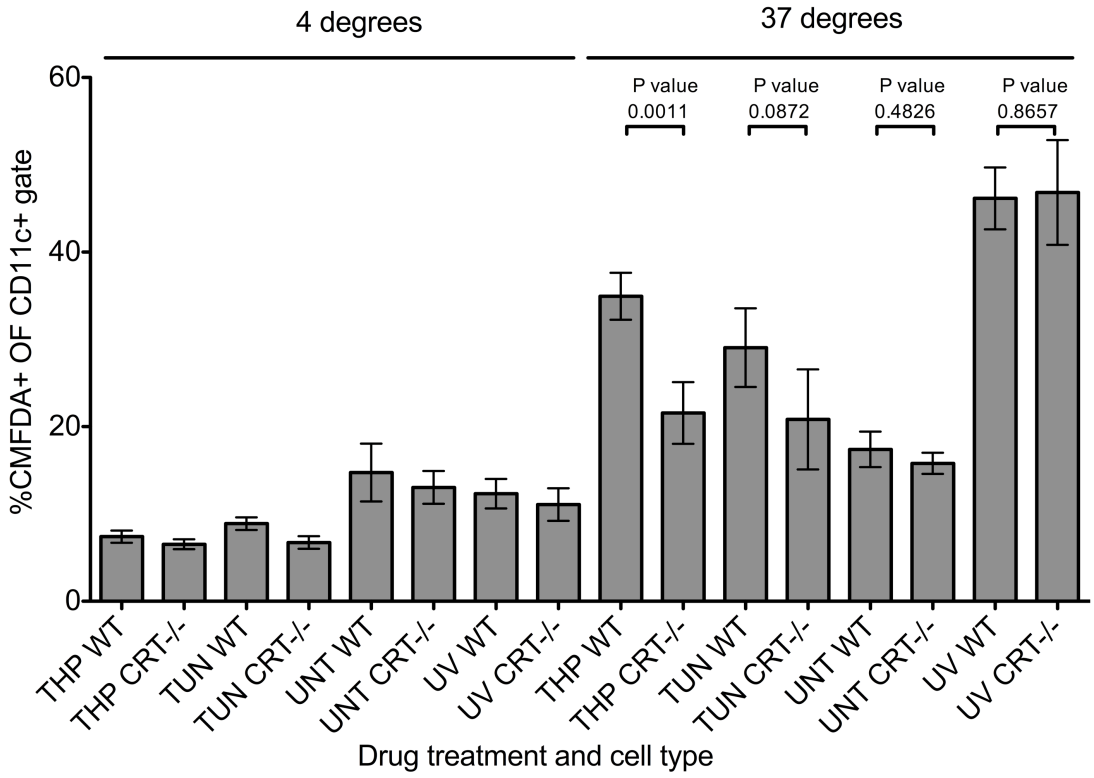

Figure 3.10 UV-treated apoptotic cells have the highest level of association with BMDC of all target cell treatment groups.
The values used to calculate the phagocytic indices shown in Fig. 3.9A (plotted there as the 37°C/4°C ratios) are plotted here separately as percentages of CMFDA+ events in the CD11c+ gate at 4 °C and 37 °C.

In contrast to some previous findings (Obeid et al., 2007b), we show in this chapter that THP promotes phagocytic uptake of cells via mechanisms that are, in part, CRT-dependent. Thus the inability of THP-treated cells to induce anti-tumor immunity with sufficient potency (Martins et al., 2011; Obeid et al., 2007b) is likely not related to an absence of cell-surface CRT *per se*. Other immunogenic signals absent in THP-treated cells, including HMGB1 (Apetoh et al., 2007) and elevated levels of ATP (Ghiringhelli et al., 2009) (**Fig. 3.5**), may be required to confer stronger immunogenicity to treated cells. Consequently, although THP has some potentially desirable attributes for a chemotherapeutic, including the abilities to induce stronger phagocytic uptake of treated cells by DC (**Fig. 3.9**) and elicit stronger cytokine production by DC (**Fig. 3.1 and 3.3**),

these appear to be insufficient signals to confer anti-tumor immune protection (Martins et al., 2011). These observations are highly relevant to the ongoing clinical trials evaluating THP pro-drugs for the treatment of advanced solid tumors (ClinicalTrials.gov Identifier: NCT01056029, (Janssen et al., 2006)). Because phagocytic uptake and cytokine levels can influence T cell priming steps, our results highlight the importance of further research investigating the impacts of different forms of ER stress on the priming of CD8 and CD4 T cell responses.

CHAPTER FOUR
Discussion

Given the range of necessary, basic cellular processes carried out by the ER, it is no surprise that deregulation or malfunction of the ER is associated with many diseases (Yoshida, 2007). Specifically, the connection between the ER stress response and diseases involving inflammation and autoimmunity generates much interest (Hummasti and Hotamisligil, 2010; Todd et al., 2008; Yoshida, 2007). Recent research suggests that parts of the ER stress response pathway are not only involved in excessive, disease-related inflammation, but are also required for mounting a complete inflammatory response to defend against infection (Martinon et al., 2010). Additionally, because of the stressful environment within a tumor, the UPR is an important survival tool for many cancer cells (Healy et al., 2009). Clearly, the ER stress response is an important area of study for understanding the etiology of many diseases, including cancer (Healy et al., 2009), neurodegenerative disorders (Yoshida, 2007), cardiovascular disease (Minamino et al., 2010), obesity and diabetes (Hummasti and Hotamisligil, 2010) and autoimmune diseases (Todd et al., 2008). Therefore, modulation of the ER stress response is a promising drug target for these and other diseases. Supporting this idea, some recent research retrospectively connects modulation of the ER stress pathway with mechanisms of action for pharmaceuticals currently in use (Obeid et al., 2007b; Yoshida, 2007).

Within the cell, ER-resident chaperones and HSPs are important in mediating the ER stress response. Given that the HSP protein family is widely implicated in modulating the immune response in a variety of ways when present outside the cell (reviewed in chapter 1), studying the mechanisms of immunomodulation by extracellular HSPs in the context of ER stress may enhance understanding of the complex interactions between ER stress and inflammation. Furthermore, additional research on immunomodulation by HSPs is needed to guide the current and future clinical efforts to use extracellular HSPs to treat disease (Testori et al., 2008).

My thesis focused on understanding several biological aspects of extracellular ER chaperones and HSPs in the context of ER stress, with a primary focus on CRT, an HSP strongly implicated in phagocytosis of apoptotic cells and induction of anti-tumor immunity. Specifically, my thesis investigated mechanisms of chaperone release from the cell, the ability of the combined presence of several extracellular HSPs to influence innate immune responses, and the ability of extracellular CRT to enhance phagocytosis. In all three cases, we investigated these areas in the context of THP- or TUN-induced ER stress.

Recently, the lab of Dr. Guido Kroemer characterized a stimulus-specific pathway for increased pre-apoptotic expression of cell-surface CRT (summarized in chapters 1 & 2), induced by stimuli such as the chemotherapeutic MTX. This mechanism of cell-surface CRT expression required calreticulin to be in complex with ERp57. However, other ER proteins were reported to be retained (with lysyl-tRNA synthetase [KARS] being the only exception (Kepp et al., 2010)). Furthermore, the mechanism described by Kroemer et al. involves transport of ERp57:CRT complexes through the secretory pathway in a manner that requires ER stress-induced PERK activation and ROS (Panaretakis et al., 2009). Finally, MTX treatment is reported not to induce detectable secretion of CRT despite high levels of CRT on the cell surface (Kepp et al., 2010). Prior to this study, Kroemer's model for cell-surface CRT induction was the only published model for pre-apoptotic cell-surface CRT expression. We sought to further characterize cellular and molecular processes involved in cell-surface CRT induction with a focus on ER stress.

In chapter 1, we characterize a novel pathway of transient, pre-apoptotic cell-surface CRT expression in response to THP-induced, ER calcium depletion. Mechanisms of THP-induced, and MTX-induced, cell-surface CRT have some similarities, but several key differences in their characteristics. Following short exposures to drug, THP-induced cell-surface CRT levels were much higher than MTX-induced cell-surface CRT (**Fig. 2.1**). Cell surface CRT was not detectable on the surface of apoptotic cells following long exposures to THP (**Fig. 2.1**). Cell-surface CRT expression in response to THP did not occur in all cell types examined (**Fig. 2.4**). Co-incident with short THP treatments, several ER chaperones are secreted: CRT, PDI, BIP and gp96 (**Fig. 2.5**). THP-induced

cell-surface CRT travels through the secretory pathway (**Fig. 2.6**). This finding rules out CRT transit through the cytosol, another recently proposed, but less-well characterized pathway for surface CRT expression on apoptotic cells (Tarr et al., 2010). In contrast with MTX, THP-induced cell surface CRT did not require the CRT:ERp57 interaction, and ERp57 was not detected on the cell surface (**Fig. 2.7**). Interestingly, we show that polypeptide binding by CRT was required for its retention on the cell surface (**Fig. 2.9**). Finally, we show that primary, apoptotic, plasma cells (a highly secretory, cell-type subject to acute and constitutive ER stress as part of its normal development and function), have high levels of cell-surface CRT easily detectable by flow cytometry. In our assays, cell surface CRT was not measurable on other apoptotic lymphocytes and splenocytes (**Fig. 2.9-11**) and a variety of other cell types tested (**Fig. 2.1**). These studies show that increases in cell-surface CRT expression can occur by mechanisms other than ERp57 co-transport, and that a measurable up-regulation of cell-surface CRT is not a universal feature of apoptotic cells.

Our published work shows that THP treatment leads to a greater induction of pre-apoptotic cell-surface CRT than MTX treatment (Peters and Raghavan, 2011b). The work of Kroemer et al. showed the opposite trend (Obeid et al., 2007b). Because of this contrast, we tested the effects of primary antibody, cell line, fixation of stained cells, and solvent used for mitoxantrone solution on cell surface CRT induction. Variations in experimental techniques included using the same anti-calreticulin antibody used in Obeid et al 2007, the same cell line used in the majority of Kroemer's work (CT26), using a different solvent to reconstitute the MTX, and experiments with and without fixation of the stained cells. Similar levels of CRT induction were obtained using the rabbit-anti-CRT antibody (Abcam) used by Kroemer and colleagues or chicken-anti-CRT (Affinity Bioreagents) antibody used by Gardai and colleagues (Gardai et al., 2005). Consequently, Figures 2.1 and 2.2 include experiments performed with both antibodies (as described in the materials and methods). Additionally solublizing MTX in ethanol instead of DMSO did not lead to higher CRT induction by MTX (data not shown). The data shown used MTX reconstituted in DMSO. However, we performed additional and experiment with MTX in ethanol. This did not improve the relative induction of cell-surface CRT by MTX (data not shown). Furthermore, cell-surface CRT induction in CT-26 cells was

unaltered by fixation of the stained cells (data not shown). We conclude that the described differences in our cell-surface CRT induction data compared to that published by Kroemer and colleagues are not due to the described experimental variations. However, there were procedural differences in the cell death stains in our protocol that may explain some of the discrepancy in the data (ie. Our cells were triple stained with CRT, a permability marker and Annexin-V).

Identifying conditions that induced cell-surface CRT expression and secretion of several ER chaperones (chapter 2), allowed us to investigate extracellular functions of several HSPs (chapter 3). Specifically, we examined whether or not CRT-high, THP-treated cells induced production of several cytokines by BMDC, or suppressed BMDC cytokine production in response to LPS. This is of great interest because several of the ER chaperones secreted by THP-treated cells are reported to strongly modulate the innate immune response in other experimental or physiological systems. Furthermore, cell-surface CRT is widely reported to have a very active role in inducing anti-tumor immune responses (reviewed in (Tesniere et al., 2008)). The use of WT & $CRT^{-/-}$ MEFs in our experiments directly assessed the contribution of the innate immune response to the role of cell-surface CRT in anti-tumor immunity. Finally, we examined phagocytic uptake by an APC (BMDC) of target cells subjected to two different types of ER stress and the effect of CRT expression by the target cells (**Fig. 3.9**).

We show that THP-treated cells and CM stimulate sterile production of IL-6, but not IL-1β, IL-12p70, TNF-α, and IL-23 despite the extracellular presence of BIP, CRT, gp96 and PDI (**Fig. 3.1 and 3.2**). Furthermore, the extracellular presence of these HSPs with or without THP-treated cells did not dampen production of IL-1β, IL-12p70, TNF-α, and IL-23 by BMDC in response to LPS (**Fig. 3.1 and 3.2**). Interestingly, the LPS-induced production of IL-1β, IL-12p70, TNF-α, and IL-23 was dramatically increased following co-incubation with THP-treated cells or cell CM (**Fig. 3.1 and 3.2**). Importantly, none of the cytokine responses measured were altered by or dependent on CRT expression by the THP-treated cell (**Fig. 3.1 and 3.2**). BMDC co-incubations with THP-treated target cells were compared to co-incubations with MTX and TUN-treated cells, and neither of the latter two conditions altered innate immune responses by BMDC (**Fig. 3.1 and 3.2**). This is quite relevant in understanding the ability of MTX-treated cells

to stimulate protective and therapeutic anti-tumor immune responses when injected into mice. Our data suggests for the first time, that the immunogenicity of MTX-treated tumor cells may be limited to its influence on the adaptive immune response (Obeid et al., 2007b). Of equal or greater importance, we used drug-treated (MTX and THP) WT and $CRT^{-/-}$ target cells as potential stimuli for BMDC cytokine production. In doing so, we convincingly demonstrated that the important role cell-surface CRT plays in inducing an anti-tumor immune response does not involve its stimulation of pro-inflammatory cytokine production by DC. An important next step of these experiments is to evaluate whether other APC subsets respond differently to cell-surface CRT *in vitro* and *in vivo*.

In order to further understand the mechanism by which THP-induced ER stress in target cells stimulated BMDC cytokine production in a paracrine manner, we compared BMDC responses to direct treatment with the two ER stress inducers TUN & THP (**Fig. 3.6**). These analyses showed that both a direct TUN or THP treatment of BMDC induce cytokine expression with a similar pattern as that observed with THP-treated cells and cell CM (**Fig. 3.1 and 3.3**). However, THP more strongly enhanced LPS-induced expression of IL-1β and much more strongly (~10 fold) induced sterile IL-6 production than TUN (Fig. 3.6). Several effects downstream of the (likely) stronger and faster calcium flux induced by THP (relative to TUN) may explain the difference in IL-1β and IL-6 production. Consistent with this possibility, Hsieh et al. showed that THP induced over 2 fold more ROS than TUN treatment of NIH3T3 MEFs. This was attributed in part to the strong calcium efflux from the ER and/or an ER overload response (EOR) induced by THP-treated cells (Hsieh et al., 2007). Notably, ROS influence many signaling pathways. In particular, ROS can induce NFκB translocation to the nucleus (ie. activation) by promoting the degradation of its endogenous inhibitor IκB (Chen et al., 2009). Therefore, increased ROS induced by THP is likely to lead to increased NFκB activation and subsequent increased IL-6 production though this mechanism, and possibly others. ROS also control the priming of the NLRP3 inflammasome, which is required for mature IL-1β secretion following LPS addition (Bauernfeind et al., 2011). Again, the increased levels of ROS induced by THP relative to TUN are implicated in the enhanced pro-inflammatory profile induced by THP treatment of BMDC. These findings are relevant to understanding inflammatory protein folding disorders involving ER

calcium depletion as a result of an EOR (Davies et al., 2009; Pahl and Baeuerle, 1997) in the presence or absence of a classically defined UPR (discussed in more depth below).

We next sought to characterize the stimulatory factor(s) released from THP treated cells. We first examined the release of the known endogenous DAMPs HMGB1 and ATP. These analyses suggested that ATP and HMGB1 are not responsible for the stimulation induced by THP-treated cells (**Fig. 3.6B-D**). BMDC had similar responses to direct THP treatment and to paracrine stimulation by washed, THP-treated target cells (and cell CM). Therefore, we investigated whether the washed, THP-treated cells released soluble THP molecules, resulting in direct BMDC stimulation by dialyzing THP CM. We established that the paracrine stimulatory factor(s) released from THP-treated target cells was/were larger than 10 kDa (**Fig. 3.7**). Because THP monomers have a molecular mass of 650 Da, these findings suggest the paracrine stimulatory factor(s) is/are likely one or more of the following: 1) an unmodified (or stress-modified) endogenous DAMP/stimulatory factor released from the THP-treated target cells; or 2) residual THP either bound to other molecules with a larger molecular mass or in multivalent complexes larger than 10 kDa (**Fig. 3.7**). Scenario 1 could still potentially be involved in the stimulation of BMDC by direct THP treatment by release of factors and their acting in an autocrine or paracrine manner in the BMDC culture.

Several lines of evidence discussed in chapter 3 lead us to favor the idea that THP molecules themselves are responsible for the stimulation of BMDC by THP-treated cells or CM from THP-treated cells. Notably, qualitatively, cytokine production resulting from ER stress occurring within TUN-treated DC was similar to that in THP-treated DC (chapter 3), and my work in chapter 2 showed that TUN does not induce release of suspected DAMPs (HSPs). This conclusion is in agreement with recent publications showing that various ER stress stimuli (not associated with a failure in ER retention) synergize with LPS ligation in macrophages and B-cells resulting in greatly enhanced cytokine production (DeLay et al., 2009; Goodall et al., 2010; Martinon et al., 2010; Smith et al., 2008). Building on these observations, Martinon et al. showed that activated XBP-1 plays a role in enhancing pro-inflammatory cytokine production in response to PRR ligation that is independent from its role in inducing UPR (Martinon et al., 2010). This role for XBP-1s was not demonstrated for sterile IL-6 production during ER stress,

however, it may still be relevant to my observations of sterile IL-6 production in response to THP & TUN (chapter 3). Together, my results suggest that any endogenous factors released from THP-treated target cells, such as the HSPs BIP or gp96, are unable to significantly suppress or induce innate immune responses. This possibility is consistent with the inability of cell-surface (**Fig. 3.1**) or secreted (**Fig. 3.3**) CRT to influence innate immune responses, examined more directly with $CRT^{-/-}$ MEFs.

Interestingly, we showed that BMDC phagocytosed ER stressed target cells at levels significantly above background uptake of dead cells in the UNT target control (**Fig. 3.9-3.10**). As shown in Figure 3.9C the average levels of viable [AnnV(-), & 7AAD(-)] cells is 82-91% for the UNT, TUN & THP target cells and 22-23% for UV-treated apoptotic cells. It is interesting to speculate that with THP and TUN-treated target cells, we observed PS-independent phagocytic uptake of the viable cells rather than PS-dependent uptake of the 10-20% of dead cells. Although our experiments did not directly test this possibility, comparing the relative levels of dead cells and phagocytosis under each condition suggests PS-independent uptake of viable cells. As indicated in chapter 3, if phagocytic uptake of these viable, ER stressed cells is occurring, it is likely due to the down-regulation of don't eat me signals.

We showed in chapter 2 that TUN & THP caused significant down-regulation of a constitutively-expressed cell surface protein, MHC-I (**Fig. 2.4**). Although MHC-I is not a 'don't eat me' signal, this observation demonstrates that ER stress results in the down-regulation of at least one cell-surface protein. This observation is consistent with the hypothesis that a don't eat-me signal could be down-regulated by ER stress. Furthermore, the UPR-induced block in translation of non-essential proteins [reviewed in (Todd et al., 2008)] is a potential cause of down-regulation of some cell-surface proteins during ER stress. Another potential mechanism of down-regulation of specific cell-surface proteins during ER stress may be the induction of specific 'sheddases.' Sheddases, such as members of the "A Disintegrin And Metalloprotease" (ADAM) family can proteolytically cleave the ecto-domain of integral membrane proteins. It is possible that ER stress induces shedding of specific cell-surface proteins by altering the expression or activation of sheddases. Knock-out mice exist for several ADAM family members (reviewed in (Reiss and Saftig, 2009)). Use of cells from these mice would allow

examination of the role of various ADAM family members in down-regulation of constitutively expressed cell-surface proteins in response to ER stress. In conclusion, ER stress may down-regulate 'don't-eat me' signals through various mechanisms, and further investigations of these observations are needed.

Other papers demonstrated phagocytic uptake of live cells by blocking 'don't eat-me' signals or receptors for 'don't eat me' signals (Chao et al., 2010; Gardai et al., 2005; Park et al., 2008). However, to my knowledge, our work provides the first suggestion that ER stress could potentially promote phagocytic uptake by APCs via interference with expression of don't eat me signals. This possibility has interesting implications for the maintenance of peripheral tolerance and the loss of peripheral tolerance and deserves further study. Specifically, the ability of various types of ER stress to down-regulate known don't-eat me signals should be examined.

In order for PS-independent phagocytic uptake to occur, eat-me signal(s) must be present on the cell surface. Although we didn't detect distinctive signals for cell-surface CRT in most situations we examined using flow cytometry, most papers examining viable cells by microscopy show CRT on the surface of viable cells (Gardai et al., 2005; Kuraishi et al., 2007; Obeid et al., 2007a; Panaretakis et al., 2009; Park et al., 2008; Tufi et al., 2008). Therefore, it is possible that cell-surface CRT may play a role in the uptake of TUN cells, despite the fact that we did not detect surface CRT by flow cytometry. Supporting this idea, TUN WT cells' total association (37 degree condition) with BMDC was higher than that seen with TUN $CRT^{-/-}$ cells (**Fig. 3.9** – 37 degree condition), although this difference did not achieve statistical significance (p=0.0872, n=4) (**Fig. 3.9**). As described earlier, total association is a measure of the target cells adhered to the outside of the BMDC (measured by co-incubations at $4^{o}C$) and the target cells phagocytosed by BMDC. In the context of TUN-treated cells, CRT may act to bridge targets to BMDC. These types of differences were not detected with the UV-treated targets (**Fig. 3.9**), where phosphatidylserine exposure and other cellular changes could promote bridging and uptake. The experiments of Figures 3.9 & 3.10 showed a relatively high degree of variation due in large part to the relatively low phagocytic indices when measuring BMDC phagocytosis of target cells by this assay. The magnitudes of our phagocytic indices are consistent with previously published examples of these assays

(Kopecka et al., 2011; Obeid, 2008; Obeid et al., 2007b). The low positive signal results in a greater influence of natural experimental variability. Furthermore, data measuring phagocytic uptake of TUN-treated (n=4) and UV-treated (n=8) $CRT^{-/-}$ targets were particularly variable. These factors considered, it remains possible, or even likely, that cell-surface CRT plays a role in the uptake of TUN-treated cells.

In the context of a different type of ER stress (THP-induced ER calcium depletion) a role for cell-surface CRT in inducing uptake by BMDCs is quite unambiguous. We showed that BMDC phagocytosed CRT high, ER calcium-depleted cells at levels similar to those of UV-treated apoptotic cells, in a manner significantly enhanced by CRT (**Fig. 3.9-3.10**). It should be noted that ~80% of the UV-treated apoptotic cells were positive for the strong eat-me signal PS (**Fig. 3.9C**). As mentioned, Figure 3.9 indirectly suggests that PS-negative viable THP-treated cells are phagocytosed by BMDC. Consistent with this possibility, other reports suggest that BMDCs can phagocytose CRT-high, PS negative cells in the context anthracyclin-treated pre-apoptotic cells (Obeid, 2008; Obeid et al., 2007b).

Our report of high levels of cell-surface CRT significantly enhancing uptake of THP-treated (likely PS negative) cells is also consistent with CRT's described role as an 'eat-me' signal on the surface of apoptotic, PS positive cells (Gardai et al., 2005; Kuraishi et al., 2007). However macrophages or fibroblasts were used as the phagocytes in the previous demonstration of CRT-dependent uptake of mammalian apoptotic cells (Gardai et al., 2005). CRT dependent uptake of apoptotic cells was also described in *Drosophila*, but it is already known that PS is not used as an eat-me signal in *Drosophila* (Kuraishi et al., 2007). Therefore, to my knowledge, our analysis of the relative contributions of PS-mediated uptake and CRT-mediated uptake of mammalian UV-treated apoptotic cells is the first such examination with DC (**Fig. 3.9-3.10**). Although we weren't able to measure UV-induced increases in cell-surface CRT by flow (**Fig. 3.9B**), it is quite possible that some cell-surface CRT is present. As discussed, evaluations of UNT cells often detect only background levels of cell-surface CRT by flow (similar to what we see with UNT cells and UV-treated cells) (Obeid, 2008; Obeid et al., 2007b), yet fluorescence microscopy typically reveals cell-surface CRT on UNT neutrophils and transformed cell lines (Gardai et al., 2005; Obeid et al., 2007a; Paidassi et al., 2011;

Panaretakis et al., 2009; Park et al., 2008; Tufi et al., 2008). These observations support the idea that although we didn't detect any specific increases in CRT surface expression following UV-treatment, it may still be present on the surface. This possibility is further supported by findings from at least two other groups that UV induces CRT cell-surface expression (Gardai et al., 2005; Obeid et al., 2007a; Paidassi et al., 2011).

Regardless, our analysis of uptake of UV WT & $CRT^{-/-}$ MEFs by BMDC reveals the important finding that BMDC are not dependent on CRT expression in the target cell for uptake of apoptotic cells. However, these experiments must be conducted in other DC subsets to confidently extend these conclusions into *in vivo* situations. As mentioned, macrophage (J774, peritoneal, and human-monocyte derived)-mediated phagocytosis was suggested to be highly dependent of CRT expression in apoptotic target cells (Gardai et al., 2005), which contrasts with our findings in BMDC. In many cases, DC and not macrophages are the cells responsible for professional antigen presentation during T-cell priming (reviewed in (Savina and Amigorena, 2007)). Therefore, more research investigating the relative contributions of PS and CRT-mediated signaling in the phagocytic uptake of apoptotic cells by various DC subsets is needed. Such studies would contribute to the understanding of mechanisms of DC-induced peripheral tolerance and adaptive immune responses to cell-associated antigens.

More questions remain regarding precisely how cell-surface CRT expression on dying tumor cells drives the anti-tumor immune responses reported by Kroemer and colleagues (reviewed in (Zitvogel et al., 2010)). My work clearly demonstrates that cell surface CRT does not induce proinflammatory cytokine expression by BMDC (chapter 3). In the absence of PS surface exposure CRT surface expression significantly enhances uptake of targets by DC (chapter 3, this thesis and (Obeid et al., 2007b)). However, my work shows for the first time that BMDC (or any DC subset) uptake of apoptotic cells killed by UV light is not affected by CRT expression in the target cell. This finding suggests that CRT may not enhance delivery of apoptotic-cell associated antigens to DC. However, different DC subsets could differ in expression of CRT specific receptors and in their abilities to mediate CRT-dependent uptake of apoptotic targets.

Consequently, the recent finding that lymph node resident, CD11c+CD169+ 'macrophages' are required for cross-priming anti-tumor immune responses to

subcutaneously injected apoptotic tumor cells is particularly interesting (Asano et al., 2011). Subcutaneous vaccination is the route used to show that surface CRT-high dying tumor cells are highly immunogenic (Obeid et al., 2007b). In contrast, a CD8α+CD103+CD207+ DC subset in the spleen was recently suggested to be responsible for tolerance induction to blood-born apoptotic cells (Qiu et al., 2009). PS exposed on apoptotic cells is known to be dominantly immunosuppressive and cell-surface CRT is required for induction of many experimentally induced, protective anti-tumor immune responses (Green et al., 2009). Therefore I propose that the APC subsets responsible for generating tolerance to cell-associated antigens (such as splenic CD8α+CD103+CD207+ DC) receive PS-mediated signals from apoptotic cells that promote T-cell tolerance to presented antigens. Furthermore, I propose that APC subsets responsible for activating T-cells specific to cell-associated antigens (such as LN-resident CD11c+CD169+ macrophages), preferentially receive signals from apoptotic cell-surface CRT (rather than PS) that enhance T-cell activation against presented antigens. The signals from cell-surface CRT may alter antigen processing and presentation, or may simply prevent PS-mediated immunosuppression. An important note in considering my proposed model, is that Qiu et al. showed uptake of apoptotic cells by CD11c+CD169+ macrophages was PS-dependent. To suggest this, they showed that blockade of PS on apoptotic target cells with a mutant MFG-E8 blocked apoptotic cell uptake (Asano et al., 2011). However CRT co-localizes with PS in clusters on the apoptotic cell surface (Gardai et al., 2005), so it is possible that protein binding to PS sterically blocks access of macrophage receptors for CRT on the apoptotic cell surface. In conclusion, my results showing CRT-independent phagocytosis of apoptotic cells by DCs warrant further investigation on how different 'eat-me' signals differentially effect antigen presentation by various APC subsets.

Thapsigargin as a chemotherapeutic

Unlike many current chemotherapies that are cytotoxic to proliferating cells, thapsigargin is cytotoxic to both proliferating and quiescent cells (ie., cells in growth arrest) (Denmeade et al., 2003). Some cancers, such as prostate cancer, have many non-proliferative or slowly proliferative cells (Denmeade et al., 2003). Furthermore, some

prostate cancer cells are resistant to a current therapeutic regiment of choice because of a lack of a sustained rise in intracellular calcium (and subsequent apoptosis) in response to a current treatment. These observations led to the development of thapsigargin prodrugs that are targeted to prostate cancer cells. Phase I clinical trials are currently evaluating dosage and pharmacokinetics of targeted THP pro-drugs in patients with advanced solid tumors (ClinicalTrials.gov Identifier: NCT01056029, (Janssen et al., 2006)).

Because apoptosis is usually immunosuppressive, the search of chemotherapeutics that induce immunogenic cell death is of interest. The pursuit of clinical applications for THP was part of the justification for the work described in this thesis that investigated the immunological consequences of thapsigargin. The previous work from G. Kroemer and colleagues suggests that thapsigargin does not induce immunogenic cell death in mouse tumor immunization models (Martins et al., 2011; Obeid et al., 2007b). However, in Kroemer's studies, THP-treated tumor cell vaccines induced tumor growth in the vaccination flank (Martins et al., 2011). This finding suggests that the preparation contained too many live cells and this needs to be re-examined.

My work contributes to knowledge about the potential immunological properties of thapsigargin-mediated cell death. I showed that thapsigargin induces high levels of cell-surface calreticulin (chapter 2), phagocytic uptake of treated cells, and pro-inflammatory cytokine production by BMDC (chapter 3). Despite these effects, THP-treated tumor cells may prove not to be a stimulator of anti-tumor immunity for several reasons.

First, Torchinski et al. showed phagocytosis of infected apoptotic cells by DC resulted in production of IL-6 and TGF-β (Torchinsky et al., 2010). Furthermore, Torchinski et al. showed that the conditioned media from these DC induced differentiation of naïve CD4 T-cells into a FoxP3(-), IL-10 producing immunosuppressive T-cell subset (in addition to the Th17 cells induced by the conditioned media from the described DC, which was the focus of the paper) (Torchinsky et al., 2010). Relevant to this, I showed that BMDC exposed to THP or THP-treated cells produce sterile IL-6 (chapter 3). As mentioned, a vaccine with THP-killed tumor cells cannot have any pre-apoptotic cells or it will induce the growth of a tumor in the

vaccination flank prior to the induction of an immune response (Martins et al., 2011). Therefore, vaccination with THP-killed cells will likely have mostly PS-positive apoptotic cells that lack high levels of cell-surface CRT (chapter 2). The BMDC or macrophages phagocytosing these THP-treated tumor cells may produce TGF-β in response to the PS (reviewed in (Green et al., 2009)). Consequently, APC phagocytosing apoptotic THP-treated cells may drive the differentiation of tumor-specific CD4-T-cells into an IL-10 producing immunosuppressive phenotype. However, in a more clinically relevant therapeutic system (or in the clinical trials), the THP-killed tumor cells may be phagocytosed prior to PS-exposure due to a high-level of pre-apoptotic cell-surface CRT (chapter 2). In this situation, it is possible that TGF-β would not be produced and effective anti-tumor immune responses may be induced. The second reason THP may not prove to be an immunogenic chemotherapeutic is due to high levels of NO shown by others to be induced by THP (Hsieh et al., 2007). This is suggested because NO production by iNOS activation in DC was recently shown to be required for apoptotic cell-mediated immunosuppression by DC (Ren et al., 2008). However, these studies used dexamethasone-induced apoptosis that may not induce cell-surface CRT. Additionally, a different group recently showed that iNOS activation and subsequent NO production in anthracyclin-treated tumor cells was required for cell-surface CRT expression and phagocytic uptake by DC (De Boo et al., 2009). It is likely that the effects of NO production in DC are context specific, and is a possibility that requires further investigation. The final reason THP may not prove to be an immunogenic chemotherapeutic in some situations is that its ability to induce high levels of cell-surface CRT appears to be cell-type specific. Therefore it is of interest to characterize the immunogenicity of more clinically-relevant cell-types (prostate cancer cells) treated with THP. As a first step, we showed that human multiple myeloma's (RPMI8226 and H929) do not show detectable THP-induced increases in cell-surface CRT (**Fig. 2.2B**).

ER calcium depletion and inflammatory disorders

Together, this work identifies important differences between ER stress that is induced primarily by protein misfolding (due to pharmacological inhibition of the ER glycosylation machinery (TUN)) versus that induced primarily by ER calcium depletion

(due to inhibition of calcium uptake into the ER (THP)). Primarily we showed that THP but not TUN treatment induces a global handicap in ER retention leading to abnormal secretion (and surface expression in some cases) of ER resident proteins (chapter 2). Furthermore, direct THP treatment of BMDC induces ~10 fold more sterile IL-6 and ~2 fold more LPS-stimulated IL-1β production than TUN treatment, (**Fig. 3.6**). These observations suggest that these two drugs may elicit different types of ER stress.

The idea that THP and TUN-mediated ER stress are distinct is consistent with a model originally proposed in 1995, wherein the ER responds differently to overload occurring in the absence of protein misfolding (EOR), than it does to accumulation of misfolded proteins in the ER (UPR) (Pahl and Baeuerle, 1995). The EOR model consists of ER overload leading to ER calcium depletion, reactive oxygen species generation and activation of NFκB (Pahl and Baeuerle, 1996). The existence of an EOR that doesn't induce the UPR was supported by some early observations surrounding the accumulation of a clinically relevant mutant anti-trypsin protein in the ER of hepatocytes. Specifically, in 1990, Graham et al. showed that mutant protein accumulation in the ER did not lead to upregulation of BIP (one of many downstream effects of UPR activation) yet did lead to NFκB activation (Graham et al., 1990). However, PERK activation by ER stress also leads to NFκB activation, and a lack of BIP upregulation did not entirely rule out activation of the UPR (Deng et al., 2004). Furthermore, many of the stimuli used to initially characterize the EOR (Pahl and Baeuerle, 1996) are also now known to induce UPR. Therefore, for many years, it was difficult to identify physiological (or convincing experimental) conditions where the ER becomes overloaded, yet does not have an accumulation of misfolded proteins, and has a stress response distinct from the UPR. Because of this, research on, and understanding of, the EOR is less extensive than that of the UPR.

Recently, however, the existence of an 'EOR' completely distinct from the UPR was confirmed (Davies et al., 2009; Hidvegi et al., 2005). Study of familial dementia caused by mutant neuroserpin proteins that accumulate and polymerize in the ER revealed an EOR completely independent from the UPR (Davies et al., 2009). Like the originally proposed EOR (Pahl and Baeuerle, 1996), Davies et al. showed that the activation of NFκB (a transcription factor involved in the induction of immune

responses) in response to mutant neuroserpin accumulation in the ER required ER calcium flux into the cytosol (Davies et al., 2009). Furthermore, inflammation is associated with the etiology of dementia caused by mutant neuroserpin EOR (Leonard, 2007). My data in Figure 3.6 suggest that the ER calcium flux associated with EOR is likely much more pro-inflammatory than UPR, which supports the view that an EOR is an important factor driving the pathogenic inflammation in this disease and other diseases where an EOR is implicated.

In atherosclerosis, ER overload of a different kind is implicated in inducing inflammation. Macrophages in atherosclerotic plaques take up free cholesterol (FC). This leads to an abnormal increase ('overload') in the cholesterol composition of the ER membrane known as membrane 'stiffening' (Li et al., 2004). Such stiffening is suggested to inactivate SERCA by increasing the structural order of the ER membrane and restricting the movement of SERCA (Li et al., 2004). Interestingly, in the model of neuroserpin polymer accumulation in the ER, Davies et al, proposed that 'Ordered Protein Response' (OPR) was a better term than EOR to describe the effects of neuroserpin accumulation in the ER (Davies et al., 2009). Their use of the term 'order' suggests that increased ER order (or restriction of fluidity) is a common mechanism driving ER-induced inflammation in atherosclerosis and other OPR-related diseases.

As in diseases associated neuroserpin-induced OPR, inflammation also plays a role in the pathogenesis of atherosclerosis. Inflammation in atherosclerotic plaques is linked to 2/3 of heart attacks and strokes by promoting plaque rupture (Charo and Taub, 2011). Furthermore, IL-6 controls expression of genes positively linked to the risk of atherosclerosis (Brasier, 2010). In the case of atherosclerosis, the SERCA inhibition induced by increased order of the ER was implicated in inducing inflammatory cytokines IL-6 & TNF-α (Li et al., 2005). In the case of atherosclerosis, UPR is induced (Feng et al., 2003), unlike during neuroserpin accumulation in the ER where OPR is suggested to occur independently of UPR (Davies et al., 2009). However, because inhibition of SERCA is the proposed mechanism leading to FC-loaded stress in atherosclerosis, it would most likely resemble THP treatment, and have an OPR and UPR.

My data comparing pro-inflammatory responses of BMDC subjected to TUN or THP-induced ER stress, suggests that FC loading of the macrophage ER membrane

occurring during atherosclerosis would result in much more sterile IL-6 production than compared to a situation where UPR alone is responsible for the inflammation detected. Furthermore, it is possible that macrophages in atherosclerotic plaques exhibit the other THP-induced phenotypic characteristics I have described: loss of ER retention and synergistically enhanced LPS-induced cytokine production (and possibly primed NLRP-3 inflammasomes). These potential consequences of FC loading may further contribute to atherosclerosis and should be investigated. Currently, it is unknown what signals link Davies et al.'s proposed OPR during neuroserpin polymerization within the ER, to ER calcium depletion. However, experiments measuring the freedom of SERCA movement in neuroserpin-induced ER overload may reveal that it is the increase in ER order that causes SERCA inhibition in a mechanism similar to that seen in FC-loaded macrophages.

ER stress, tolerance and autoimmunity

As stated previously, although my data suggest that HSPs like CRT, gp96 and BiP do not stimulate innate immune responses, it supports a role for promoting presentation of cell-associated antigens to T-cells through enhanced phagocytic antigen delivery to APCs (chapter 2). Some research investigators occasionally speculate about the involvement of extracellular CRT (Eggleton and Llewellyn, 1999) and gp96 (Han et al., 2010) in the pathogenesis of autoimmune diseases such as lupus and rheumatic arthritis. It is interesting to hypothesize what physiological conditions might induce the loss of ER retention in a stressed target cell (chapter 1), and sterile inflammatory cytokine production by a surrounding APC (chapter 2). The first question to answer is whether or not a physiological source of ER calcium depletion, such as an EOR/OPR, induces cell-surface CRT. This could promote uptake of a PS-negative, self-cell, subverting the typical immunosuppressive effects of PS-mediated uptake. However, in most situations this would promote peripheral tolerance through clonal deletion of the Ag-specific T-cell by presentation of antigen in the absence of co-stimulation. However, if the APC is also subjected to any type of ER stress (such as expression of some mutant proteins (Davies et al., 2009; Smith et al., 2008), a UPR (Martinon et al., 2010) (Chapter 3), or overload of the ER membrane with cholesterol (Li et al., 2005)), it will have likely have NFκB activation and produce IL-6. This combination may lead to presentation of self-antigens

by a mature APC expressing co-stimulatory molecules, and clonal expansion of a self-reactive T-cell. Obviously there are other checks and balances in place to prevent a loss of self-tolerance, but experiments directed at investigating some of these ideas may contribute to our understanding of autoimmunity.

BIBLIOGRAPHY

Afshar, N., Black, B.E., and Paschal, B.M. (2005). Retrotranslocation of the chaperone calreticulin from the endoplasmic reticulum lumen to the cytosol. Mol Cell Biol *25*, 8844-8853.

Allenspach, E.J., Lemos, M.P., Porrett, P.M., Turka, L.A., and Laufer, T.M. (2008). Migratory and lymphoid-resident dendritic cells cooperate to efficiently prime naive CD4 T cells. Immunity *29*, 795-806.

Apetoh, L., Ghiringhelli, F., Tesniere, A., Obeid, M., Ortiz, C., Criollo, A., Mignot, G., Maiuri, M.C., Ullrich, E., Saulnier, P.*, et al.* (2007). Toll-like receptor 4-dependent contribution of the immune system to anticancer chemotherapy and radiotherapy. Nat Med *13*, 1050-1059.

Asano, K., Nabeyama, A., Miyake, Y., Qiu, C.H., Kurita, A., Tomura, M., Kanagawa, O., Fujii, S., and Tanaka, M. (2011). CD169-positive macrophages dominate antitumor immunity by crosspresenting dead cell-associated antigens. Immunity *34*, 85-95.

Bak, S.P., Amiel, E., Walters, J.J., and Berwin, B. (2008). Calreticulin requires an ancillary adjuvant for the induction of efficient cytotoxic T cell responses. Mol Immunol *45*, 1414-1423.

Basu, S., and Srivastava, P.K. (1999). Calreticulin, a peptide-binding chaperone of the endoplasmic reticulum, elicits tumor- and peptide-specific immunity. J Exp Med *189*, 797-802.

Bauernfeind, F., Bartok, E., Rieger, A., Franchi, L., Nunez, G., and Hornung, V. (2011). Cutting Edge: Reactive Oxygen Species Inhibitors Block Priming, but Not Activation, of the NLRP3 Inflammasome. J Immunol.

Blais, J.D., Filipenko, V., Bi, M., Harding, H.P., Ron, D., Koumenis, C., Wouters, B.G., and Bell, J.C. (2004). Activating transcription factor 4 is translationally regulated by hypoxic stress. Mol Cell Biol *24*, 7469-7482.

Blander, J.M. (2008). Phagocytosis and antigen presentation: a partnership initiated by Toll-like receptors. Ann Rheum Dis *67 Suppl 3*, iii44-49.

Blass, S., Union, A., Raymackers, J., Schumann, F., Ungethum, U., Muller-Steinbach, S., De Keyser, F., Engel, J.M., and Burmester, G.R. (2001). The stress protein BiP is overexpressed and is a major B and T cell target in rheumatoid arthritis. Arthritis Rheum *44*, 761-771.

Booth, C., and Koch, G.L. (1989). Perturbation of cellular calcium induces secretion of luminal ER proteins. Cell *59*, 729-737.

Bost, K.L., and Mason, M.J. (1995). Thapsigargin and cyclopiazonic acid initiate rapid and dramatic increases of IL-6 mRNA expression and IL-6 secretion in murine peritoneal macrophages. J Immunol *155*, 285-296.

Braakman, I., and Bulleid, N.J. (2010). Protein Folding and Modification in the Mammalian Endoplasmic Reticulum. Annu Rev Biochem.

Brasier, A.R. (2010). The nuclear factor-kappaB-interleukin-6 signalling pathway mediating vascular inflammation. Cardiovasc Res *86*, 211-218.

Bruneau, N., Lombardo, D., Levy, E., and Bendayan, M. (2000). Roles of molecular chaperones in pancreatic secretion and their involvement in intestinal absorption. Microsc Res Tech *49*, 329-345.

Burdakov, D., Petersen, O.H., and Verkhratsky, A. (2005). Intraluminal calcium as a primary regulator of endoplasmic reticulum function. Cell Calcium *38*, 303-310.

Carpio, M.A., Lopez Sambrooks, C., Durand, E.S., and Hallak, M.E. (2010). The arginylation-dependent association of calreticulin with stress granules is regulated by calcium. Biochem J *429*, 63-72.

Casares, N., Pequignot, M.O., Tesniere, A., Ghiringhelli, F., Roux, S., Chaput, N., Schmitt, E., Hamai, A., Hervas-Stubbs, S., Obeid, M.*, et al.* (2005). Caspase-dependent immunogenicity of doxorubicin-induced tumor cell death. J Exp Med *202*, 1691-1701.

Chao, M.P., Jaiswal, S., Weissman-Tsukamoto, R., Alizadeh, A.A., Gentles, A.J., Volkmer, J., Weiskopf, K., Willingham, S.B., Raveh, T., Park, C.Y.*, et al.* (2010). Calreticulin is the dominant pro-phagocytic signal on multiple human cancers and is counterbalanced by CD47. Sci Transl Med *2*, 63ra94.

Charo, I.F., and Taub, R. (2011). Anti-inflammatory therapeutics for the treatment of atherosclerosis. Nat Rev Drug Discov *10*, 365-376.
Chen, K., Craige, S.E., and Keaney, J.F., Jr. (2009). Downstream targets and intracellular compartmentalization in Nox signaling. Antioxid Redox Signal *11*, 2467-2480.
Cheng, W.F., Hung, C.F., Chen, C.A., Lee, C.N., Su, Y.N., Chai, C.Y., Boyd, D.A., Hsieh, C.Y., and Wu, T.C. (2005). Characterization of DNA vaccines encoding the domains of calreticulin for their ability to elicit tumor-specific immunity and antiangiogenesis. Vaccine *23*, 3864-3874.
Coe, H., and Michalak, M. (2009). Calcium binding chaperones of the endoplasmic reticulum. Gen Physiol Biophys *28 Spec No Focus*, F96-F103.
Cohen, J.J., Duke, R.C., Fadok, V.A., and Sellins, K.S. (1992). Apoptosis and programmed cell death in immunity. Annu Rev Immunol *10*, 267-293.
Corrigall, V.M., Bodman-Smith, M.D., Brunst, M., Cornell, H., and Panayi, G.S. (2004). Inhibition of antigen-presenting cell function and stimulation of human peripheral blood mononuclear cells to express an antiinflammatory cytokine profile by the stress protein BiP: relevance to the treatment of inflammatory arthritis. Arthritis Rheum *50*, 1164-1171.
Corrigall, V.M., Bodman-Smith, M.D., Fife, M.S., Canas, B., Myers, L.K., Wooley, P., Soh, C., Staines, N.A., Pappin, D.J., Berlo, S.E.*, et al.* (2001). The human endoplasmic reticulum molecular chaperone BiP is an autoantigen for rheumatoid arthritis and prevents the induction of experimental arthritis. J Immunol *166*, 1492-1498.
Dancourt, J., and Barlowe, C. (2010). Protein sorting receptors in the early secretory pathway. Annu Rev Biochem *79*, 777-802.
Davies, M.J., Miranda, E., Roussel, B.D., Kaufman, R.J., Marciniak, S.J., and Lomas, D.A. (2009). Neuroserpin polymers activate NF-kappaB by a calcium signaling pathway that is independent of the unfolded protein response. J Biol Chem *284*, 18202-18209.
De Boo, S., Kopecka, J., Brusa, D., Gazzano, E., Matera, L., Ghigo, D., Bosia, A., and Riganti, C. (2009). iNOS activity is necessary for the cytotoxic and immunogenic effects of doxorubicin in human colon cancer cells. Mol Cancer *8*, 108.
Del Cid, N., Jeffery, E., Rizvi, S.M., Stamper, E., Peters, L.R., Brown, W.C., Provoda, C., and Raghavan, M. (2010). Modes of calreticulin recruitment to the major histocompatibility complex class I assembly pathway. J Biol Chem *285*, 4520-4535.

DeLay, M.L., Turner, M.J., Klenk, E.I., Smith, J.A., Sowders, D.P., and Colbert, R.A. (2009). HLA-B27 misfolding and the unfolded protein response augment interleukin-23 production and are associated with Th17 activation in transgenic rats. Arthritis Rheum *60*, 2633-2643.

Delpino, A., and Castelli, M. (2002). The 78 kDa glucose-regulated protein (GRP78/BIP) is expressed on the cell membrane, is released into cell culture medium and is also present in human peripheral circulation. Biosci Rep *22*, 407-420.

Deng, J., Lu, P.D., Zhang, Y., Scheuner, D., Kaufman, R.J., Sonenberg, N., Harding, H.P., and Ron, D. (2004). Translational repression mediates activation of nuclear factor kappa B by phosphorylated translation initiation factor 2. Mol Cell Biol *24*, 10161-10168.

Denmeade, S.R., Jakobsen, C.M., Janssen, S., Khan, S.R., Garrett, E.S., Lilja, H., Christensen, S.B., and Isaacs, J.T. (2003). Prostate-specific antigen-activated thapsigargin prodrug as targeted therapy for prostate cancer. J Natl Cancer Inst *95*, 990-1000.

Devitt, A., Parker, K.G., Ogden, C.A., Oldreive, C., Clay, M.F., Melville, L.A., Bellamy, C.O., Lacy-Hulbert, A., Gangloff, S.C., Goyert, S.M.*, et al.* (2004). Persistence of apoptotic cells without autoimmune disease or inflammation in CD14-/- mice. J Cell Biol *167*, 1161-1170.

Di Jeso, B., Park, Y.N., Ulianich, L., Treglia, A.S., Urbanas, M.L., High, S., and Arvan, P. (2005). Mixed-disulfide folding intermediates between thyroglobulin and endoplasmic reticulum resident oxidoreductases ERp57 and protein disulfide isomerase. Mol Cell Biol *25*, 9793-9805.

Drummond, I.A., Lee, A.S., Resendez, E., Jr., and Steinhardt, R.A. (1987). Depletion of intracellular calcium stores by calcium ionophore A23187 induces the genes for glucose-regulated proteins in hamster fibroblasts. J Biol Chem *262*, 12801-12805.

Dupuis, M., Schaerer, E., Krause, K.H., and Tschopp, J. (1993). The calcium-binding protein calreticulin is a major constituent of lytic granules in cytolytic T lymphocytes. J Exp Med *177*, 1-7.

Eggleton, P., and Llewellyn, D.H. (1999). Pathophysiological roles of calreticulin in autoimmune disease. Scand J Immunol *49*, 466-473.

Eggleton, P., Ward, F.J., Johnson, S., Khamashta, M.A., Hughes, G.R., Hajela, V.A., Michalak, M., Corbett, E.F., Staines, N.A., and Reid, K.B. (2000). Fine specificity of autoantibodies to calreticulin: epitope mapping and characterization. Clin Exp Immunol *120*, 384-391.

Ellgaard, L., Molinari, M., and Helenius, A. (1999). Setting the standards: quality control in the secretory pathway. Science *286*, 1882-1888.

Elliott, M.R., and Ravichandran, K.S. (2010). Clearance of apoptotic cells: implications in health and disease. J Cell Biol *189*, 1059-1070.

Elrod-Erickson, M.J., and Kaiser, C.A. (1996). Genes that control the fidelity of endoplasmic reticulum to Golgi transport identified as suppressors of vesicle budding mutations. Mol Biol Cell *7*, 1043-1058.

Fadok, V.A., Voelker, D.R., Campbell, P.A., Cohen, J.J., Bratton, D.L., and Henson, P.M. (1992). Exposure of phosphatidylserine on the surface of apoptotic lymphocytes triggers specific recognition and removal by macrophages. J Immunol *148*, 2207-2216.

Feder, M.E., and Hofmann, G.E. (1999). Heat-shock proteins, molecular chaperones, and the stress response: evolutionary and ecological physiology. Annu Rev Physiol *61*, 243-282.

Feng, B., Yao, P.M., Li, Y., Devlin, C.M., Zhang, D., Harding, H.P., Sweeney, M., Rong, J.X., Kuriakose, G., Fisher, E.A*., et al.* (2003). The endoplasmic reticulum is the site of cholesterol-induced cytotoxicity in macrophages. Nat Cell Biol *5*, 781-792.

Franz, S., Herrmann, K., Furnrohr, B.G., Sheriff, A., Frey, B., Gaipl, U.S., Voll, R.E., Kalden, J.R., Jack, H.M., and Herrmann, M. (2007). After shrinkage apoptotic cells expose internal membrane-derived epitopes on their plasma membranes. Cell Death Differ *14*, 733-742.

Frickel, E.M., Riek, R., Jelesarov, I., Helenius, A., Wuthrich, K., and Ellgaard, L. (2002). TROSY-NMR reveals interaction between ERp57 and the tip of the calreticulin P-domain. Proc Natl Acad Sci U S A *99*, 1954-1959.

Frleta, D., Yu, C.I., Klechevsky, E., Flamar, A.L., Zurawski, G., Banchereau, J., and Palucka, A.K. (2009). Influenza virus and poly(I:C) inhibit MHC class I-restricted presentation of cell-associated antigens derived from infected dead cells captured by human dendritic cells. J Immunol *182*, 2766-2776.

Gallucci, S., Lolkema, M., and Matzinger, P. (1999). Natural adjuvants: endogenous activators of dendritic cells. Nat Med *5*, 1249-1255.

Gao, B., and Tsan, M.F. (2003). Recombinant human heat shock protein 60 does not induce the release of tumor necrosis factor alpha from murine macrophages. J Biol Chem *278*, 22523-22529.

Gardai, S.J., McPhillips, K.A., Frasch, S.C., Janssen, W.J., Starefeldt, A., Murphy-Ullrich, J.E., Bratton, D.L., Oldenborg, P.A., Michalak, M., and Henson, P.M. (2005). Cell-surface calreticulin initiates clearance of viable or apoptotic cells through trans-activation of LRP on the phagocyte. Cell *123*, 321-334.

Gass, J.N., Jiang, H.Y., Wek, R.C., and Brewer, J.W. (2008). The unfolded protein response of B-lymphocytes: PERK-independent development of antibody-secreting cells. Mol Immunol *45*, 1035-1043.

Gaut, J.R., and Hendershot, L.M. (1993). Mutations within the nucleotide binding site of immunoglobulin-binding protein inhibit ATPase activity and interfere with release of immunoglobulin heavy chain. J Biol Chem *268*, 7248-7255.

Ghiringhelli, F., Apetoh, L., Tesniere, A., Aymeric, L., Ma, Y., Ortiz, C., Vermaelen, K., Panaretakis, T., Mignot, G., Ullrich, E.*, et al.* (2009). Activation of the NLRP3 inflammasome in dendritic cells induces IL-1beta-dependent adaptive immunity against tumors. Nat Med *15*, 1170-1178.

Ginzkey, C., Eicker, S.O., Marget, M., Krause, J., Brecht, S., Westphal, M., Hugo, H.H., Mehdorn, H.M., Steinmann, J., and Hamel, W. (2010). Increase in tumor size following intratumoral injection of immunostimulatory CpG-containing oligonucleotides in a rat glioma model. Cancer Immunol Immunother *59*, 541-551.

Gold, L.I., Eggleton, P., Sweetwyne, M.T., Van Duyn, L.B., Greives, M.R., Naylor, S.M., Michalak, M., and Murphy-Ullrich, J.E. (2010). Calreticulin: non-endoplasmic reticulum functions in physiology and disease. FASEB J *24*, 665-683.

Goodall, J.C., Wu, C., Zhang, Y., McNeill, L., Ellis, L., Saudek, V., and Gaston, J.S. (2010). Endoplasmic reticulum stress-induced transcription factor, CHOP, is crucial for dendritic cell IL-23 expression. Proc Natl Acad Sci U S A *107*, 17698-17703.

Gorlach, A., Klappa, P., and Kietzmann, T. (2006). The endoplasmic reticulum: folding, calcium homeostasis, signaling, and redox control. Antioxid Redox Signal *8*, 1391-1418.

Graham, K.S., Le, A., and Sifers, R.N. (1990). Accumulation of the insoluble PiZ variant of human alpha 1-antitrypsin within the hepatic endoplasmic reticulum does not elevate the steady-state level of grp78/BiP. J Biol Chem *265*, 20463-20468.

Granados, D.P., Tanguay, P.L., Hardy, M.P., Caron, E., de Verteuil, D., Meloche, S., and Perreault, C. (2009). ER stress affects processing of MHC class I-associated peptides. BMC Immunol *10*, 10.

Green, D.R., Ferguson, T., Zitvogel, L., and Kroemer, G. (2009). Immunogenic and tolerogenic cell death. Nat Rev Immunol *9*, 353-363.

Han, J.M., Kwon, N.H., Lee, J.Y., Jeong, S.J., Jung, H.J., Kim, H.R., Li, Z., and Kim, S. (2010). Identification of gp96 as a novel target for treatment of autoimmune disease in mice. PLoS One *5*, e9792.

Handford, P.A. (2000). Fibrillin-1, a calcium binding protein of extracellular matrix. Biochim Biophys Acta *1498*, 84-90.

Healy, S.J., Gorman, A.M., Mousavi-Shafaei, P., Gupta, S., and Samali, A. (2009). Targeting the endoplasmic reticulum-stress response as an anticancer strategy. Eur J Pharmacol *625*, 234-246.

Hebert, D.N., Bernasconi, R., and Molinari, M. (2010). ERAD substrates: which way out? Semin Cell Dev Biol *21*, 526-532.

Hebert, D.N., and Molinari, M. (2007). In and out of the ER: protein folding, quality control, degradation, and related human diseases. Physiol Rev *87*, 1377-1408.

Henderson, B., Calderwood, S.K., Coates, A.R., Cohen, I., van Eden, W., Lehner, T., and Pockley, A.G. (2010). Caught with their PAMPs down? The extracellular signalling actions of molecular chaperones are not due to microbial contaminants. Cell Stress Chaperones *15*, 123-141.

Henderson, B., and Pockley, A.G. (2010). Molecular chaperones and protein-folding catalysts as intercellular signaling regulators in immunity and inflammation. J Leukoc Biol *88*, 445-462.

Hidvegi, T., Schmidt, B.Z., Hale, P., and Perlmutter, D.H. (2005). Accumulation of mutant alpha1-antitrypsin Z in the endoplasmic reticulum activates caspases-4 and -12, NFkappaB, and BAP31 but not the unfolded protein response. J Biol Chem *280*, 39002-39015.

Hoffmann, P.R., deCathelineau, A.M., Ogden, C.A., Leverrier, Y., Bratton, D.L., Daleke, D.L., Ridley, A.J., Fadok, V.A., and Henson, P.M. (2001). Phosphatidylserine (PS) induces PS receptor-mediated macropinocytosis and promotes clearance of apoptotic cells. J Cell Biol *155*, 649-659.

Hong, C., Qiu, X., Li, Y., Huang, Q., Zhong, Z., Zhang, Y., Liu, X., Sun, L., Lv, P., and Gao, X.M. (2010). Functional analysis of recombinant calreticulin fragment 39-272: implications for immunobiological activities of calreticulin in health and disease. J Immunol *185*, 4561-4569.

Howe, C., Garstka, M., Al-Balushi, M., Ghanem, E., Antoniou, A.N., Fritzsche, S., Jankevicius, G., Kontouli, N., Schneeweiss, C., Williams, A.*, et al.* (2009). Calreticulin-dependent recycling in the early secretory pathway mediates optimal peptide loading of MHC class I molecules. EMBO J *28*, 3730-3744.

Hsieh, Y.H., Su, I.J., Lei, H.Y., Lai, M.D., Chang, W.W., and Huang, W. (2007). Differential endoplasmic reticulum stress signaling pathways mediated by iNOS. Biochem Biophys Res Commun *359*, 643-648.

Hummasti, S., and Hotamisligil, G.S. (2010). Endoplasmic reticulum stress and inflammation in obesity and diabetes. Circ Res *107*, 579-591.

Ivashkiv, L.B. (2008). A signal-switch hypothesis for cross-regulation of cytokine and TLR signalling pathways. Nat Rev Immunol *8*, 816-822.

Iwakoshi, N.N., Lee, A.H., Vallabhajosyula, P., Otipoby, K.L., Rajewsky, K., and Glimcher, L.H. (2003). Plasma cell differentiation and the unfolded protein response intersect at the transcription factor XBP-1. Nat Immunol *4*, 321-329.

Janssen, S., Rosen, D.M., Ricklis, R.M., Dionne, C.A., Lilja, H., Christensen, S.B., Isaacs, J.T., and Denmeade, S.R. (2006). Pharmacokinetics, biodistribution, and antitumor efficacy of a human glandular kallikrein 2 (hK2)-activated thapsigargin prodrug. Prostate *66*, 358-368.

Jeffery, E., Peters, L.R., and Raghavan, M. (2011). The polypeptide binding conformation of calreticulin facilitates its cell-surface expression under conditions of endoplasmic reticulum stress. J Biol Chem *286*, 2402-2415.

Kazama, H., Ricci, J.E., Herndon, J.M., Hoppe, G., Green, D.R., and Ferguson, T.A. (2008). Induction of immunological tolerance by apoptotic cells requires caspase-dependent oxidation of high-mobility group box-1 protein. Immunity *29*, 21-32.

Kepp, O., Gdoura, A., Martins, I., Panaretakis, T., Schlemmer, F., Tesniere, A., Fimia, G.M., Ciccosanti, F., Burgevin, A., Piacentini, M.*, et al.* (2010). Lysyl tRNA synthetase is required for the translocation of calreticulin to the cell surface in immunogenic death. Cell Cycle *9*, 3072-3077.

Kerr, J.F., Wyllie, A.H., and Currie, A.R. (1972). Apoptosis: a basic biological phenomenon with wide-ranging implications in tissue kinetics. Br J Cancer *26*, 239-257.

Kirk, S.J., Cliff, J.M., Thomas, J.A., and Ward, T.H. (2010). Biogenesis of secretory organelles during B cell differentiation. J Leukoc Biol *87*, 245-255.

Kopecka, J., Campia, I., Brusa, D., Doublier, S., Matera, L., Ghigo, D., Bosia, A., and Riganti, C. (2011). Nitric oxide and P-glycoprotein modulate the phagocytosis of colon cancer cells. J Cell Mol Med *15*, 1492-1504.

Koumenis, C., Naczki, C., Koritzinsky, M., Rastani, S., Diehl, A., Sonenberg, N., Koromilas, A., and Wouters, B.G. (2002). Regulation of protein synthesis by hypoxia via activation of the endoplasmic reticulum kinase PERK and phosphorylation of the translation initiation factor eIF2alpha. Mol Cell Biol *22*, 7405-7416.

Kozlov, G., Pocanschi, C.L., Rosenauer, A., Bastos-Aristizabal, S., Gorelik, A., Williams, D.B., and Gehring, K. (2010). Structural basis of carbohydrate recognition by calreticulin. J Biol Chem *285*, 38612-38620.

Kroning, H., Kahne, T., Ittenson, A., Franke, A., and Ansorge, S. (1994). Thiol-proteindisulfide-oxidoreductase (proteindisulfide isomerase): a new plasma membrane constituent of mature human B lymphocytes. Scand J Immunol *39*, 346-350.

Krysko, D.V., Denecker, G., Festjens, N., Gabriels, S., Parthoens, E., D'Herde, K., and Vandenabeele, P. (2006). Macrophages use different internalization mechanisms to clear apoptotic and necrotic cells. Cell Death Differ *13*, 2011-2022.

Krysko, D.V., and Vandenabeele, P. (2008). From regulation of dying cell engulfment to development of anti-cancer therapy. Cell Death Differ *15*, 29-38.

Kung, G., Konstantinidis, K., and Kitsis, R.N. (2011). Programmed necrosis, not apoptosis, in the heart. Circ Res *108*, 1017-1036.

Kuraishi, T., Manaka, J., Kono, M., Ishii, H., Yamamoto, N., Koizumi, K., Shiratsuchi, A., Lee, B.L., Higashida, H., and Nakanishi, Y. (2007). Identification of calreticulin as a marker for phagocytosis of apoptotic cells in Drosophila. Exp Cell Res *313*, 500-510.

Kyewski, B., and Klein, L. (2006). A central role for central tolerance. Annu Rev Immunol *24*, 571-606.

Leach, M.R., Cohen-Doyle, M.F., Thomas, D.Y., and Williams, D.B. (2002). Localization of the lectin, ERp57 binding, and polypeptide binding sites of calnexin and calreticulin. J Biol Chem *277*, 29686-29697.

Lee, H.K., Zamora, M., Linehan, M.M., Iijima, N., Gonzalez, D., Haberman, A., and Iwasaki, A. (2009). Differential roles of migratory and resident DCs in T cell priming after mucosal or skin HSV-1 infection. J Exp Med *206*, 359-370.

Leonard, B.E. (2007). Inflammation, depression and dementia: are they connected? Neurochem Res *32*, 1749-1756.

Lev, A., Dimberu, P., Das, S.R., Maynard, J.C., Nicchitta, C.V., Bennink, J.R., and Yewdell, J.W. (2009). Efficient cross-priming of antiviral CD8+ T cells by antigen donor cells is GRP94 independent. J Immunol *183*, 4205-4210.

Li, M., Baumeister, P., Roy, B., Phan, T., Foti, D., Luo, S., and Lee, A.S. (2000). ATF6 as a transcription activator of the endoplasmic reticulum stress element: thapsigargin stress-induced changes and synergistic interactions with NF-Y and YY1. Mol Cell Biol *20*, 5096-5106.

Li, Y., Ge, M., Ciani, L., Kuriakose, G., Westover, E.J., Dura, M., Covey, D.F., Freed, J.H., Maxfield, F.R., Lytton, J.*, et al.* (2004). Enrichment of endoplasmic reticulum with cholesterol inhibits sarcoplasmic-endoplasmic reticulum calcium ATPase-2b activity in parallel with increased order of membrane lipids: implications for depletion of endoplasmic reticulum calcium stores and apoptosis in cholesterol-loaded macrophages. J Biol Chem *279*, 37030-37039.

Li, Y., Schwabe, R.F., DeVries-Seimon, T., Yao, P.M., Gerbod-Giannone, M.C., Tall, A.R., Davis, R.J., Flavell, R., Brenner, D.A., and Tabas, I. (2005). Free cholesterol-loaded macrophages are an abundant source of tumor necrosis factor-alpha and interleukin-6: model of NF-kappaB- and map kinase-dependent inflammation in advanced atherosclerosis. J Biol Chem *280*, 21763-21772.

Liu, B., Dai, J., Zheng, H., Stoilova, D., Sun, S., and Li, Z. (2003). Cell surface expression of an endoplasmic reticulum resident heat shock protein gp96 triggers MyD88-dependent systemic autoimmune diseases. Proc Natl Acad Sci U S A *100*, 15824-15829.

Llewellyn, D.H., Kendall, J.M., Sheikh, F.N., and Campbell, A.K. (1996). Induction of calreticulin expression in HeLa cells by depletion of the endoplasmic reticulum Ca2+ store and inhibition of N-linked glycosylation. Biochem J *318 (Pt 2)*, 555-560.

Llewellyn, D.H., Roderick, H.L., and Rose, S. (1997). KDEL receptor expression is not coordinatedly up-regulated with ER stress-induced reticuloplasmin expression in HeLa cells. Biochem Biophys Res Commun *240*, 36-40.

Malhotra, J.D., and Kaufman, R.J. (2007). Endoplasmic reticulum stress and oxidative stress: a vicious cycle or a double-edged sword? Antioxid Redox Signal *9*, 2277-2293.

Mancino, L., Rizvi, S.M., Lapinski, P.E., and Raghavan, M. (2002). Calreticulin recognizes misfolded HLA-A2 heavy chains. Proc Natl Acad Sci U S A *99*, 5931-5936.

Mariathasan, S., Weiss, D.S., Newton, K., McBride, J., O'Rourke, K., Roose-Girma, M., Lee, W.P., Weinrauch, Y., Monack, D.M., and Dixit, V.M. (2006). Cryopyrin activates the inflammasome in response to toxins and ATP. Nature *440*, 228-232.

Martin, V., Groenendyk, J., Steiner, S.S., Guo, L., Dabrowska, M., Parker, J.M., Muller-Esterl, W., Opas, M., and Michalak, M. (2006). Identification by mutational analysis of amino acid residues essential in the chaperone function of calreticulin. J Biol Chem *281*, 2338-2346.

Martinon, F., Chen, X., Lee, A.H., and Glimcher, L.H. (2010). TLR activation of the transcription factor XBP1 regulates innate immune responses in macrophages. Nat Immunol *11*, 411-418.

Martins, I., Kepp, O., Galluzzi, L., Senovilla, L., Schlemmer, F., Adjemian, S., Menger, L., Michaud, M., Zitvogel, L., and Kroemer, G. (2010). Surface-exposed calreticulin in the interaction between dying cells and phagocytes. Ann N Y Acad Sci *1209*, 77-82.

Martins, I., Kepp, O., Schlemmer, F., Adjemian, S., Tailler, M., Shen, S., Michaud, M., Menger, L., Gdoura, A., Tajeddine, N*., et al.* (2011). Restoration of the immunogenicity of cisplatin-induced cancer cell death by endoplasmic reticulum stress. Oncogene *30*, 1147-1158.

Mezghrani, A., Courageot, J., Mani, J.C., Pugniere, M., Bastiani, P., and Miquelis, R. (2000). Protein-disulfide isomerase (PDI) in FRTL5 cells. pH-dependent thyroglobulin/PDI interactions determine a novel PDI function in the post-endoplasmic reticulum of thyrocytes. J Biol Chem *275*, 1920-1929.

Michalak, M., Groenendyk, J., Szabo, E., Gold, L.I., and Opas, M. (2009). Calreticulin, a multi-process calcium-buffering chaperone of the endoplasmic reticulum. Biochem J *417*, 651-666.

Michalak, M., Robert Parker, J.M., and Opas, M. (2002). Ca2+ signaling and calcium binding chaperones of the endoplasmic reticulum. Cell Calcium *32*, 269-278.

Minamino, T., Komuro, I., and Kitakaze, M. (2010). Endoplasmic reticulum stress as a therapeutic target in cardiovascular disease. Circ Res *107*, 1071-1082.

Morel, P.A., and Turner, M.S. (2011). Dendritic cells and the maintenance of self-tolerance. Immunol Res.

Munoz, L.E., Peter, C., Herrmann, M., Wesselborg, S., and Lauber, K. (2010). Scent of dying cells: the role of attraction signals in the clearance of apoptotic cells and its immunological consequences. Autoimmun Rev *9*, 425-430.

Murphy, F.J., Hayes, M.P., and Burd, P.R. (2000). Disparate intracellular processing of human IL-12 preprotein subunits: atypical processing of the P35 signal peptide. J Immunol *164*, 839-847.

Murshid, A., Gong, J., and Calderwood, S.K. (2008). Heat-shock proteins in cancer vaccines: agents of antigen cross-presentation. Expert Rev Vaccines *7*, 1019-1030.

Obeid, M. (2008). ERP57 membrane translocation dictates the immunogenicity of tumor cell death by controlling the membrane translocation of calreticulin. J Immunol *181*, 2533-2543.

Obeid, M., Panaretakis, T., Joza, N., Tufi, R., Tesniere, A., van Endert, P., Zitvogel, L., and Kroemer, G. (2007a). Calreticulin exposure is required for the immunogenicity of gamma-irradiation and UVC light-induced apoptosis. Cell Death Differ *14*, 1848-1850.

Obeid, M., Tesniere, A., Ghiringhelli, F., Fimia, G.M., Apetoh, L., Perfettini, J.L., Castedo, M., Mignot, G., Panaretakis, T., Casares, N.*, et al.* (2007b). Calreticulin exposure dictates the immunogenicity of cancer cell death. Nat Med *13*, 54-61.

Ogura, Y., Sutterwala, F.S., and Flavell, R.A. (2006). The inflammasome: first line of the immune response to cell stress. Cell *126*, 659-662.

Oizumi, S., Strbo, N., Pahwa, S., Deyev, V., and Podack, E.R. (2007). Molecular and cellular requirements for enhanced antigen cross-presentation to CD8 cytotoxic T lymphocytes. J Immunol *179*, 2310-2317.

Okada, T., Haze, K., Nadanaka, S., Yoshida, H., Seidah, N.G., Hirano, Y., Sato, R., Negishi, M., and Mori, K. (2003). A serine protease inhibitor prevents endoplasmic reticulum stress-induced cleavage but not transport of the membrane-bound transcription factor ATF6. J Biol Chem *278*, 31024-31032.

Pahl, H.L., and Baeuerle, P.A. (1995). A novel signal transduction pathway from the endoplasmic reticulum to the nucleus is mediated by transcription factor NF-kappa B. EMBO J *14*, 2580-2588.

Pahl, H.L., and Baeuerle, P.A. (1996). Activation of NF-kappa B by ER stress requires both Ca2+ and reactive oxygen intermediates as messengers. FEBS Lett *392*, 129-136.

Pahl, H.L., and Baeuerle, P.A. (1997). The ER-overload response: activation of NF-kappa B. Trends Biochem Sci *22*, 63-67.

Paidassi, H., Tacnet-Delorme, P., Verneret, M., Gaboriaud, C., Houen, G., Duus, K., Ling, W.L., Arlaud, G.J., and Frachet, P. (2011). Investigations on the C1q-calreticulin-phosphatidylserine interactions yield new insights into apoptotic cell recognition. J Mol Biol *408*, 277-290.

Panaretakis, T., Joza, N., Modjtahedi, N., Tesniere, A., Vitale, I., Durchschlag, M., Fimia, G.M., Kepp, O., Piacentini, M., Froehlich, K.U.*, et al.* (2008a). The co-translocation of ERp57 and calreticulin determines the immunogenicity of cell death. Cell Death Differ *15*, 1499-1509.

Panaretakis, T., Joza, N., Modjtahedi, N., Tesniere, A., Vitale, I., Durchschlag, M., Fimia, G.M., Kepp, O., Piacentini, M., Froehlich, K.U.*, et al.* (2008b). The co-translocation of ERp57 and calreticulin determines the immunogenicity of cell death. Cell Death Differ.

Panaretakis, T., Kepp, O., Brockmeier, U., Tesniere, A., Bjorklund, A.C., Chapman, D.C., Durchschlag, M., Joza, N., Pierron, G., van Endert, P.*, et al.* (2009). Mechanisms of pre-apoptotic calreticulin exposure in immunogenic cell death. EMBO J *28*, 578-590.

Panayi, G.S., and Corrigall, V.M. (2006). BiP regulates autoimmune inflammation and tissue damage. Autoimmun Rev *5*, 140-142.

Panayi, G.S., and Corrigall, V.M. (2008). BiP, an anti-inflammatory ER protein, is a potential new therapy for the treatment of rheumatoid arthritis. Novartis Found Symp *291*, 212-216; discussion 216-224.

Park, Y.J., Liu, G., Lorne, E.F., Zhao, X., Wang, J., Tsuruta, Y., Zmijewski, J., and Abraham, E. (2008). PAI-1 inhibits neutrophil efferocytosis. Proc Natl Acad Sci U S A *105*, 11784-11789.

Patel, V.A., Longacre, A., Hsiao, K., Fan, H., Meng, F., Mitchell, J.E., Rauch, J., Ucker, D.S., and Levine, J.S. (2006). Apoptotic cells, at all stages of the death process, trigger characteristic signaling events that are divergent from and dominant over those triggered by necrotic cells: Implications for the delayed clearance model of autoimmunity. J Biol Chem *281*, 4663-4670.

Peters, L.R., and Raghavan, M. (2011a). Endoplasmic Reticulum Calcium Depletion Impacts Chaperone Secretion, Innate Immunity, and Phagocytic Uptake of Cells. J Immunol.

Peters, L.R., and Raghavan, M. (2011b). Endoplasmic reticulum calcium depletion impacts chaperone secretion, innate immunity, and phagocytic uptake of cells. J Immunol *187*, 919-931.

Petrovski, G., Zahuczky, G., Katona, K., Vereb, G., Martinet, W., Nemes, Z., Bursch, W., and Fesus, L. (2007a). Clearance of dying autophagic cells of different origin by professional and non-professional phagocytes. Cell Death Differ *14*, 1117-1128.

Petrovski, G., Zahuczky, G., Majai, G., and Fesus, L. (2007b). Phagocytosis of cells dying through autophagy evokes a pro-inflammatory response in macrophages. Autophagy *3*, 509-511.

Pfeffer, S.R. (2007). Unsolved mysteries in membrane traffic. Annu Rev Biochem *76*, 629-645.

Qiu, C.H., Miyake, Y., Kaise, H., Kitamura, H., Ohara, O., and Tanaka, M. (2009). Novel subset of CD8{alpha}+ dendritic cells localized in the marginal zone is responsible for tolerance to cell-associated antigens. J Immunol *182*, 4127-4136.

Raghavan, M., Del Cid, N., Rizvi, S.M., and Peters, L.R. (2008). MHC class I assembly: out and about. Trends Immunol *29*, 436-443.
Ravichandran, K.S. (2010). Find-me and eat-me signals in apoptotic cell clearance: progress and conundrums. J Exp Med *207*, 1807-1817.
Reed, R.C., Berwin, B., Baker, J.P., and Nicchitta, C.V. (2003). GRP94/gp96 elicits ERK activation in murine macrophages. A role for endotoxin contamination in NF-kappa B activation and nitric oxide production. J Biol Chem *278*, 31853-31860.
Reimold, A.M., Iwakoshi, N.N., Manis, J., Vallabhajosyula, P., Szomolanyi-Tsuda, E., Gravallese, E.M., Friend, D., Grusby, M.J., Alt, F., and Glimcher, L.H. (2001). Plasma cell differentiation requires the transcription factor XBP-1. Nature *412*, 300-307.
Reiss, K., and Saftig, P. (2009). The "a disintegrin and metalloprotease" (ADAM) family of sheddases: physiological and cellular functions. Semin Cell Dev Biol *20*, 126-137.
Ren, G., Su, J., Zhao, X., Zhang, L., Zhang, J., Roberts, A.I., Zhang, H., Das, G., and Shi, Y. (2008). Apoptotic cells induce immunosuppression through dendritic cells: critical roles of IFN-gamma and nitric oxide. J Immunol *181*, 3277-3284.
Ren, Y., Stuart, L., Lindberg, F.P., Rosenkranz, A.R., Chen, Y., Mayadas, T.N., and Savill, J. (2001). Nonphlogistic clearance of late apoptotic neutrophils by macrophages: efficient phagocytosis independent of beta 2 integrins. J Immunol *166*, 4743-4750.
Rizvi, S.M., Mancino, L., Thammavongsa, V., Cantley, R.L., and Raghavan, M. (2004). A polypeptide binding conformation of calreticulin is induced by heat shock, calcium depletion, or by deletion of the C-terminal acidic region. Mol Cell *15*, 913-923.
Rock, K.L., and Kono, H. (2008). The inflammatory response to cell death. Annu Rev Pathol *3*, 99-126.
Rodriguez-Manzanet, R., Sanjuan, M.A., Wu, H.Y., Quintana, F.J., Xiao, S., Anderson, A.C., Weiner, H.L., Green, D.R., and Kuchroo, V.K. (2010). T and B cell hyperactivity and autoimmunity associated with niche-specific defects in apoptotic body clearance in TIM-4-deficient mice. Proc Natl Acad Sci U S A *107*, 8706-8711.
Rutkowski, D.T., and Kaufman, R.J. (2004). A trip to the ER: coping with stress. Trends Cell Biol *14*, 20-28.

Saito, Y., Ihara, Y., Leach, M.R., Cohen-Doyle, M.F., and Williams, D.B. (1999). Calreticulin functions in vitro as a molecular chaperone for both glycosylated and non-glycosylated proteins. EMBO J *18*, 6718-6729.

Sambrook, J.F. (1990). The involvement of calcium in transport of secretory proteins from the endoplasmic reticulum. Cell *61*, 197-199.

Sato, K., and Nakano, A. (2007). Mechanisms of COPII vesicle formation and protein sorting. FEBS Lett *581*, 2076-2082.

Savina, A., and Amigorena, S. (2007). Phagocytosis and antigen presentation in dendritic cells. Immunol Rev *219*, 143-156.

Schenten, D., and Medzhitov, R. (2011). The control of adaptive immune responses by the innate immune system. Adv Immunol *109*, 87-124.

Schild, H., and Rammensee, H.G. (2000). gp96--the immune system's Swiss army knife. Nat Immunol *1*, 100-101.

Schroder, M., and Kaufman, R.J. (2005). The mammalian unfolded protein response. Annu Rev Biochem *74*, 739-789.

Schulze, C., Munoz, L.E., Franz, S., Sarter, K., Chaurio, R.A., Gaipl, U.S., and Herrmann, M. (2008). Clearance deficiency--a potential link between infections and autoimmunity. Autoimmun Rev *8*, 5-8.

Scorrano, L., Oakes, S.A., Opferman, J.T., Cheng, E.H., Sorcinelli, M.D., Pozzan, T., and Korsmeyer, S.J. (2003). BAX and BAK regulation of endoplasmic reticulum Ca2+: a control point for apoptosis. Science *300*, 135-139.

Selzner, N., Selzner, M., Graf, R., Ungethuem, U., Fitz, J.G., and Clavien, P.A. (2004). Water induces autocrine stimulation of tumor cell killing through ATP release and P2 receptor binding. Cell Death Differ *11 Suppl 2*, S172-180.

Sipione, S., Ewen, C., Shostak, I., Michalak, M., and Bleackley, R.C. (2005). Impaired cytolytic activity in calreticulin-deficient CTLs. J Immunol *174*, 3212-3219.

Skalet, A.H., Isler, J.A., King, L.B., Harding, H.P., Ron, D., and Monroe, J.G. (2005). Rapid B cell receptor-induced unfolded protein response in nonsecretory B cells correlates with pro- versus antiapoptotic cell fate. J Biol Chem *280*, 39762-39771.

Smith, J.A., Turner, M.J., DeLay, M.L., Klenk, E.I., Sowders, D.P., and Colbert, R.A. (2008). Endoplasmic reticulum stress and the unfolded protein response are linked to

synergistic IFN-beta induction via X-box binding protein 1. Eur J Immunol *38*, 1194-1203.

Sonnichsen, B., Fullekrug, J., Nguyen Van, P., Diekmann, W., Robinson, D.G., and Mieskes, G. (1994). Retention and retrieval: both mechanisms cooperate to maintain calreticulin in the endoplasmic reticulum. J Cell Sci *107 (Pt 10)*, 2705-2717.

Spisek, R., Charalambous, A., Mazumder, A., Vesole, D.H., Jagannath, S., and Dhodapkar, M.V. (2007). Bortezomib enhances dendritic cell (DC)-mediated induction of immunity to human myeloma via exposure of cell surface heat shock protein 90 on dying tumor cells: therapeutic implications. Blood *109*, 4839-4845.

Srivastava, P. (2002). Roles of heat-shock proteins in innate and adaptive immunity. Nat Rev Immunol *2*, 185-194.

Srivastava, P.K., DeLeo, A.B., and Old, L.J. (1986). Tumor rejection antigens of chemically induced sarcomas of inbred mice. Proc Natl Acad Sci U S A *83*, 3407-3411.

Stuart, L.M., Takahashi, K., Shi, L., Savill, J., and Ezekowitz, R.A. (2005). Mannose-binding lectin-deficient mice display defective apoptotic cell clearance but no autoimmune phenotype. J Immunol *174*, 3220-3226.

Tager, M., Kroning, H., Thiel, U., and Ansorge, S. (1997). Membrane-bound proteindisulfide isomerase (PDI) is involved in regulation of surface expression of thiols and drug sensitivity of B-CLL cells. Exp Hematol *25*, 601-607.

Tamura, Y., Hirohashi, Y., Kutomi, G., Nakanishi, K., Kamiguchi, K., Torigoe, T., and Sato, N. (2011). Tumor-produced secreted form of binding of immunoglobulin protein elicits antigen-specific tumor immunity. J Immunol *186*, 4325-4330.

Tarr, J.M., Young, P.J., Morse, R., Shaw, D.J., Haigh, R., Petrov, P.G., Johnson, S.J., Winyard, P.G., and Eggleton, P. (2010). A mechanism of release of calreticulin from cells during apoptosis. J Mol Biol *401*, 799-812.

Tesniere, A., Panaretakis, T., Kepp, O., Apetoh, L., Ghiringhelli, F., Zitvogel, L., and Kroemer, G. (2008). Molecular characteristics of immunogenic cancer cell death. Cell Death Differ *15*, 3-12.

Testori, A., Richards, J., Whitman, E., Mann, G.B., Lutzky, J., Camacho, L., Parmiani, G., Tosti, G., Kirkwood, J.M., Hoos, A.*, et al.* (2008). Phase III comparison of vitespen, an autologous tumor-derived heat shock protein gp96 peptide complex vaccine, with

physician's choice of treatment for stage IV melanoma: the C-100-21 Study Group. J Clin Oncol *26*, 955-962.

Thastrup, O., Cullen, P.J., Drobak, B.K., Hanley, M.R., and Dawson, A.P. (1990). Thapsigargin, a tumor promoter, discharges intracellular Ca2+ stores by specific inhibition of the endoplasmic reticulum Ca2(+)-ATPase. Proc Natl Acad Sci U S A *87*, 2466-2470.

Todd, D.J., Lee, A.H., and Glimcher, L.H. (2008). The endoplasmic reticulum stress response in immunity and autoimmunity. Nat Rev Immunol *8*, 663-674.

Torchinsky, M.B., Garaude, J., and Blander, J.M. (2010). Infection and apoptosis as a combined inflammatory trigger. Curr Opin Immunol *22*, 55-62.

Torchinsky, M.B., Garaude, J., Martin, A.P., and Blander, J.M. (2009). Innate immune recognition of infected apoptotic cells directs T(H)17 cell differentiation. Nature *458*, 78-82.

Tsan, M.F., and Gao, B. (2009). Heat shock proteins and immune system. J Leukoc Biol *85*, 905-910.

Tufi, R., Panaretakis, T., Bianchi, K., Criollo, A., Fazi, B., Di Sano, F., Tesniere, A., Kepp, O., Paterlini-Brechot, P., Zitvogel, L.*, et al.* (2008). Reduction of endoplasmic reticulum Ca2+ levels favors plasma membrane surface exposure of calreticulin. Cell Death Differ *15*, 274-282.

Turnbull, I.R., and Colonna, M. (2007). Activating and inhibitory functions of DAP12. Nat Rev Immunol *7*, 155-161.

Ulianich, L., Terrazzano, G., Annunziatella, M., Ruggiero, G., Beguinot, F., and Di Jeso, B. (2011). ER stress impairs MHC Class I surface expression and increases susceptibility of thyroid cells to NK-mediated cytotoxicity. Biochim Biophys Acta *1812*, 431-438.

Voll, R.E., Herrmann, M., Roth, E.A., Stach, C., Kalden, J.R., and Girkontaite, I. (1997). Immunosuppressive effects of apoptotic cells. Nature *390*, 350-351.

Waser, M., Mesaeli, N., Spencer, C., and Michalak, M. (1997). Regulation of calreticulin gene expression by calcium. J Cell Biol *138*, 547-557.

Wiest, D.L., Bhandoola, A., Punt, J., Kreibich, G., McKean, D., and Singer, A. (1997). Incomplete endoplasmic reticulum (ER) retention in immature thymocytes as revealed by

surface expression of "ER-resident" molecular chaperones. Proc Natl Acad Sci U S A *94*, 1884-1889.

Winnay, J.N., Boucher, J., Mori, M.A., Ueki, K., and Kahn, C.R. (2010). A regulatory subunit of phosphoinositide 3-kinase increases the nuclear accumulation of X-box-binding protein-1 to modulate the unfolded protein response. Nat Med *16*, 438-445.

Yamasaki, S., and Anderson, P. (2008). Reprogramming mRNA translation during stress. Curr Opin Cell Biol *20*, 222-226.

Yoo, J.Y., and Desiderio, S. (2003). Innate and acquired immunity intersect in a global view of the acute-phase response. Proc Natl Acad Sci U S A *100*, 1157-1162.

Yoshida, H. (2007). ER stress and diseases. FEBS J *274*, 630-658.

Zanin-Zhorov, A., Cahalon, L., Tal, G., Margalit, R., Lider, O., and Cohen, I.R. (2006). Heat shock protein 60 enhances CD4+ CD25+ regulatory T cell function via innate TLR2 signaling. J Clin Invest *116*, 2022-2032.

Zhang, K., Shen, X., Wu, J., Sakaki, K., Saunders, T., Rutkowski, D.T., Back, S.H., and Kaufman, R.J. (2006). Endoplasmic reticulum stress activates cleavage of CREBH to induce a systemic inflammatory response. Cell *124*, 587-599.

Zhang, Y., Liu, R., Ni, M., Gill, P., and Lee, A.S. (2010). Cell surface relocalization of the endoplasmic reticulum chaperone and unfolded protein response regulator GRP78/BiP. J Biol Chem *285*, 15065-15075.

Zitvogel, L., Kepp, O., and Kroemer, G. (2010). Decoding cell death signals in inflammation and immunity. Cell *140*, 798-804.